

HERE TODAY, GONE TOMORROW:  
FLOW VARIABILITY, LARVAL DISPERSAL  
AND FISHERIES MANAGEMENT IN HAWAI'I

A DISSERTATION SUBMITTED TO THE GRADUATE DIVISION OF THE  
UNIVERSITY OF HAWAI'I AT MĀNOA IN PARTIAL FULFILLMENT OF THE  
REQUIREMENTS FOR THE DEGREE OF

DOCTOR OF PHILOSOPHY

IN

OCEANOGRAPHY

DECEMBER 2012

By

Ana Carolina Vaz

Dissertation Committee:

Kelvin Richards, Chairperson

Brian Bowen

Christopher Kelley

Claire Paris

Brian Powell

Keywords: Lagrangian Coherent Structures, larval dispersal, eddy variability, reserves

Copyright 2012

by

Ana Carolina Vaz

To Paul, Lucia & Angela

## Acknowledgements

Thank you to my advisor, Kelvin Richards, for your guidance, mentoring, discussions, encouragement, flexibility and patience during the last six years. Thank you for supporting me to pursue my research interests. Thanks to Christopher Kelley for the time you invested in this research. Your ideas, enthusiasm, discussions, reviews, and biological insights were all most helpful. Also, thank you for offering me opportunities to share my research with managers, making it useful for solving real life problems. Thanks for Claire Paris for embarking in this project. Thank you for sharing your knowledge of biophysical processes, for providing the biophysical models (BOLTS and CMS) used here, for thoughtful ideas, and for the great opportunities to work with you and your group in Miami. Thank you to Brian Bowen and Brian Powell for participating in the committee, comments and suggestions along the entire work development.

Due to the interdisciplinary nature of my dissertation, I benefited from discussions and mentoring from many different researchers. A special thanks to Yanli Jia (IPRC), who provided the regional HYCOM velocity fields. Also, for all your comments, ideas and support throughout this dissertation. Thanks to Bruce Mundy's (NOAA), whose research inspired me to write my Ph.D. project while in Brazil, and who has been a wonderful source of information. Thank you Mr. Mundy for sharing a little of your vast knowledge with me. Thanks for David Itano (PRFRP) for your collaboration in the yellowfin tuna project and for your insights. My sincere gratitude is extended to Robert Humphreys (NOAA), Margareth McManus (UHM), Jeff Drazen (UHM), Kathleen Rutemberg (UHM), Jeanne Wexler (ITTCC), Josefina Olascoaga (RMSAS), Don Olson (RMSAS), Frank Parrish (NOAA), Rob Toonen (UHM), Saulo Soares (UHM), Joana Tavares, Carolina Parada (UDEC), Paulo Calil (FURG), Ashwanth Srinivasan (RSMAS), Don Kobayashi (NOAA), Kim Andrews and Michelle Gaither for helpful discussions at different stages of this project, as well as for providing invaluable references and data. Thanks for Francesco D'Ovidio, for providing the FSLE routines used in Chapter 2.

Support for this work was partially provided by the Coordenação de Aperfeiçoamento de Pessoal de Nível Superior (CAPES), Ministério da Educação, Brasil, and the Fulbright Program. Additional funding was provided by Cooperative Agreement NA09OAR4320075 between the Joint Institute for Marine and Atmospheric Research (JIMAR) and the National Oceanic and Atmospheric Administration (NOAA); and by the Research Corporation of the University of Hawai'i (RCUH) through a Dissertation Completion Award (2010).

My sincere gratitude to all Oceanography professors, researchers and graduate students, for helping me be a better oceanographer! Special thanks to the graduate students of the entering classes of 2006 and 2007. Thanks to the department staff, particularly Nancy Koike, Kristin Momohara, and Catalpa Kong, as well as Susan Yago from personnel, all SOEST, IPRC, PFRP, JIMAR and ISS staff for all of your assistance

and for making my life manageable. I am also indebted to my past oceanography professors and friends, all contributed to my professional formation. Thanks in particular to my former advisors Osmar Moller Jr. (FURG) and Edmo Campos (USP), for encouraging me to pursue my research interests and a Ph.D abroad. Thanks are due also to José Henrique Muelbert (FURG) and Carolina Parada (UDEC), for teaching me about individual-based models and for mentoring in the implementation of my first IBM.

An essential part of this long Ph.D. journey were my friends and family, who filled my glass when it was half-empty (literally and not), gave encouragement, ideas, discussions, informal English lessons, made my adaption to American and graduate student life easier and funnier, and were present in every stage of this dissertation. Thanks to the Bamboo housemates, and all my friends in Hawai‘i, especially Paula, Joana, Lucia, Irina, Marcos, Saulo, Eric, Claire & Petra, Dani, Dave & Maiara, Eric & Aki, Melanie, Caro & Jorge, and Lora. I am blessed to have friends like you in my life! For the friends in Miami which helped the time there be more productive and fun, in particular to Tania. Thanks to my Brazilian friends, for your friendship and support despite the physical distance, in particular to Dri, and the “spices”: Ana, Hel, Ká & Vi. My gratitude to Celene, Jeronimo, Lais, Regis, Stella and César, por todo carinho, and for keeping an eye on and giving support to my moms. A big thank you to my entire family! In Brazil, thanks in particular to my aunts Joana and Ziza, and to Li, César and Manu for their love and support. In the USA, thank you for the fabulous family I am so lucky to have become a part of: Tutu, Paula, Steve, Sam, Abby, Amanda and Jonnie, for your love, support, enthusiasm and for sharing Paul with me; to Madilyn, Emma and Jackson, thank you for your love, your smiles and for constantly reminding me that the world is a place of wonders, where exciting discoveries wait for us everyday!

This dissertation is a result of a long journey, which somehow started 24 years ago when I, then a nine year old, decided that I would be an oceanographer. My mom, Lucia, and my aunt, Angela were an integral part of every step in this journey to make my dream come true: no words can express my gratitude to you. You took it graciously when I decided to live in the other side of the world to follow my dream, and never wavered in your support and belief in my potential. Thank you for giving me the love for knowledge and for your unconditional love.

And during this journey, I met my best friend, Paul. Because of your love, friendship, and unwavering support, I was able to overcome many challenges of research and graduate student life with confidence and grace. Thank you so very much! Your love, enthusiasm, courage, curiosity and intelligence make me a better person and a better researcher, everyday. Thank you for being the perfect partner to ride with through the waters of life: you give me the certainty that we will ride to reach all of our dreams and beyond. Eu te amo!

## Abstract

A contemporary challenge in marine ecology is understanding population connectivity driven by transport during early life stages. Connectivity results from a complex combination of biological traits and physical mechanisms. This dissertation begins by investigating the influence of physical mechanisms on particle transport around the Island of Hawai‘i. Particle dispersion was determined by using an individual-based model (IBM) and the flow fields derived from a global and a regional implementations of an ocean circulation model. To understand the underlying physical processes of transport, coherent structures were located in the flow field, recurrent physical features were identified, and how particle transport related to them was observed. Results showed that the eddy flow increased connectivity and influenced retention, as well as that both the flow field and dispersal patterns were highly variable. In this scenario, eddy events influenced transport in distinct ways, and the timing of release played an important role in the dispersal and resulting connectivity. Differences were found in the transport of particles and emerging connectivity patterns when comparing the two model implementations, highlighting that modeling studies should use hydrodynamical model flows representing the scales of variability affecting dispersion. Then, the IBM was adapted for fish species, and connectivity patterns along the Hawaiian Archipelago of three bottomfish: *E. coruscans*, *E. carbunculus*, and *P. filamentosus* were investigated. These species appeared to share common features in their connectivity patterns driven by larval transport, as follows: i) limited connectivity between the Papahānaumokuākea Marine National Monument (PMNM) and the Main Hawaiian Islands (MHI); ii) greater

connectivity among islands in the PMNM than in the MHI; iii) existence of four, mostly self-contained, dispersal zones along the Archipelago; and iv) islands from Kauai to Necker connected the PMNM and the MHI through larval dispersal, acting as ecological corridors. When the MHI's bottomfish restricted fishing areas (BRFAs) were considered, it was found that these reserves are potentially replenishing depleted fishing areas by larval export, but rely on larval subsidy from the fishing sites to sustain their populations. Thus, the efficiency of the reserve network could be improved by the protection of additional bottomfish habitat, distributed in new or expanded reserves. Finally, dispersal characteristics of yellowfin tuna (*T. albacares*) around the MHI were investigated. The physical environment appeared favorable for retention of yellowfin tuna larvae. However, retention is not the main factor optimizing the spawning season of this species in the archipelago, and other factors, such as favorable water temperature and food availability, are likely contributing to spawning seasonality. The distribution of larvae by the time evolving eddy field was highly variable. Apart from nearshore regions, no additional persistent dispersal pathways or accumulation zones were observed.

# Contents

Acknowledgments. . . . .	iv
Abstract. . . . .	vi
List of Tables. . . . .	x
List of Figures. . . . .	xi
List of Abbreviations and Symbols. . . . .	xvii
<b>1 Introduction. . . . .</b>	<b>1</b>
1.2 Background. . . . .	6
1.2.1 Location and fluid environment. . . . .	6
1.2.2 Biological environment . . . . .	7
1.3 Dissertation Structure . . . . .	9
1.3.1 Physical environment and larval transport. . . . .	9
1.3.2 Larval transport, connectivity and management . . . . .	9
<b>2 Flow variability and its impact on connectivity for the island of Hawai‘i. . . . .</b>	<b>11</b>
2.1 Introduction. . . . .	11
2.1.1 Physical environment of the Hawai‘i Island. . . . .	14
2.2. Material and Methods. . . . .	15
2.2.1 Hydrodynamic model. . . . .	15
2.2.2 Individual-based model . . . . .	17
2.2.3 Finite Size Lyapunov Exponents . . . . .	18
2.3 Results. . . . .	20
2.3.1 Lagrangian Coherent Structures. . . . .	20
2.3.2 Connectivity patterns . . . . .	23
2.4 Discussion. . . . .	25



<b>3 First estimation of larval supply and connectivity of reserves in the Hawaiian Archipelago</b> .....	38
3.1 Introduction .....	38
3.2 Methods .....	40
3.2.1 Hydrodynamic model .....	40
3.2.2 Individual-based model .....	42
3.2.3 Sensitivity Analyses .....	42
3.2.4 Comparison of regional and global HYCOM .....	45
3.2.5 Adaptation to bottomfish species .....	46
3.2.6 Evaluation of potential reserves .....	48
3.3. Results .....	49
3.3.1 Papahānaumokuākea Marine National Monument and Main Hawaiian Islands .....	49
3.3.2 Reserves within the Main Hawaiian Islands .....	51
3.3.3 Potential reserves .....	53
3.4 Discussion .....	54
3.4.1 Connectivity along the archipelago .....	54
3.4.2 Reserves within the Main Hawaiian Islands .....	58
3.4.3 Evaluation of potential reserves .....	59
3.4.4 Future directions .....	61
<b>4 Early life stage dispersal of yellowfin tuna (<i>Thunnus albacares</i>) in the Hawaiian Region</b> .....	79
4.1. Introduction .....	79
4.2 Methodology .....	80
4.2.1 Hydrodynamic model .....	80
4.2.2 Individual-based model .....	81

4.2.3	Adaption to Yellowfin tuna. . . . .	83
4.2.4	Sensitivity analyses. . . . .	83
4.3	Results . . . . .	86
4.4	Discussion . . . . .	88
4.4.1	Patterns of larval retention . . . . .	88
4.4.2	Larval retention and seasonality of spawning. . . . .	90
4.4.3	Onshore-offshore distributions. . . . .	91
<b>5</b>	<b>Conclusions.</b> . . . . .	<b>104</b>
5.1	Future directions . . . . .	107
	<b>Bibliography.</b> . . . . .	<b>108</b>

## List of Tables

3.1	Parameters tested in the sensitivity analyses and their respective values. . . . .	63
3.2	Preferred depth and spawning season for the three deep-water bottomfish species considered in this study. The preferential depth range corresponds to the range where 93% of occurrences for a determined species were registered, based on literature reviews, and Hawai‘i Undersea Research Laboratory (HURL) database ( <a href="http://www.soest.hawaii.edu/HURL/index.html">http://www.soest.hawaii.edu/HURL/index.html</a> ) . . . . .	64
3.3	Area (km <sup>2</sup> ) of essential fish habitat (EFH) available for each reserve and number of released eggs for the scaled experiment. The number of released eggs was based on the habitat area of each reserve. Reserve “O” corresponds to the Kaho‘olawe Island Reserve . . . . .	65
4.1	Table relating the wind velocity (at 10 m) categories and the mortality index applied per day at each one of the 0.2 x 0.2 degree bins. The percentage of larval survival for each mortality index illustrates a hypothetical case where a constant mortality was applied for 30 days.	94

## List of Figures

2.1	Sea surface height (SSH, cm, color) as: (a) measured from a satellite (an average over 7 days centered on 16 July 2009), simulated for 18 July 2009 by (b) the regional HYCOM and (c) the global HYCOM. Vectors indicate the surface geostrophic velocity derived from SSH. . . . .	29
2.2	Long-term mean surface geostrophic velocity (color, m/s) derived from Sea Surface Height (SSH) for (a) satellite measurements, (b) regional HYCOM, and (c) global HYCOM . . . . .	30
2.3	Release (source) and destination (sink) sites around the Hawai‘i Island. Each of the 53 sites has 10 km of diameter and were grouped into 3 areas to facilitate analysis. These areas are indicated by colors in the graph: south (yellow), leeward (blue) and windward (green). . . . .	31
2.4	Attracting Lagrangian Coherent Structures (LCSs, unstable manifolds, $d^{-1}$ ) for surface, 30 and 100 meters, calculated from the (a) regional, and (b) global HYCOM for 18 of July 2009. The velocity field was integrated for 30 days backward in time. . . . .	32
2.5	Distribution of particles, repelling LCSs (stable manifolds, red) and attracting LCSs (unstable manifolds, black) ( $d^{-1}$ ) at 25 of July (a), 30 of July (b), 7 of August (c) and 15 of August (d) 2009 for the regional HYCOM. In this figure, particles were released on 18 of July 2009 and tracked for 7, 12, 20 and 28 days (respectively) at 30 meters. The velocity field was integrated forward (backward) in time for determining the stable (unstable) manifolds. Particles are colored according to the face of the island where they were released . . . . .	33
2.6	Distribution of particles and attracting Lagrangian Coherent Structures (LCSs, unstable manifolds, $d^{-1}$ ) for surface, 30 and 100 meters, at 10 of August 2009 for the regional HYCOM. In this figure, particles were released on 18 of July 2009 and tracked for 23 days. The velocity field was integrated backward in time for determining the unstable manifolds. Particles are colored according to the face of the island where they were released. . . . .	34

2.7	Connectivity matrices for the Hawai‘i Island from June 2009 to May 2010. Particles were released at surface (a,b) and 30 m (c,d) and advected by velocities from the regional (a,c) and global HYCOM (b,d). The probability at each cell (i,j) is given by the number of particles leaving the spawning site i and arriving at the settlement site j, divided by the number of particles leaving the spawning site i and arriving at any settlement site. Therefore, when calculating the probability matrix, only the retained particles were considered . . . . .	35
2.8	Connectivity matrices showing all source/destination sites for the Hawai‘i Island from June 2009 to May 2010. Particles were released at surface (a,b) and 30 m (c,d) and advected by velocities from the regional (a,c) and global HYCOM (b,d). The probability at each cell (i,j) is given by the number of particles leaving the spawning site i and arriving at the settlement site j, divided by the number of particles leaving the spawning site i and arriving at any settlement site. Therefore, when calculating the probability matrix, only the retained particles were considered. . . . .	36
2.9	Connectivity matrices for the Hawai‘i Island for 2009 (a) and 2010 (b) summer (July to September). Particles were released at surface and advected by velocities from the regional HYCOM. The probability at each cell (i,j) is given by the number of particles leaving the spawning site i and arriving at the settlement site j, divided by the number of particles leaving the spawning site i and arriving at any settlement site. Therefore, when calculating the probability matrix, only the retained particles were considered . . . . .	37
3.1	Study Area. The location of the Papahānaumokuākea Marine National Monument (PMNM), Main Hawaiian Islands (MHI) and mean currents are indicated in the map. The background represents the geostrophic zonal velocity from AVISO, averaged from 2004 to 2011. NEC stands for the North Equatorial Current, HLCC for Hawaiian Lee Counter Current, HLC for the Hawaiian Lee Current, and STCC for Subtropical Counter Current. White areas represent release/destination sites at 75 m depth. . . . .	66
3.2	Map of the Main Hawaiian Islands. The polygons are a 14 km wide region around the land contour at 75 m. The bottomfish reserves (BRFAs) are shown in blue, and are named with the letters from A to M. The Kaho‘olawe Island Reserve is also shown in blue, and is indicated with the letter O. The red polygons are the “fishing” sites: zones where bottomfish is found and are open to bottomfish fisheries. . . . .	67

3.3	Local retention and export per island considering different diffusion coefficients. For one year, 100 larvae were released every five days at 75 m and dispersed for 30 days using global HYCOM flow fields. Larvae were actively buoyant and presented ontogenic vertical migration (OVM). The proportion of retained larvae was given as: (number of viable larvae)/(total larvae released) and was based on 72 releases for each diffusion coefficient . . . . .	68
3.4	Local retention and export per island considering larvae advected using velocities from the regional and global HYCOM. For one year, 100 larvae were released every five days at 75 m and dispersed for 30 days using global and regional HYCOM velocities. Larvae were actively buoyant and presented ontogenic vertical migration (OVM). The proportion of retained larvae was given as: (number of viable larvae)/(total larvae released) and was based on 72 releases for each implementation of HYCOM. . . . .	69
3.5	Difference between the connectivity matrices for larvae advected with velocities from the global and regional HYCOM. Positive (negative) values represent higher retention using velocities from the global (regional) HYCOM. This figure shows the probability of transport among all release and destination polygons (see polygons on Figure 2), and it is based on 84 releases for each implementation of HYCOM. For two years, from June to December 100 larvae were released every 5 days at 75 meters depth and dispersed for 30 days. Larvae were actively buoyant and presented ontogenic vertical migration . . . . .	70
3.6	(a) Connectivity matrix for opakapaka ( <i>Pristipomoides filamentosus</i> ) for a pelagic larval duration (PLD) of 30 days, based on 210 releases. (b) Variance of the connectivity matrices calculated considering twelve scenarios: three species, two PLDs and ontogenic vertical migration (OVM) schemes, based on 1920 releases. The shaded areas represent the transport among the Papahānaumokuākea Marine National Monument (PMNM) and the Main Hawaiian Islands (MHI). Black boxes represent zones where larvae released are mostly locally-retained. At (a) the probability at each cell (i,j) is given by the number of particles leaving the spawning site i and arriving at the settlement site j, divided by the number of particles leaving the spawning site i and arriving at any settlement site. Therefore, when calculating the probability matrix, only the retained larvae were considered . . . . .	72

3.7	Limits of the self-contained zones (black boxes). Most of the larvae released at each one of these zones is locally retained. The mean and standard deviation of the probability of local retention is indicated for each group of islands. These values were calculated considering twelve scenarios: three species, two PLDs and ontogenic vertical migration (OVM) schemes, based on 1920 releases. White areas represent release/destination sites at 75 m depth . . . . .	73
3.8	(a) Connectivity matrix for larvae released inside reserves; (b) Destination of viable larvae released inside each reserve; (c) Proportion of larvae received by each reserve. Both proportions and the connectivity matrix are averaged for the three species and for pelagic larval durations (PLD) of 30 and 60 days, based on 384 releases. (a-b) were calculated considering only larvae released inside reserves; (c) considered larvae released (and retained) at fishing sites and reserves. . . . .	74
3.9	Proportion of (a) viable larvae released per spawning site, (b) viable larvae at destination sites, and (c) number of connections. Existing reserves boundaries are shown in black. The 40% of the sites presenting the higher values of viable larvae release, larval retention and number of connections, were defined as the best spawning, destination and most connected sites, respectively. Proportions are based on the total number of viable larvae, not considering larvae dispersed to the ocean. Values were averaged for three species and two pelagic larval durations, based on 384 releases. . . . .	75
3.10	Candidate sites for future reserve designation are shown in red. Existing reserves boundaries are shown in blue. Candidate areas were evaluated on three aspects regarding larval dispersal: i) efficiency as release sites; ii) efficiency as retention sites; iii) connectivity. Indicators of habitat suitability and presence of bottomfish species were also considered (Parke, 2006, Christopher Kelley, <i>personal communication</i> , Hawai‘i Division of Aquatic Resources) . . . . .	76

3.11	Pounds of bottomfish caught per fishery reporting zone of the Hawai‘i Division of Aquatic Resources (HDAR), from 2005 to 2011. Bottomfish reported include the following species: <i>Pristipomoides filamentosus</i> (opakapaka), <i>Etelis carbunculus</i> (ehu), <i>Etelis coruscans</i> (onaga), <i>Epinephelus quernus</i> (hapu‘upu‘u), <i>Pristipomoides sieboldi</i> (kalekale), <i>Aphareus rutilans</i> (lehi), <i>Seriola dumerili</i> (kahala) and <i>Pristipomoides zonatus</i> (gindai). It is important to highlight that prior to 2011 the catch from Middle Bank (northern most squares) could be recorded as part of the Papahānaumokuākea Marine National Monument (PMNM) catch. In 2011, after the closure of the PMNM, 5,750 lbs of bottomfish were recorded as caught in the Middle Bank region, representing most of the catches in the region from 2005 to 2011. . . . .	77
3.12	Location of the Hawai‘i Division of Aquatic Resources (HDAR) fishery reporting zones, indicating the area of bottomfish habitat (m <sup>2</sup> ) per zone. From Parke (2006). . . . .	78
4.1	Spawning locations for yellowfin tuna. Blue areas (hereafter “inshore”) are within 20 nm (37 km) of the 400 m isobath. Pink areas (“offshore”) are from 20 nm to 50 nm (37 to 92 km) of the 400 m isobath. . . . .	95
4.2	Number of eggs released per spawning area, by month of release. Percentage of spawning was based the proportion of mature yellowfin tuna in spawning condition captured per month from 1994 to 1996, as described on Itano (2000). The classification of mature females in fully yolked, atretic and spawning conditions was defined by the histological interpretation of preserved ovarian material (c.f. Itano, 2000). . . . .	96
4.3	Average of proportion of larvae found within 20 nm (37 km, blue lines) and from 20 nm to 50 nm (37 to 92 km, pink line) of the Hawaiian Islands, by dispersal days. Lines show the proportion of retention from different mortality schemes, based on 100 simulations each. Larvae were released every 5 days during the yellowfin tuna spawning season for 2011. . . . .	97
4.4	Average of proportion of larvae found within 20 nm (37 km, blue lines) and from 20 nm to 50 nm (37 to 92 km, pink line) of the Hawaiian Islands, by dispersal days. Lines show the proportion of retention from different vertical migration schemes, based on 100 simulations each. Larvae were released every 5 days during the yellowfin tuna spawning season from 2009 to 2011. . . . .	98



4.5	Average of the monthly probability distribution functions (PDFs) of larval distributions at 26 days of dispersal. Individual PDFs are given by the number of larvae found in each 0.2 x 0.2 degree bins at 26 days of dispersal, divided by the area (km <sup>2</sup> ) of the bins. Monthly PDFs were averaged for the yellowfin tuna spawning season from 2009 to 2011. . . . .	99
4.6	Trajectories of larvae dispersed for 30 days by the regional HYCOM flow fields averaged from 2009 to 2011. Colors are used to highlight dispersal from different areas. . . . .	100
4.7	Monthly average and standard deviations of the proportion of yellowfin tuna larvae found within: (a) 20 nm (37 km) and (b) from 20nm to 50 nm (37 to 92 km) off the Hawaiian Islands; based on 100 simulations. Larvae were released every 5 days during the yellowfin tuna spawning season from 2009 to 2011. . . . .	101
4.8	Average of the proportion of larvae found within 20 nm of the Hawaiian Islands, evolving with dispersal days, released at (a) inshore and (b) offshore spawning sites. Lines show the proportion of retention for larvae released at different sites, based on 100 simulations each. Larvae were released every 5 days during the yellowfin tuna spawning season from 2009 to 2011. . . . .	102
4.9	Mean (black) and standard deviations (red) of the monthly onshore-offshore dispersal kernels of (a) hatching eggs (1 day of dispersal), (b) feeding larvae (6 days of dispersal), (c) post-flexion larvae transitioning to piscivory (16 days of dispersal), (d) transitional juvenile (26 days of dispersal). Mean and standard deviations are based on 100 simulations, during the spawning season of yellowfin tuna from 2009 to 2011. The dispersal kernels are based on the number of larvae within 90 km of the Hawaiian Islands, not considered dispersion to the open ocean. Larval stages were based on Margulies <i>et al.</i> (2007), Wexler <i>et al.</i> (2011) and Jeanne Wexler ( <i>personal communication</i> ) . . . . .	103

## List of Abbreviations and Symbols

BRFA	Bottomfish restricted fishing areas
BOLTS	Biophysical Lagrangian Transport System
CMS	Connectivity modeling system
EFH	Essential fish habitat
EKE	Eddy kinetic energy ( $m^2s^{-2}$ )
FADS	Feeding aggregating devices
FSLE	Finite size Lyapunov exponent
HDAR	Hawai‘i Division of Aquatic Resources
HLC	Hawaiian Lee Current
HLCC	Hawai‘i Lee Counter Current
HURL	Hawai‘i Undersea Research Laboratory
HYCOM	HYbrid Coordinate Ocean Model
IBM	Individual-based model
LCS	Lagrangian Coherent Structure
MHI	Main Hawaiian Islands
MPA	Marine protected area
NEC	North Equatorial Current
NHRC	North Hawaiian Ridge Current
NWHI	Northwestern Hawaiian Islands
OVM	Ontogenic vertical migration
PDF	Probability density function
PLD	Pelagic larval duration
PMNM	Papahānaumokuākea Marine National Monument
PV	Potential vorticity
STCC	Subtropical Counter Current
SSH	Sea surface height
SST	Sea surface temperature
$\zeta$	Relative vorticity
$f$	Coriolis parameter ( $s^{-1}$ )
$\lambda$	Finite size Lyapunov exponent ( $days^{-1}$ )
$\kappa$	diffusivity parameter ( $m^2/s$ )

# Chapter 1

## Introduction

This dissertation concerns the study of biological-physical interactions. This is an interdisciplinary area of research, where many questions remain without answer (Sammarco and Leon, 1994, Mann and Lazier, 2006). One of these unanswered questions concerns the processes shaping the fate of the early phases of marine organisms. Most species of marine organisms present a pelagic planktonic phase, during which they are small and have limited locomotion capabilities. While their dispersal to nursery grounds or other suitable areas is essential for their survival and successful recruitment, their transport is highly influenced by physical processes occurring across a broad range of spatio-temporal scales (Okubo, 1994, Cowen *et al.*, 2007). Therefore, a persistent challenge to understanding larval survival is a better comprehension of their dispersal pathways. Almost a century ago, the pioneering work of Hjort (1914) showed the major role currents play in the and recruitment of larvae. Today, we know that the physical processes underlying larval transport have a great impact on population dynamics. The occurrence of appropriate circulation patterns to transport and retain larvae, that are necessary for their survival, can influence fish spawning strategies and recruitment (Sinclair, 1988, Bakun and Parrish, 1991, Hugget *et al.*, 2003, Karnauskas *et al.*, 2011). At the same time, larval dispersal influences how different populations are connected, with effects on their genetics and demographics (Cushing, 1988, Paris *et al.*, 2007, Kool

*et al.*, 2009). Thus, the knowledge of larval dispersal pathways, physical mechanisms of transport, and connectivity is essential not only to understand the survival of specific cohorts of larvae, but also to comprehend the ecology of marine populations (Cushing, 1988). Further, larval dispersal has scientific, social, economic and ecological implications and it is vital information in the designation of management measures for the conservation of marine populations (Fogarty and Botsford, 2007, Gaines *et al.*, 2007).

The world's oceans have suffered rapid degradation in the past decades through a combination of pollution, destruction of coastal environments, and overexploitation of marine resources, resulting in a loss of diversity and biomass. Within this scenario, measures have been taken to protect and rebuild marine populations, including implementation of catch quotas, fishing gear regulations, and the establishment of marine reserves. Marine reserves are areas where some or all extractive activities are prohibited. One of the benefits of reserves is to protect breeding stocks composed of older and larger individuals, which produce higher quality eggs in greater numbers when compared to younger fish of the same species (Man *et al.*, 1995, Berkeley *et al.*, 2004). Those eggs and larvae can be dispersed over large distances, enhancing populations outside reserve boundaries (Lubchenco *et al.*, 2003, Pelc *et al.*, 2010, Christie *et al.*, 2011, Di Franco *et al.*, 2012, Harrison *et al.*, 2012). Therefore, larval dispersal from reserves may help replenish fishery resources and connect populations in different reserves. Thus, it is important to understand larval dispersal pathways in order to design efficient reserves with the objective of conservation and replenishment of fisheries populations. Surprisingly, despite the conspicuous role of larval drift in promoting the expected

benefits of a reserve network, this information is scarce and rarely taken into account in the designation process (Gaines *et al.*, 2003, Gerber *et al.*, 2003).

Empirical studies accounting for larval dispersal are almost nonexistent. They are prohibitively expensive due to the small size of eggs and larvae, and their low density in the environment (Paris and Cowen, 2004). As a consequence, modeling techniques have been developed to indirectly evaluate larval dispersal and population connectivity. Such models can generate dispersal characteristics not yet available from *in situ* studies. In the following chapters, I used two versions of a biological modeling system (Paris *et al.*, 2007, Paris *et al.*, submitted) that are Lagrangian<sup>1</sup> implementations of an Individual-based model (IBM). IBMs treat “*individuals as unique, discrete entities,*” (Grimm *et al.*, 1999) with their own attributes such as position, age and behavior, which vary in time and space, and are influenced by environmental conditions. Given that processes determining larval dispersal and survival have a distinct effect on each individual organism, those models are an excellent framework for studying these processes (Crowder *et al.*, 1992, Paris *et al.*, 2007). The IBM used here accounts for physical-biological interactions in fish early life history and is designed to estimate population connectivity, defined as the probability of exchange of individuals between distinct populations (Cowen *et al.*, 2007). It is important to mention that this dissertation focuses on the connectivity driven by the transport of early life stages, and does not consider exchanges driven by the migration of adults.

---

<sup>1</sup> Lagrangian methods define flow characteristics by following the evolution of marked fluid parcels as a function of time.

In the following chapters, this IBM is applied to study the dispersal patterns of distinct species: a pelagic fish, the yellowfin tuna (*Thunnus albacares*), and three bottomfishes: onaga (*Etelis coruscans*), ehu (*Etelis carbunculus*), and opakapaka (*Pristipomoides filamentosus*). In all cases, the understanding of their early life stage dispersal has direct applications for fisheries management. Biophysical modeling techniques are necessary to answer questions related to population connectivity, identification of breaks, quantification of transport and retention (Cowen *et al.*, 2006, Baums *et al.*, 2006, Almany *et al.*, 2009). Yet, we also need to understand underlying mechanisms of larval transport, represented by physical oceanographic features. The occurrence of diffusion, mixing, instabilities, and the presence of coherent structures, condition transport in the ocean at specific scales, affecting connectivity and larval transport. To provide insight and understanding regarding the connectivity, Lagrangian techniques were applied to locate the Lagrangian Coherent Structures (LCSs) in the flow, identify recurrent physical features, and show how they related to larval dispersion (d'Ovidio *et al.*, 2008, Beron-Vera *et al.*, 2008, Olascoaga *et al.*, 2008, Haller and Yuan, 2000).

Recent studies concluded that the yellowfin tuna caught in Hawai'i's inshore fisheries are locally spawned, which contradicts the prevailing view that all tuna are highly migratory (Siebert and Hampton, 2003, Schaefer *et al.*, 2007, Wells *et al.*, 2011). However, questions regarding the origin of the tuna fished and the degree of dispersal at early life stages still remain unanswered. Yellowfin tuna also show a clear seasonal spawning cycle in the Hawaiian Islands (Itano, 2000). It is unknown if the optimization

of the spawning is related to larval retention. To answer those questions, the dispersal kernels and local retention were estimated, providing supplemental information on the origin of yellowfin tuna available to Hawai'i fisheries. The seasonal larval retention patterns were also estimated, in order to investigate their influence on the spawning strategy of yellowfin tuna. The main motivation to study bottomfish connectivity was the redesign of the Bottomfish Restricted Fishing Areas (BRFAs), a type of marine reserve throughout the Main Hawaiian Islands (MHI). Those reserves were implemented with a specific objective: to help rebuild the stocks of selected bottomfish species. The designation process took into account the best available information about their populations. However, little is known of their connectivity and larval transport. To understand the effectiveness of the BRFAs in rebuilding populations and replenishing fishery's stocks, bottomfish connectivity in the entire Hawaiian Archipelago and between reserves was estimated.

Fisheries activities are an essential part of life in the Hawaiian Islands. For centuries, islanders have been closely tied to the ocean for subsistence and recreation, and the consumption of seafood is an integral part of local culture (Pooley, 1987, Lowe, 2004, Spalding, 2010). Before foreign interventions in the late eighteenth century, Native Hawaiians lived a system of *malama i ka 'aina, malama i ke kai, a malama i kou kino* ("take care of the land, take care of the sea, [as you would] take care of your own body") (Lowe, 2004). Rigid *kapus* (sacred rules/prohibitions) governed fishing activities to ensure sustainability. Moreover, knowledge, respect and appreciation of the ocean and its resources were transmitted generationally, ensuring its stewardship. I hope this

dissertation is a modest contribution to the understanding of the fish populations inhabiting Hawaiian waters, and to their protection and continuity for centuries to come.

## **1.2 Background**

### **1.2.1 Location and fluid environment**

The Hawaiian Ridge is in the center of the North Pacific Subtropical Gyre. The “Main Hawaiian Islands” (MHI), those between the Island of Hawai‘i and Kaua‘i, are the most populated islands. They include Hawai‘i, Maui, Moloka‘i, Lana‘i, Kaho‘olawe, O‘ahu, and Kaua‘i. Northwest of Kaua‘i are the Northwestern Hawaiian Islands (NWHI), a chain of small islands, atolls and shoals that stretches for more than 2000 km (Figure 3.1). The NWHI were proclaimed the Papahānaumokuākea Marine National Monument (PMNM) in 2006 (Presidential Proclamation 8031, 2006) and by 2009 all commercial fishing in the region was prohibited. The regional circulation is controlled by both local and remote forcing, particularly the westward flowing North Equatorial Current (NEC) and the wind field which, locally, is affected by the presence of the main islands. Flow in the study area has a high spatial and temporal variability that is the result of variations in the wind forcing and intrinsic instabilities of the oceanic flow (Lumpkin, 1998, Flament *et al.*, 2001, Calil *et al.*, 2008). The region is one of high variability, as confirmed by the high mean Eddy Kinetic Energy ( $EKE = \langle u'^2 \rangle + \langle v'^2 \rangle$ ) calculated from sea surface height (SSH) anomaly (see Figure 2 of Calil *et al.*, 2008). Such variability changes larval dispersal patterns and must be adequately understood. The characteristics of wind flow interacting with the islands' orography are complex. The obstruction of trade winds by



high mountains on Maui and Hawai‘i is the major forcing mechanism for vigorous eddies found on the leeward side of the islands (Lumpkin, 1998, Jia *et al.*, 2011). Both anticyclonic and cyclonic eddies are observed in the area and while cyclonic eddies tend to propagate to the northwest, anticyclonic ones primarily propagate west-southwest, and their signal can be detected more than 4000 km west of Hawai‘i (Mitchum, 1995). Therefore, the major issues investigated here are: i) how the varying eddy field influence dispersal kernels and connectivity patterns? and ii) what mechanisms play a role in the transport and retention of larvae?

### **1.2.2 Biological environment**

Genetic analyses of numerous species in the Hawaiian region point to the presence of shared population breaks along the island chain (Toonen *et al.*, 2011). These breaks are observed through a large range of taxa, including but not limited to gastropods, echinoderms, arthropods and fish (Bird *et al.*, 2007, Eble *et al.*, 2009, Rivera *et al.*, 2011, Toonen *et al.*, 2011). Considering that many species are sedentary or show limited adult movement, these breaks can potentially be related to the characteristics of the dispersal during their early life stages. Despite the fact that these species present distinct biological traits such as reproduction strategies, larval mobility and pelagic larval duration, the location of their population breaks are often concordant, indicating that such breaks are likely defined by circulation features.

Connectivity in highly fragmented environments, such as in oceanic islands, relies on mechanisms different from those typically employed in coastal environments (Paris *et*

*al.*, 2002, Paris *et al.*, 2008, Munday *et al.*, 2009). Since the 1970's, eddies have been regarded as the mechanism responsible for enhancing nearshore larval retention in oceanic islands, thereby increasing the chances of larval survival. It was suggested that coral reef fish developed spawning strategies that benefit from this retention mechanism, spawning in eddies close to the islands' coasts (Sale, 1970, Johannes, 1978). Whether eddies influence larval retention is still a matter of debate in the Hawaiian region (Boehlert and Mundy, 1994, Walsh, 1987, Lobel, 1989, Lobel and Robinson, 1986). Pioneering studies applied modeling techniques to address questions related to larval transport and population connectivity in the Hawaiian Islands (Polovina *et al.*, 1999, Kobayashi, 2006, Kobayashi and Polovina, 2006, Rivera *et al.*, 2011), bringing new insights about larval drift dynamics, and showing the potential of modeling techniques to increase our understanding of connectivity in the study area. However, those studies could not capture patterns observed in the population genetics of marine organisms (Toonen *et al.*, 2011), resulting in several unanswered questions. This research focuses on some of those questions, specifically i) how do uncertainties in the hydrodynamic model implementations can change the simulated connectivity patterns? ii) how do biological traits influence larval dispersal? iii) how do the local flow regime within BRFA's influences the amount of viable larvae spawned inside the reserves and the intensity of larval fluxes to other reserves and fishing sites? and iv) are the frequency and intensity of yellowfin tuna spawning related to larval retention patterns?

### **1.3 Dissertation Structure**

The overarching goal of this research is to provide the scientific knowledge necessary to improve the designation process of fisheries management regulations in the Hawaiian region, by understanding the pathways of larval dispersal. The specific goal of this dissertation is twofold: i) to gain knowledge about population connectivity in the Hawaiian region and ii) to determine the impact of the flow on larval dispersion characteristics around Hawai‘i.

#### **1.3.1 Physical environment and larval transport**

Chapter 2 explores how the variable eddying field influences dispersal kernels and connectivity patterns. Particle dispersion was determined by using an IBM and the flow fields derived from global and regional implementations of an ocean circulation model. In order to understand the underlying physical processes of transport, coherent structures were located in the flow field by the calculation of the Finite Size Lyapunov Exponents. Recurrent physical features were identified, and it was observed how particle transport is related to them. In addition, it was determined how different hydrodynamic model implementations affect estimates of transport at a local scale.

#### **1.3.2. Larval transport, connectivity and management**

Chapter 3 examines the connectivity of selected bottomfish species driven by the transport of early life stages. A range of biological traits were implemented in the biological model to test their effect on larval dispersal, and in shaping the demographics

of bottomfish populations. The connectivity was estimated between the MHI and the PMNM, driven by the transport of early life stages. In addition, breaks for larval transport at ecological time scales were identified, and compared to demographic information available for bottomfish species. Finally, this information was linked to fisheries management issues. Two addressed key questions regarding the location of the reserves were: i) are the reserves efficient in supporting populations through larval retention and connectivity? Thus, how much of the larvae released at a reserve will be locally retained or exported to another protected site was assessed and; ii) are the reserves potentially effective at replenishing fisheries resources through larval dispersal? This question was addressed by estimating the larval export from BRFA's to fishery sites. These questions are typically asked when evaluating the efficiency of a reserve network to rebuild fish stocks and sustain their own populations via larval production and dispersal (Hastings and Botsford, 2003, Leis, 2006, Pelc *et al.*, 2010).

Chapter 4 explores the larval dispersal patterns of a pelagic species, the yellowfin tuna (*Thunnus albacares*). How different biological traits would affect yellowfin tuna larvae retention around the Hawaiian Islands was tested. It was also evaluated whether larvae spawned around the Hawaiian Islands are locally retained, their retention seasonality and what spawning sites produce higher amounts of viable larvae. Finally, the onshore-offshore larval distributions were estimated and its significance for yellowfin tuna larval survival was explored.

## Chapter 2

### Flow variability and its impact on connectivity for the island of Hawai'i

#### 2.1. Introduction

One of the most important and exciting contemporary areas of research in marine ecology is the characterization of population connectivity (Cowen *et al.*, 2006, Cowen *et al.*, 2007, Paris, 2010). The connectivity of populations has ecological, economic, and management implications (Fogarty and Botsford, 2006, Gaines *et al.*, 2007, Steneck *et al.*, 2009). Connectivity patterns of marine organisms with a pelagic early life stage are shaped by a complex combination of biological traits and flow characteristics (Paris *et al.*, 2007, Werner *et al.*, 2007, Cowen and Sponaugle, 2009). This study focused on the latter, and its objective was twofold: i) investigate how the variability of the physical environment affects transport patterns and ii) identify mechanisms that play a role in the transport and retention of larvae. Our study site was the island of Hawai'i, part of the Hawaiian Ridge located in the center of the North Pacific Subtropical Gyre (Figure 2.1a). The oceanic flow around the island is dominated by an energetic field of mesoscale eddies, both locally and remotely generated (Lumpkin and Flament, 2001, Calil *et al.*, 2008, Jia *et al.*, 2011). Particularly important factors for the regional circulation are the westward flowing North Equatorial Current (NEC, Figure 2.2a) and the wind field, locally affected by the presence of the main islands.

Connectivity in oceanic islands relies on mechanisms different from those typically acting on coastal environments (Paris *et al.*, 2002, Munday *et al.*, 2009). Since the 1970s, eddies have been regarded as the mechanism responsible for enhancing nearshore larval retention around oceanic islands, thereby increasing the chances of larval survival. It has been suggested that coral reef fish have developed spawning strategies that benefit from this retention mechanism; spawning in eddies close to the islands' coasts (Sale, 1970, Johannes, 1978). Available evidence from *in situ* larval sampling, drifters, recruitment studies, and genetic parentage analyses indicated that eddies influence larval retention in the Hawaiian region (Lobel and Robinson, 1986, Walsh, 1987, Lobel and Robinson, 1988, Lobel, 1989, Boehlert and Mundy, 1994, Christie *et al.*, 2010). However, due to limitations of sampling methodologies, these studies were restricted to small temporal and spatial scales. Thus, the net effect of the eddy field on larval transport and connectivity is still unknown. The lack of adequate tools to account for larval dispersal is not a problem unique to the study region. Due to the small size of larvae and relative scarcity in the environment, *in situ* studies accounting for their dispersal remain prohibitively expensive, making data extremely rare (Paris and Cowen, 2004). Numerical modeling techniques have been developed to indirectly evaluate larval dispersal, population connectivity, and generate dispersal characteristics not yet available from empirical data (Botsford *et al.*, 2009). Biophysical models have been particularly useful in answering questions related to population connectivity (Cowen *et al.*, 2006), identification of breaks (Baums *et al.*, 2006), and quantification of transport and retention (Almany *et al.*, 2009). Moreover, biophysical models are useful to identify the underlying

physical mechanisms that provide transport pathways used by vertically migrating larvae (Paris and Cowen, 2004, Ayata *et al.*, 2010). These pathways result from coherent structures in the time evolving turbulent flow that are typically characterized by Lagrangian methods and emerge as regions in the fluid where tracer dynamics are largely distinct from their neighboring regions (Haller and Yuan, 2000). In an evolving two-dimensional flow, Lagrangian Coherent Structures (LCSs) can be characterized as material fluid lines. Of particular interest are those material lines that represent regions of rapid divergence and convergence in the flow; stable and unstable manifolds, respectively (Haller and Yuan, 2000, d'Ovidio *et al.*, 2008, Olascoaga *et al.*, 2008). Attracting LCSs (unstable manifolds) act as attractors of particles, and also as barriers to transport in the cross LCS direction (Lehan *et al.*, 2007, Calil and Richards, 2010, Rypina *et al.*, 2010). On the other hand, trajectories tend to be repelled from stable manifolds, thus also known as repelling LCSs. Therefore, the identification of LCSs provides a powerful aid to the determination of transport processes affecting larval transport and dispersal.

Here we determined particle dispersion by using an individual-based model (IBM, Paris *et al.*, 2007 for description), and the flow fields derived from a regional implementation of the HYbrid Coordinate Ocean Model (HYCOM, Jia *et al.*, 2011). To understand the underlying physical processes of transport, we located the LCSs in the flow field by calculating the Finite Size Lyapunov Exponents (FSLEs, Haller and Yuan, 2000), identified recurrent features, and observed how particle transport is related to them. Moreover, we compared how a different implementation of HYCOM (Global HYCOM, c.f. Material and Methods) changed the dispersal patterns. Both models

reproduced the eddy field (Figure 2.1), however eddies were strongly reproduced in the regional HYCOM and weakly imprinted in the global HYCOM. Dissimilarities between the two models hold true when considering longer periods of time (Figure 2.2), and arose from differences in their implementations (Jia *et al.*, 2011). Specifically, we aimed to understand if changes in the physical environment, including those due to changes in the hydrodynamic models, affected dispersal patterns. Further, we investigated the influence exerted by eddies in the transport of particles.

### **2.1.1 Physical environment of the Hawai‘i Island**

The presence of vigorous eddies, whose existence has been described since the 1960’s, remains one of the most remarkable circulation features around Hawai‘i Island (Patzert, 1969, Wyrski, 1982). An understanding of their dynamics and impacts on biogeochemical properties of the environment has improved in the last 15 years (Lumpkin, 1998, Calil *et al.*, 2008, Dickey *et al.*, 2008, Rii *et al.*, 2008, Jia *et al.*, 2011) through a combination of improved datasets and numerical modeling. High Eddy Kinetic Energy (EKE) values were observed in the leeward of the Hawai‘i Island as a consequence of this eddy field, where both cyclonic and anticyclonic eddies occur (Calil *et al.*, 2008, Jia *et al.*, 2011). The major forcing mechanism of this eddy field is the deviation of the northeasterly trade winds by the high mountains located on Maui and Hawai‘i (Haleakalā and Mauna Kea, respectively). The deviation of the winds create a wake in the atmosphere in the leeward of the Hawai‘i Island, which results in the input of vorticity in the ocean by the associated curl of the wind-stress (Qiu *et al.*, 1997, Lumpkin,



1998, Qiu and Durland, 2002, Calil *et al.*, 2008, Jia *et al.*, 2011). This is also the major forcing mechanism of the Hawai‘i Lee Counter Current (HLCC, Figure 2.2a), a narrow eastward current, located between the opposite circulation eddy fields, around 19°N to 20°N (Xie *et al.*, 2001, Qiu and Durland, 2002, Jia *et al.*, 2011). On the east side of the Hawai‘i Island, the North Hawaiian Ridge Current (NHRC, Figure 2.2a), flows mainly northwestward along the Hawaiian Ridge. The NHRC is a weak feature, presenting periodic absence or reversal of flow (Firing *et al.*, 1999). This current originates when the interior ocean flow, generally directed westward in the region, bifurcates when meeting the Hawaiian ridge and acts as a western boundary current (Qiu *et al.*, 1997). The southern branch of the bifurcation joins the westward flowing North Equatorial Current (NEC), to the south of the Hawai‘i island.

## **2.2 Material and Methods**

### **2.2.1 Hydrodynamic model**

This study used the hydrodynamic model HYCOM (Bleck, 2002). A global ocean prediction system based on HYCOM (referred here as “global HYCOM”) provides hindcast analysis (from 2003), by assimilating remotely sensed and *in situ* ocean observations, such as sea surface height (SSH) and sea surface temperature (SST), using the Navy Coupled Ocean Data Assimilation (NCODA) system (Chassignet *et al.*, 2007, Cummings, 2005). The global HYCOM’s horizontal resolution is 0.08°, approximately 8.3 km in the Hawai‘i region. In the vertical, it has 32 layers. The bathymetry is based on the Smith and Sandwell database ([http://www7320.nrlssc.navy.mil/DBDB2\\_WWW/](http://www7320.nrlssc.navy.mil/DBDB2_WWW/)).

The surface winds and thermal fluxes are from the Navy Operational Global Atmospheric Prediction System (NOGAPS, [http://www.nrlmry.navy.mil/metoc/nogaps/nogaps\\_char.html](http://www.nrlmry.navy.mil/metoc/nogaps/nogaps_char.html)) at a resolution of  $0.5^\circ$ . The Hawai'i regional HYCOM ("regional HYCOM" hereafter) is configured in a nested subdomain covering the Main Hawaiian Islands (MHI,  $16\text{-}26^\circ\text{N}$ ,  $150\text{-}166^\circ\text{W}$ ) within the global HYCOM, which supplies model fields for initialization and at the four open lateral boundaries. It has 32 vertical layers as in the global HYCOM, and a horizontal resolution of  $0.04^\circ$  ( $\sim 4$  km). Away from the lateral boundary zones where open boundary conditions are applied, the bathymetry was replaced by the General Bathymetric Chart of the Oceans database (GEBCO,  $1/60^\circ$ , <http://www.gebco.net/>) which captures the regional relief features providing an improved representation of the islands' coastlines. The regional HYCOM is forced at the surface with output from a regional atmospheric model, the Weather Research Forecasting system (WRF, <http://www.soest.hawaii.edu/MET/Faculty/wrf/arw/index.html>), with a resolution of  $0.06^\circ$ . No data assimilation is applied in the regional HYCOM (c.f. Jia *et al.* 2011). The regional current system, including the North Equatorial Current (NEC), the Hawai'i Lee Counter Current (HLCC), the Hawai'i Lee Current (HLC) and the North Hawai'i Ridge Current (NHRC), were well represented in the regional HYCOM (Figure 2.2). East of the island, model solutions differed from observations significantly. Of particular note was the strong southeastward flow along the northeast facing shore of the island in the global HYCOM, which appeared to be a persistent feature, as reflected in the time-averaged flow field (Figure 2.2c). Such a flow did not exist in observations (Figure 2.2a) or in the regional HYCOM solution (Figure 2.2b).

### 2.2.2 Individual-based model

An IBM (c.f. Paris *et al.*, 2007) was used to address larval transport and connectivity questions. The particle displacement was given by both deterministic and turbulent velocities. The deterministic movement was simulated by a fourth order Runge-Kutta integration scheme of the simulated velocity field. The turbulence was modeled by simple diffusion (Paris *et al.*, 2007) using a horizontal coefficient of diffusivity of  $0.2 \text{ m}^2/\text{s}$  estimated from Okubo (1971). In this study, 100 particles were released every five days from May 2009 to October 2010, and dispersed for 30 days at six depth levels: 0, 10, 30, 50, 100 and 200 meters. Those depths were chosen because of their importance for the dispersal of several species of larvae, which are the focus of the next chapters. The number of larvae and interval of release were defined after sensitivity analyses of the IBM (following North *et al.*, 2009). No vertical behavior was implemented, so particles acted as 2D passive particles. Despite the lack of vertical behavior, other larval traits were assimilated to the particles, such as a plastic pelagic larval duration<sup>2</sup> (PLD), and a mortality rate to account to differences in the recruitment due to the decline in abundance over the competency period (Paris *et al.*, 2007). Particles older than 20 days found within the limits of retention sites were considered retained, and removed from the simulation. This 20 day period simulates the start of the transition period of the particles. The mortality coefficient used was  $0.83 \times 10^{-3} \text{ day}^{-1}$ , calculated so the e-folding time scale of the particles was equal to their dispersal time. The release and retention sites were the 10 km wide region around the island of Hawai‘i, subdivided into 53 polygons with 10 km of

---

<sup>2</sup> Pelagic larval duration plasticity represents the ability of the organisms to settle or transition to juvenile stages at variable periods of time

diameter (Figure 2.3). The polygons were grouped according to the face of the island where they are located: south, leeward (west side) and windward (east side). Here, larval (particle) connectivity and other quantities, such as theoretical larval transport, dispersal, local retention and export were calculated following Paris *et al.*(2007), Cowen *et al.* (2007) and Botsford *et al.* (2009). Local retention (c.f. Paris and Cowen, 2004) was the fraction of particles settling at the site where they were released. The connectivity patterns were represented by a matrix of probabilities, where the rows were the release (spawning) site, or source polygon  $i$ , and the columns were the particles final destination, or sink polygon  $j$  (Paris *et al.*, 2007). The content of each matrix cell element represented the probability of particles leaving the spawning site and arriving at a settlement site, while the cell elements  $i=j$  represented the probability of local retention. The probability at each cell  $(i,j)$  was given by the number of particles leaving spawning site  $i$  and arriving at settlement site  $j$ , divided by the number of particles leaving spawning site  $i$  and arriving at any settlement site. Therefore, when calculating the probability matrix, only the retained particles were considered in the analyses. For the period of the experiment, from 10 to 30% of the released particles were retained.

### **2.2.3 Finite Size Lyapunov Exponents**

To provide insight and understanding of connectivity, LCSs in the flow were identified and related to dispersion characteristics. Locations of unstable and stable manifolds were estimated by computing the FSLEs (Artale *et al.*, 1997, Aurell *et al.*, 1997). To calculate the FSLEs, the drift of pairs of particles was simulated by tracking the

positions of the particles in a given velocity field (d'Ovidio *et al.*, 2004). The FSLEs,  $\lambda$ , are given by  $\lambda = \log(d_f/d_0)/\tau$ , where  $\tau$  is the time taken by two particles, initially separated by a distance  $d_0$ , to reach a final distance  $d_f$ . High values of the FSLEs, computed by integrating the particle trajectories forward (backward) in time, identify the repelling (attracting) LCSs. Therefore strongly positive values of  $\lambda$  represent areas of high divergence for particle trajectories while negative values of  $\lambda$  represent areas to which particle trajectories converge. The methodology to compute the LCSs used a 2D flow field. Results were calculated taking  $d_0=1$  km and  $d_f=60$  km, which is approximately the first mode of the baroclinic Rossby Radius in the region (Chelton *et al.*, 1998). The forward and backward FSLEs were calculated every day from June 2009 to March 2010, for 0, 10, 30, 50, 100 and 200 meters, using output from both the global and the regional HYCOM. The period of integration was 30 days, which was the same period of larval dispersal. To observe the flow variation and its relation to the particle transport, we plotted and analyzed the FSLEs and particle positions for all aforementioned depths from June 2009 to March 2010. Recurrent features, and how particle transport related to them were identified. This chapter presents LCSs obtained using only the regional HYCOM flow field. The velocity field from the global HYCOM produced sparse and weak LCSs (Figure 2.4), most likely due to the discontinuity in the eddying flow field through the application of data assimilation, therefore this method cannot be used with the global HYCOM for the time scale of interest to this work.

## 2.3 Results

### 2.3.1 Lagrangian Coherent Structures

To exemplify the highly dynamic and complex nature of the flow we considered particles released at 30 m depth on July 18, 2009 (Figure 2.5) advected using the regional HYCOM flow field. In the following figures, the attracting LCS are the ridges where  $\lambda$  reaches negative values, representing lines of compression on the flow (Joseph and Legras, 2002). The repelling LCS were therefore the regions with positive values of  $\lambda$ , representing lines of strong stretching and stirring in the flow (d'Ovidio *et al.*, 2004). Typical values for the FSLEs ranged from 0.14 to 1 days<sup>-1</sup>, representing mixing times for mesoscale distances of 4 to 28 days. The longer mixing times were bounded by the time of integration of the velocity field for the calculation of the FSLEs (30 days). The maximum values of  $\lambda$  plotted for both attracting and repelling LCSs, -0.5 and 0.5 days<sup>-1</sup>, respectively, represented more than 99% of all  $\lambda$  values (different from 0) for the study region.

The attractive nature of the unstable manifolds was evident (see Video 2.1 for the evolution of the unstable manifolds and particle trajectories). At the time of release the flow in the northern tip of the island was dominated by a vortex dipole to the west of Maui and Hawai'i (Figure 2.1b). Seven days after particle release, LCSs are wrapped up by the vortex dipole with a strong unstable manifold leading back to the northern tip of the island (Figure 2.5a, dipole formed by vortex A3 and C). The position of this structure was such that particles from the leeward side of the island (blue points) were attracted onto the unstable manifold and subsequently advected around the cyclonic vortex C,

which by day 28 was centered at 19.5°N, 158°W, well away from the island (Figure 2.5d). At this time, particles originating from the south side of the island (yellow) that had traveled around the southern tip were starting to be entrained by the vortex.

At the southern tip of the island, there was also a strong unstable manifold at the time of particle release, which was associated with a strong anticyclonic vortex shed a few days earlier (Video 2.1). Particles released from both the leeward and southern sides were captured by the attracting structure. As the anticyclonic eddy moved westward (seen in the SW corner of Figure 2.1a), the strong stretching by two smaller anticyclonic eddies (A1 and A2, Figure 2.5a and Figure 2.5b) disrupted the original LCS, creating a new unstable manifold (seen in Figure 2.5b oriented approximately north/south). Particles were then attached to this new feature. In addition, this unstable manifold was intersected by a stable manifold (at 18.4°N, 156.2°W, Figure 2.5a: a hyperbolic point). The presence of the stable manifold split the particles with a mix of leeward and southern released particles heading south and predominantly leeward particles heading north (Figures 2.5a and 2.5b). The latter particles were entrained by the northern anticyclonic eddy (A1, Figures 2.5b). This anticyclonic eddy (A1) remained off the leeward shore for more than two weeks. By August 6 (Figure 2.5c) a number of particles from the southern and windward regions had also been entrained by the outer rings of the vortex. On August 14, 28 days after release, the evolving eddying flow had created a colorful mosaic of particles in the lee of the Hawai‘i Island (Figure 2.5d).

The transport and dispersion of particles were also affected by rather subtle changes in the LCSs. To illustrate, the unstable manifolds and position of particles

released at the same time at different depths were compared (Figure 2.6). The strength of the LCSs varied with depth, although similar features were discernible at all levels. The unstable manifold emanating from the northern tip, at 100 m depth, captured particles predominantly from the windward side (green), rather than leeward (blue) particles, as was the case at 30 m depth. The less distinct feature at the surface failed to capture any particles. Similarly, the anticyclonic vortex A3, centered at 19°N, 156.8°W, entrained windward (green) particles at its outer rings only at 30 m depth (Figure 2.5d, Figure 2.6). The origin of the particles and the number of particles retained differed among depths. For this example (Figure 2.6), the position of the particles relative to the core of the vortex was one of the factors influencing the number of particles reaching leeward receiving sites. At 30 m depth, the particles were closer to the center of the anticyclonic eddy located on the leeward coast, and 3% of the particles released on July 18 reached leeward sites during their competency period (define here as 20 to 30 days). In contrast, at 100 m depth the particles were located mainly in the vortex outer rings and 7% of the released particles reached the leeward coast, because they were recirculated close to shore.

The pattern of particle transport (such as that shown in Figure 2.5) was controlled by the history of the time evolving LCSs. Although initially we were able to follow the transport of particles by individual flow features, the time evolution of the flow quickly produced a complex picture of stirring of particles (as seen in tracer fields produced by many simple time evolving flows: c.f. Otinno, 1989). The eddy “events” described above are frequent occurrences in the lee of the islands, and contribute to the elevated EKE of



the region (Calil *et al.*, 2008). The time mean of the FSLEs was similarly elevated in the lee of Hawai‘i, although there was no discernible structure in either the annual or seasonal mean, indicating the absence of persistent transport barriers or pathways. Strong LCSs are seen in the observed flow as given by the gridded, satellite derived, SSH field (c.f. Fig 10 from Calil and Richards, 2010). As shown above, the LCSs shaped and controlled the transport and dispersion of particles in the regional HYCOM and were considerably stronger and more distinct than in the global HYCOM (Figure 2.4). Indeed particle trajectories in the global HYCOM exhibited much less coherency. To investigate the net effect of the eddy flow we next considered the retention and connectivity of populations on different sides of the island.

### **2.3.2 Connectivity patterns**

The annual connectivity (June 2009 to May 2010) obtained for the two models (Figure 2.7, Figure 2.8) presented many differences, as expected considering the differences in the flow representation. At the surface, the largest contrast between the two models was the probability of local retention along the leeward coast, very high in the regional HYCOM (Figure 2.7a) and almost absent in the global HYCOM (Figure 2.7b). The opposite was true for the transport from leeward to windward, moderately high in the global HYCOM and almost absent in the regional HYCOM. At 30 meters, the largest disagreement between the annual connectivity pattern for the two models was for particles released at the windward and south regions. The regional HYCOM showed mainly local retention in the three areas (Figure 2.7c), while the global HYCOM

connectivity (Figure 2.7d) showed particle fluxes from the south to the leeward sites, and from windward to south.

The connectivity pattern for the regional HYCOM not only varied with depth but also with time. We calculated monthly averages and standard deviations of the proportion of retained particles for distinct time periods, and the results indicated that retention levels varied with time. For example, the connectivity obtained with the regional HYCOM presented both monthly and inter-annual variability, as reflected by the results for the summers of 2009 and 2010 (Figure 2.9). Despite the variability, there were consistent connectivity patterns for the study period. The three regions around Hawai'i Island showed high local retention. The windward region was generally the poorer exporter of particles to other regions. The south showed the largest particle export, with a strong flow directed to the leeward side. The transport from the south to leeward was only interrupted during two months: June and December of 2009. In both cases, the formation of an anticyclonic eddy took place and created a barrier to the transport from south to leeward. This transport pattern is corroborated by recent genetic studies of parentage analysis (Christie *et al.*, 2010) which found that larvae of yellow tang (*Zebrasoma flavescens*) originating in the south of Hawai'i Island joined leeward populations. According to our modeling results, such fluxes appeared as a recurrent pattern. Local retention on the leeward coast found in our model results was also detected by the genetic parentage study (Christie *et al.*, 2010), and it was suggested by drifters trajectories and larval sampling along an eddy on the leeward coast (Lobel and Robinson, 1986, Lobel and Robinson, 1988, Lobel, 2011).

To assess the impact of the mean flow on the connectivity, we calculated connectivity matrices for particles dispersed by the mean flow field of the regional HYCOM. The mean flow was obtained from averaging daily velocities from June 2009 to May 2010 for the surface, 30, and 100 meters depth. Transport patterns observed for the time evolving flow (results not shown) were also observed for the mean flow, such as local retention and transport from the south to the leeward. However, there were important differences. The time evolving flow field increased the connectivity among all areas around the Hawai'i Island. Using the averaged flow field, we observed that most of the particle export occurred among adjacent spawning grounds, while in the time evolving regional HYCOM exchange occurred among distant spawning grounds (as shown in Figure 2.8). Specifically, the time evolving flow also increased the probability of transport from south to leeward and the probability of local retention on the leeward coast. These results highlight the importance of the eddy field in increasing connectivity and influencing retention.

## **2.4 Discussion**

The picture emerging from the analysis of unstable and stable manifolds for the modeled flow in the study region was dynamic and complex, as was also found by previous studies of advection near an island (Rypina *et al.*, 2010). Despite the complexity of the flow and the resulting LCSs, it was possible to identify particular features in the FSLEs fields such as dipoles, eddies and hyperbolic points, that had a strong influence on particle trajectories (Figure 2.5). Although unstable manifolds clearly acted as particle

attractors, in a time evolving flow even subtle changes to the location and strength of the LCSs resulted in profound changes to the transport of particles and the pattern of connectivity. It was not surprising, therefore, that LCSs varying in both depth and time, produced patterns of transport and connectivity that varied at daily, monthly, seasonal, and inter-annual time scales.

Results using the regional HYCOM provided information about the role of eddies in retention, and consolidated conflicting conclusions from previous empirical research. The eddy field was responsible for increasing connectivity and influencing retention. We observed that eddies could entrap and recirculate particles close to the coast, agreeing with larval sampling and drifter studies from the Hawai‘i Island (Lobel and Robinson, 1986, Lobel and Robinson, 1988, Lobel, 2011). However, eddies could also lower retention by transporting larvae offshore, as observed by Walsh (1987) when studying reef fish recruitment. In short, both cyclonic and anticyclonic features were observed to influence the transport of particles in four distinct, and even opposing, ways: i) by increasing the transport of particles from distinct regions, ii) by enhancing local retention, iii) by entrapping particles and transporting them away from the coast, therefore decreasing retention, and iv) by creating a barrier for the transport among different faces of Hawai‘i Island. Large cyclonic and anticyclonic features can dominate the flow in the region on temporal scales from days to weeks, and are the most studied features in the region. However, we observed that eddies with a smaller spatial scale were important for the transport and retention of particles (Leis, 1982). Although eddies influenced particle transport, the presence of an eddy and associated LCSs themselves did not guarantee that

enhanced or reduced retention took place. Given such complex and dynamical patterns, we did not find a simple correlation between eddy occurrence and retention over long periods of time. This reinforces the conclusion that both the timing and location of spawning also play a role in the retention of larvae (Karnauskas *et al.*, 2011, Sponaugle *et al.*, 2005).

The connectivity patterns between the global and regional HYCOM were distinct, resulting from differences in their representation of the flow field. Strong LCSs were seen in the observed flow as given by the gridded, satellite derived, SSH field (c.f. Figure 10 from Calil and Richards, 2010). As shown, the LCSs shaped and controlled the transport and dispersion of particles in the regional HYCOM and were considerably stronger and more distinct than in the global HYCOM for spatio-temporal scales of interest considered (Figure 2.4, Figure 2.5, Video 2.1). Those results corroborate the importance of the coherent eddy field on particle dispersal. For the regional HYCOM, despite the high variability, there were recurrent connectivity patterns. The most frequently observed patterns for the regional HYCOM were: i) local retention for the three areas and, ii) a flow from south to leeward. Both patterns for the leeward coast agree with observational studies (Christie *et al.*, 2010, Lobel, 2011). Our results indicated that such fluxes were recurrent and persistent throughout the year. Spatially explicit differences among the receiving sites around the island were also evident. Overall, the leeward was the most efficient retention site while the south received the smallest amount of particles. The high variability observed for both the FSLEs fields and connectivity patterns and the

differences between the regional and global implementations of HYCOM highlight the need for modeling studies to use flow fields that represent such scales of variability.

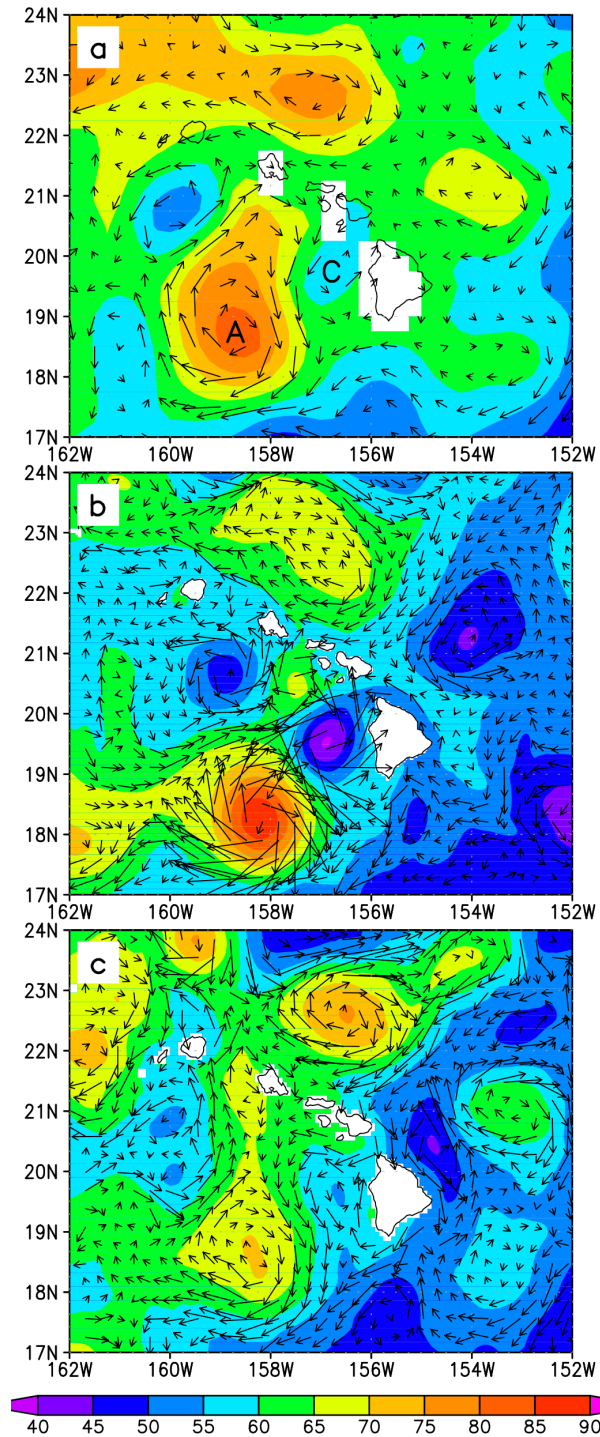


Figure 2.1. Sea surface height (SSH, cm, color) as: (a) measured from a satellite (an average over 7 days centered on 16 July 2009), simulated for 18 July 2009 by (b) the regional HYCOM and (c) the global HYCOM. Vectors indicate the surface geostrophic velocity derived from SSH.

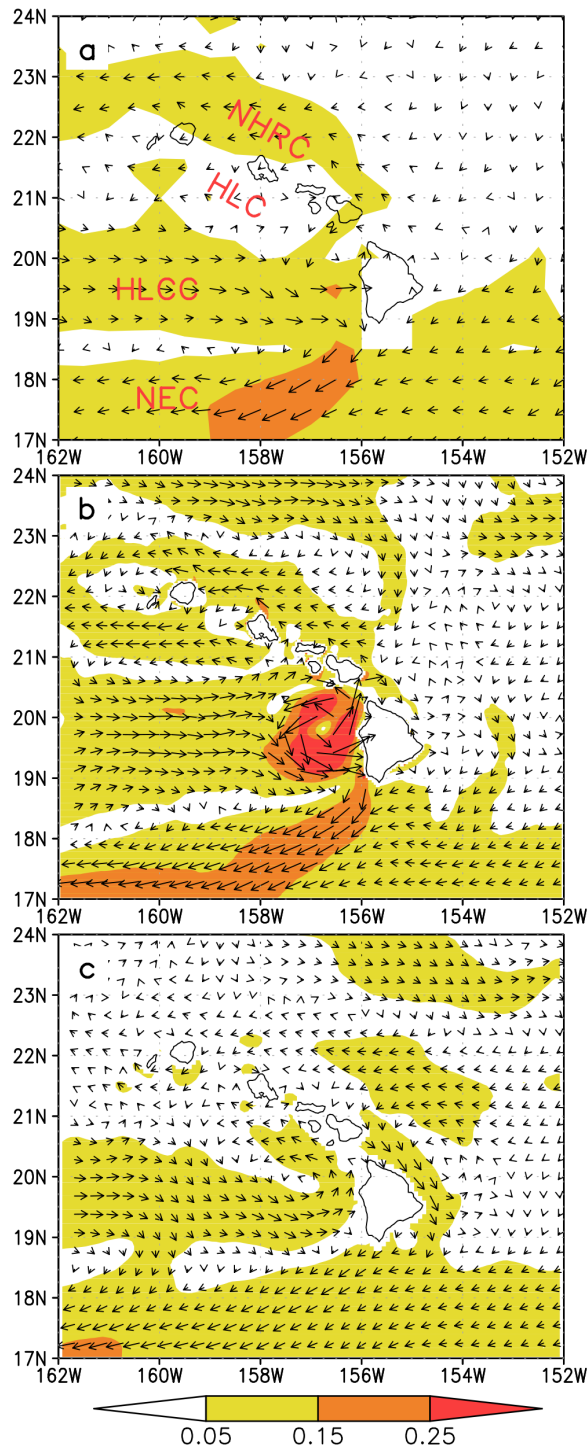


Figure 2.2. Long-term mean surface geostrophic velocity (color, m/s) derived from Sea Surface Height (SSH) for (a) satellite measurements, (b) regional HYCOM, and (c) global HYCOM.



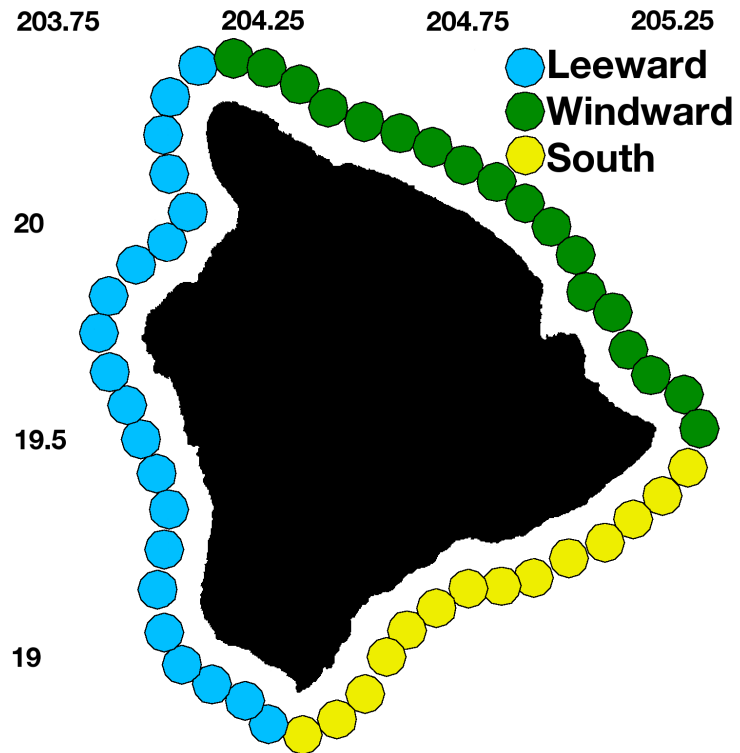


Figure 2.3. Release (source) and destination (sink) sites around the Hawai'i Island. Each of the 53 sites has 10 km of diameter and were grouped into 3 areas to facilitate analysis. These areas are indicated by colors in the graph: south (yellow), leeward (blue) and windward (green).

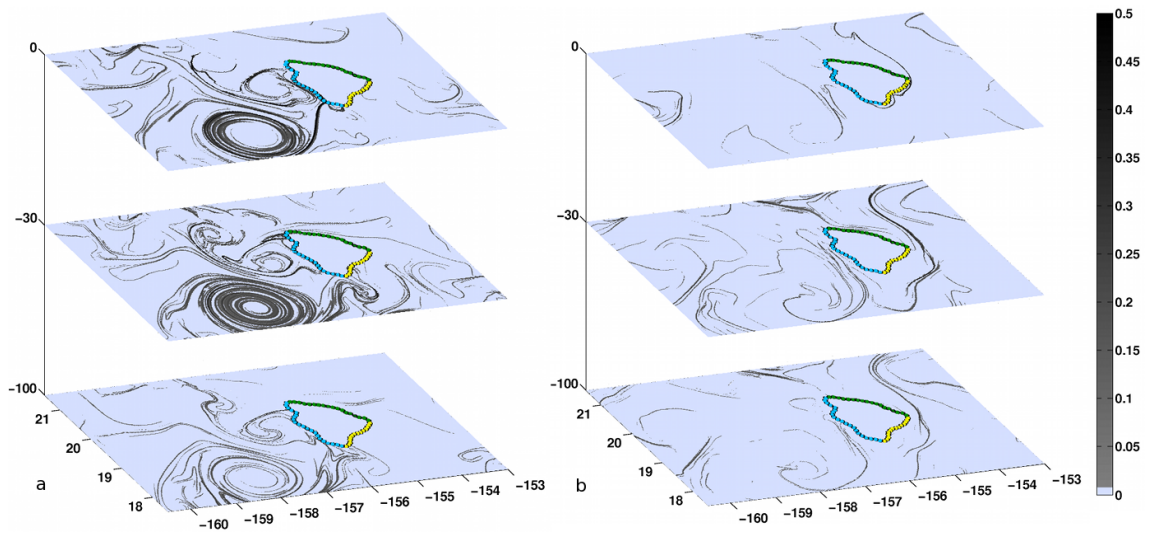


Figure 2.4. Attracting Lagrangian Coherent Structures (LCSs, unstable manifolds,  $d^{-1}$ ) for surface, 30 and 100 meters, calculated from the (a) regional, and (b) global HYCOM for 18 of July 2009. The velocity field was integrated for 30 days backward in time.

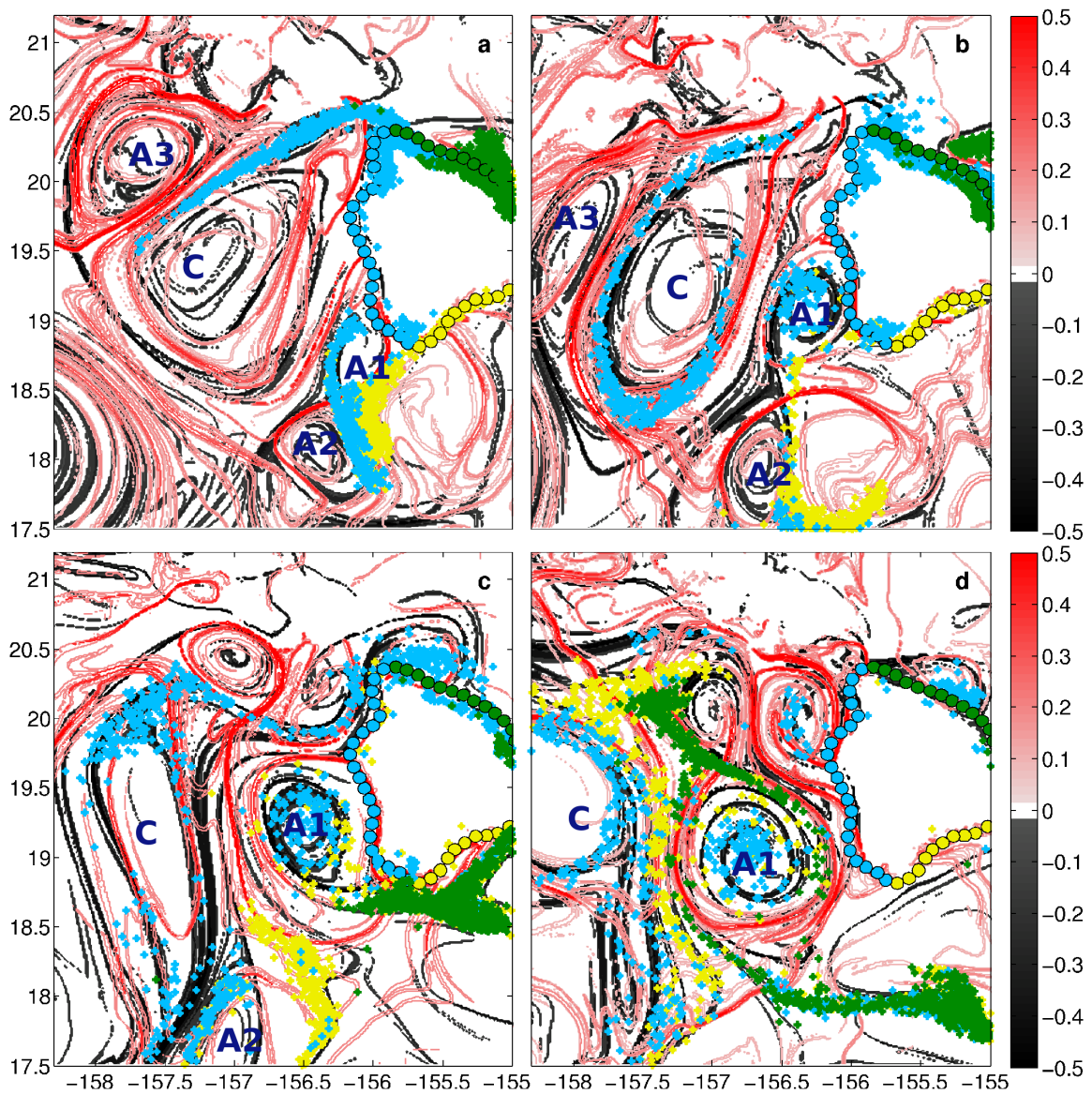


Figure 2.5. Distribution of particles, repelling LCSs (stable manifolds, red) and attracting LCSs (unstable manifolds, black) ( $d^{-1}$ ) at 25 of July (a), 30 of July (b), 7 of August (c) and 15 of August (d) 2009 for the regional HYCOM. In this figure, particles were released on 18 of July 2009 and tracked for 7, 12, 20 and 28 days (respectively) at 30 meters. The velocity field was integrated forward (backward) in time for determining the stable (unstable) manifolds. Particles are colored according to the face of the island where they were released.

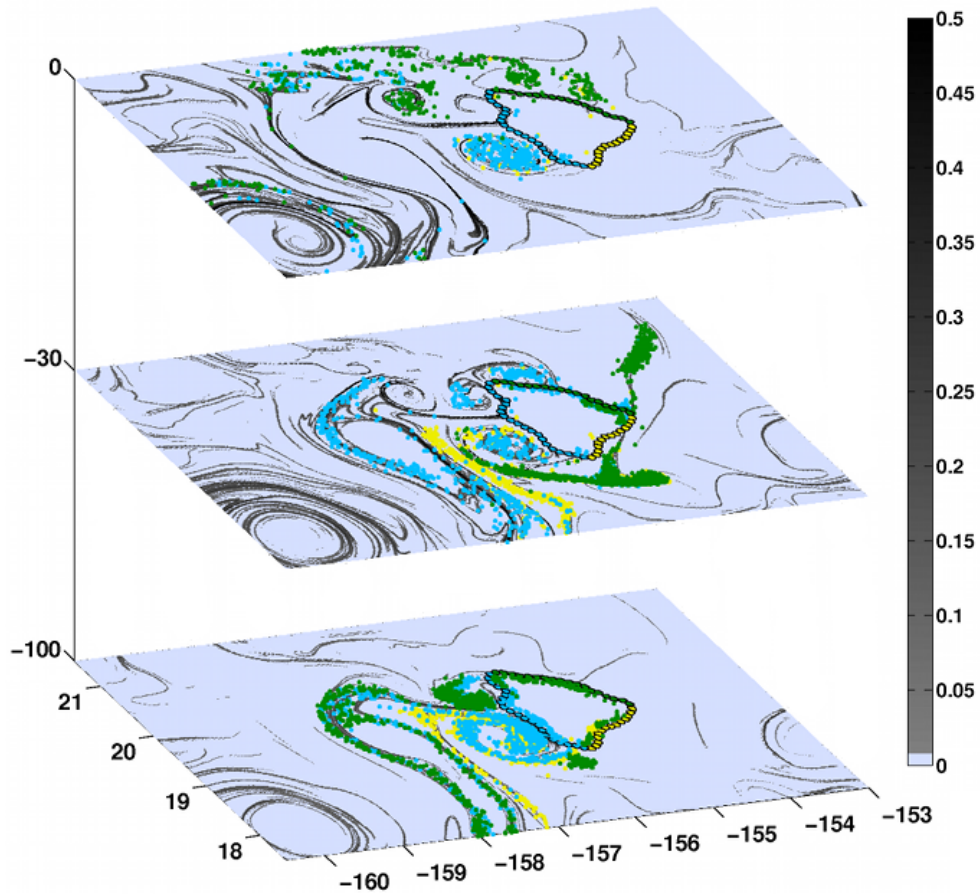


Figure 2.6. Distribution of particles and attracting Lagrangian Coherent Structures (LCSs, unstable manifolds,  $d^{-1}$ ) for surface, 30 and 100 meters, at 10 of August 2009 for the regional HYCOM. In this figure, particles were released on 18 of July 2009 and tracked for 23 days. The velocity field was integrated backward in time for determining the unstable manifolds. Particles are colored according to the face of the island where they were released.

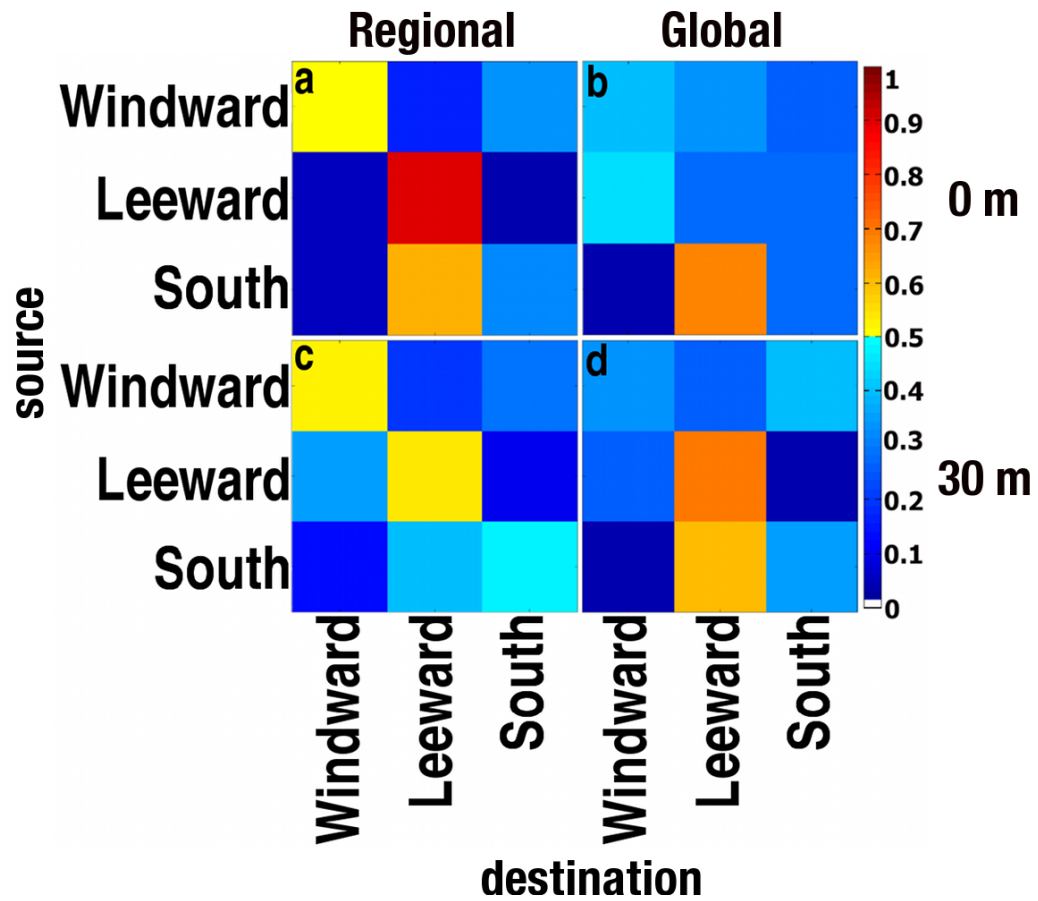


Figure 2.7. Connectivity matrices for the Hawai'i Island from June 2009 to May 2010. Particles were released at surface (a,b) and 30 m (c,d) and advected by velocities from the regional (a,c) and global HYCOM (b,d). The probability at each cell (i,j) is given by the number of particles leaving the spawning site i and arriving at the settlement site j, divided by the number of particles leaving the spawning site i and arriving at any settlement site. Therefore, when calculating the probability matrix, only the retained particles were considered.

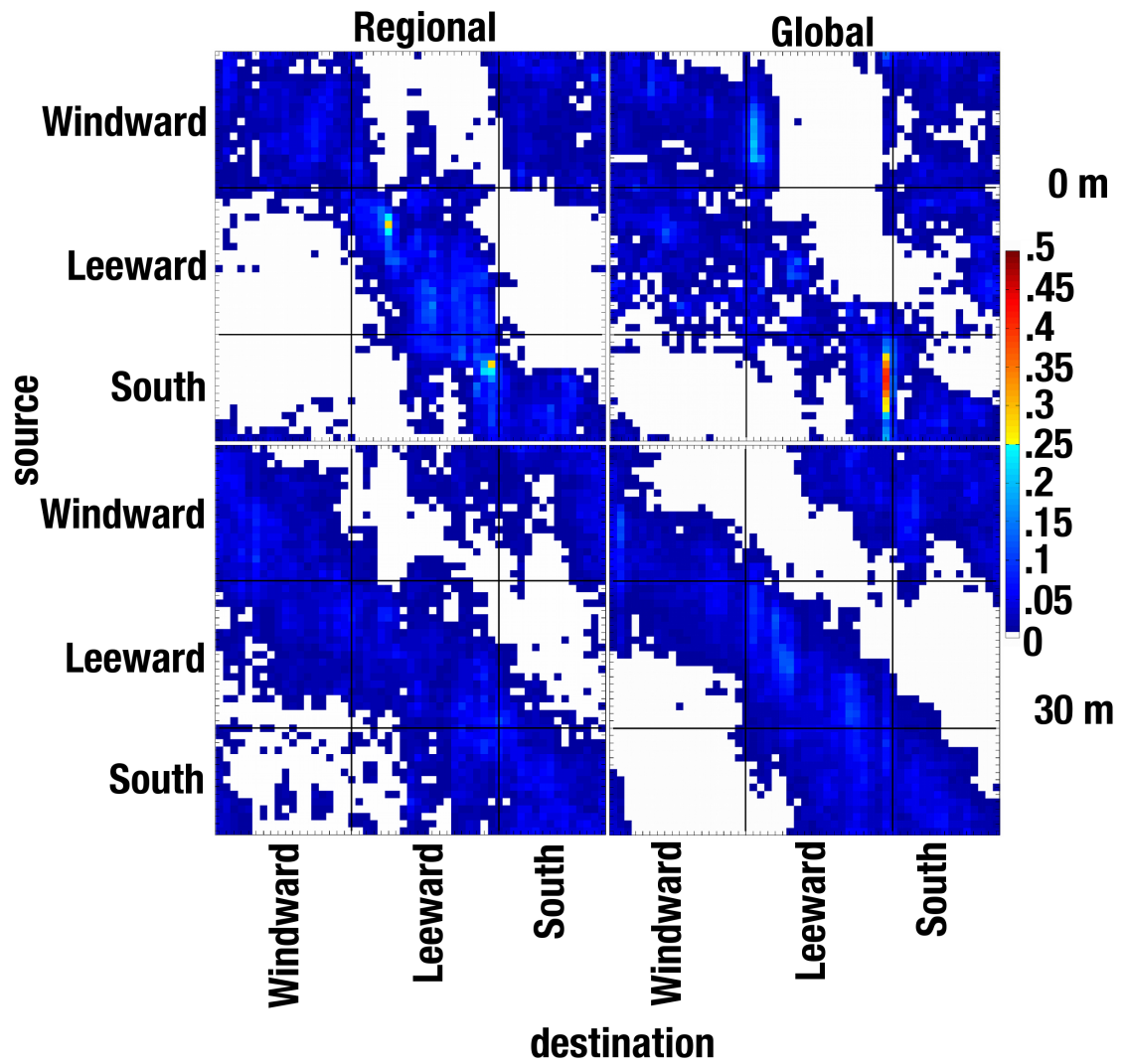


Figure 2.8. Connectivity matrices showing all source/destination sites for the Hawai'i Island from June 2009 to May 2010. Particles were released at surface (a,b) and 30 m (c,d) and advected by velocities from the regional (a,c) and global HYCOM (b,d). The probability at each cell (i,j) is given by the number of particles leaving the spawning site i and arriving at the settlement site j, divided by the number of particles leaving the spawning site i and arriving at any settlement site. Therefore, when calculating the probability matrix, only the retained particles were considered.

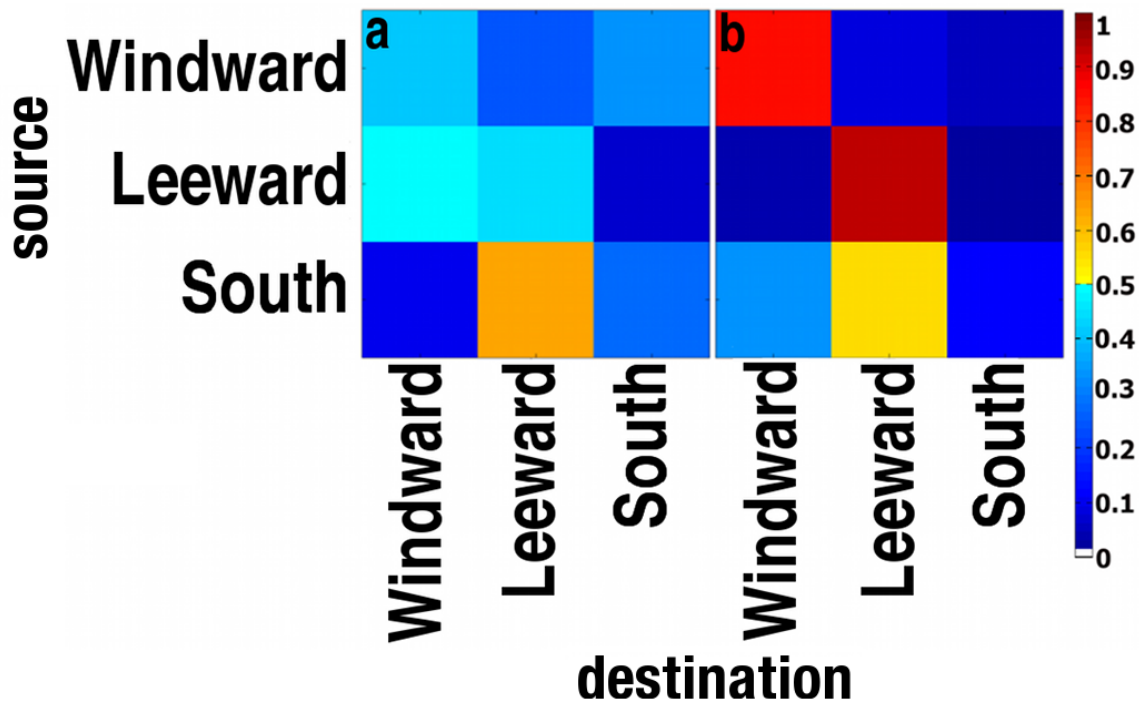


Figure 2.9. Connectivity matrices for the Hawai'i Island for 2009 (a) and 2010 (b) summer (July to September). Particles were released at surface and advected by velocities from the regional HYCOM. The probability at each cell (i,j) is given by the number of particles leaving the spawning site i and arriving at the settlement site j, divided by the number of particles leaving the spawning site i and arriving at any settlement site. Therefore, when calculating the probability matrix, only the retained particles were considered.

Supplemental Video (2.1). Animation of the distribution of particles and backward FSLEs ( $d^{-1}$ ) for surface, 30 and 100 meters, from 18 of July 2009 to 16 of August 2009 for the regional HYCOM. Each frame represents one day. Particles were released on 18 of July and are colored according to the face of the island where they were released.

## Chapter 3

### First estimation of larval supply and connectivity of reserves in the Hawaiian Archipelago

#### 3.1 Introduction

The bottomfish fishery has a long tradition in Hawai‘i and holds a prominent place in many aspects of island life (Pooley, 1987, Spalding, 2006, Zeller *et al.*, 2008). As a result, considerable effort has been given to preserving the bottomfish stocks in the islands, including the establishment of marine reserves. Reserves are a type of Marine Protected Area (MPA) where restrictions are placed on fishing and other human activities. The benefits of reserves have been well documented and include increasing ecological resilience, fish diversity, biomass and recruitment within reserve boundaries (Roberts and Hawkins, 1997, Lubchenco *et al.*, 2003, Grorud-Covert and Sponaugle, 2009, Babcock *et al.*, 2010). Furthermore, these protected areas can enhance fisheries outside their limits, particularly by larval export (Roberts and Hawkins, 2000, Christie *et al.*, 2010, Pelc *et al.*, 2010, Di Franco *et al.*, 2012, Harrison *et al.*, 2012). Larval export is considered a vital goal of many fishery reserves, because of its potential to promote the replenishment of fishery resources and the connection of populations within different reserves (Fogarty and Botsford, 2006). However, adequate larval dispersal information is rarely available for use in the reserves designation processes (Gaines *et al.*, 2003, Gerber *et al.*, 2003, Gaines *et al.*, 2010).



The Hawaiian Archipelago is located in the Central North Pacific. The populated islands between Hawai‘i and Middle Bank are the “Main Hawaiian Islands” (MHI, Figure 3.1). Northwest of Middle Bank are the Northwestern Hawaiian Islands (NWHI), a chain of small islands and atolls stretching for more than 2000 km (Figure 3.1). In 1998, nineteen Bottomfish Restricted Fishing Areas (BRFAs), were established in the MHI with the purpose of restoring the population of selected bottomfish species. A BRFA is a type of reserve where bottomfishing is the only prohibited activity within its boundaries. In 2007, the boundaries of these reserves were revised (Department of Land and Natural Resources, 2007), and their number reduced to twelve (Figure 3.2). In addition to this network, the NWHI hosts the United States’s largest marine reserve. The region was designated as the NWHI Coral Reef Ecosystem Reserve in 2001 (Executive Order No 13178, 2000 and Executive Order No 13196, 2001) and in 2006, re-designated as the Papahānaumokuākea Marine National Monument (PMNM) (Presidential Proclamation 8031, 2006). By 2009, all commercial fishing was prohibited in the PMNM. A potential benefit of the monument to bottomfish is to promote the replenishment of the MHI stocks by larval export. Available genetic evidence indicates some connectivity between the PMNM and the MHI (Rivera *et al.*, 2011, Toonen *et al.*, 2011, Gaither *et al.*, 2011). This evidence however is limited to only two bottomfish species, *Epinephelus quernus*, locally known as hapu‘upu‘u (Rivera *et al.*, 2011) and *Pristipomoides filamentosus*, or opakapaka (Gaither *et al.*, 2011). However, little is known about how much of the connectivity occurs due to transport during early life stages. Similarly, the designation of the MHI reserves took into account the best data

available for the bottomfish populations. Not considered, due to the lack of information on larval dispersal, was the reserve network's potential for larval supply and connectivity. Given this scenario in the Hawaiian Archipelago, the research goal here was twofold: i) to elucidate bottomfish population connectivity driven by the transport of early life stages, and ii) to link this knowledge to the management of their fisheries. The goal was addressed by simulating larval dispersal with a numerical model, generating information not yet available from empirical studies (Paris *et al.*, 2007, Werner *et al.*, 2007). Flow fields from a three-dimensional model (the HYbrid Coordinate Ocean Model, HYCOM) and an individual-based model (IBM) which depicted adult spawning strategies, larval behavior, and dispersal (Paris *et al.*, 2007) were used. This methodology allows the characterization of larval supply, connectivity, and breaks (Cowen *et al.*, 2006, Baums *et al.*, 2006). Specifically, connectivity between the PNMN and the MHI was evaluated. The potential of each existing reserve to sustain their own populations and rebuild bottomfish stocks was also evaluated (Hastings and Botsford, 2003, Planes *et al.*, 2009, Pelc *et al.*, 2010).

## **3.2 Methods**

### **3.2.1 Hydrodynamic model**

This study used the hydrodynamic model HYCOM (Bleck, 2002). A global ocean prediction system based on HYCOM (referred here as “global HYCOM”) provides hindcast analysis (from 2003) by assimilating remotely sensed and *in situ* ocean observations, such as sea surface height (SSH) and sea surface temperature (SST), using

the Navy Coupled Ocean Data Assimilation (NCODA) system (Chassignet *et al.*, 2007, Cummings, 2005). The global HYCOM has a horizontal resolution of  $0.08^\circ$ , approximately 8.3 km in the Hawai'i region. In the vertical, it has 32 layers. The bathymetry is based on the Smith and Sandwell database ([http://www7320.nrlssc.navy.mil/DBDB2\\_WWW/](http://www7320.nrlssc.navy.mil/DBDB2_WWW/)). The surface winds and thermal fluxes are from the Navy Operational Global Atmospheric Prediction System (NOGAPS, [http://www.nrlmry.navy.mil/metoc/nogaps/nogaps\\_char.html](http://www.nrlmry.navy.mil/metoc/nogaps/nogaps_char.html)) at a resolution of  $0.5^\circ$ . The Hawai'i regional HYCOM (aka "regional HYCOM" hereafter) is configured in a nested subdomain covering the MHI ( $16-26^\circ\text{N}$ ,  $150-166^\circ\text{W}$ ) within the global HYCOM, which supplies model fields for initialization and at the four open lateral boundaries. It has 32 vertical layers, as does the global HYCOM and a horizontal resolution of  $0.04^\circ$  (~4 km). Away from the lateral boundary zones, where open boundary conditions are applied, the bathymetry is replaced by the General Bathymetric Chart of the Oceans database (GEBCO,  $1/60^\circ$ , <http://www.gebco.net/>). This bathymetry captures the regional relief features providing an improved representation of the islands' coastlines. The regional HYCOM is forced at the surface with output from a regional atmospheric model, the Weather Research Forecasting system (WRF, <http://www.soest.hawaii.edu/MET/Faculty/wrf/arw/index.html>), with a resolution of  $0.06^\circ$ . No data assimilation is applied in the regional HYCOM (c.f. Jia *et al.*, 2011). The results obtained with the global HYCOM and the regional HYCOM were compared to address how changes in model forcing and resolution would affect the larval dispersal patterns in the region, as described below.

### 3.2.2 Individual-based Model

An individual-based, coupled biophysical modeling system was used to address larval transport and connectivity questions (detailed in Paris *et al.*, 2007). The particle displacement is given by both deterministic and turbulent velocities. The deterministic movement is simulated by a fourth order Runge-Kutta integration scheme of the simulated velocity field, while the turbulence is modeled by simple diffusion (Paris *et al.*, 2007), using a horizontal coefficient of diffusivity of 0.2 m<sup>2</sup>/s estimated from Okubo (1971). Implemented larval traits include a plastic pelagic larval duration (PLD), mortality, buoyancy and ontogenic vertical migration (OVM). The OVM of larvae was parameterized in the model by a matrix of probability density functions (PDFs). The matrix contained the probabilities of the vertical distribution of eggs/larvae for each time step. Vertical velocities were not considered to displace larvae, as it was assumed that the larvae are able to keep their vertical position, as observed by *in situ* studies (Paris and Cowen, 2004, Paris *et al.*, 2007). The PLD is parameterized by the time of advection. Model stability was evaluated by sensitive analyses (Pineda *et al.*, 2007; North *et al.*, 2009), as described below.

### 3.2.3 Sensitivity Analyses

The parameters of the biophysical model tested are given in Table 3.1. The significance of the differences in larval export and local retention among different cases was evaluated using a KS test with a 95% confidence interval. The proportion of larval export and local retention was calculated for each island and the PMNM at monthly and

yearly intervals, along with monthly averages and standard deviations. The baseline experiment had the lowest degree of complexity. In this case, 100 larvae were released every 5 days at 75 m and tracked for 30 days. The eggs followed a buoyancy scheme based on climatological values of water density for the region, and egg density values for a snapper (*Pagrus major*) from Kitajima *et al.* (1993), ranging from 1021 to 1023 g/cm<sup>3</sup>. The OVM was derived from observations of larval lutjanids from Boherlet and Mundy (1996) in the Hawaiian region and ontogenic migration surveys for Lutjanidae in the Atlantic Ocean (Huebert, 2009). The diffusivity was 0.2 m<sup>2</sup>/s (Okubo, 1971). For each sensitivity experiment, the tested parameter was the only model configuration changed. The spawning and retention sites were a 10 km wide region around the island contour at the depth of spawning, subdivided into 10 km radius polygons. For connectivity comparison, the polygons were grouped by islands (Figure 3.2).

The model reached stability at 30 larvae released per spawning site, which is valid for diffusivities within the interval  $0.009 \leq \kappa \leq 0.2$  m<sup>2</sup>/s. The velocity decorrelation time scale results showed that velocities were decorrelated for a lag of 5 days. The tested release intervals did not significantly change the proportion of larvae locally retained or exported. Changes to the diffusion coefficient, however, were significant for larval export and retention. Still, the only value tested for diffusion coefficient that led to significantly different results was 0.9 m<sup>2</sup>/s, while no significant difference occurred in the range  $0.009 \leq \kappa \leq 0.2$  m<sup>2</sup>/s (Figure 3.3). For the cases where eggs and larvae did not move vertically in the water column, the dispersion of larvae released in different layers was significantly different, which indicated the need to test different schemes for egg

buoyancy and behavior. Changing the velocity at which the eggs ascend through the water column in the buoyancy experiment did not significantly alter the larval export and local retention, nor the connectivity matrices. Considering different depths of spawning for larvae exhibiting OVM, the depth of spawning significantly affected the patterns for the three species when larvae migrated to the surface (OVM scheme *ii*, see Table 3.1 for description). However, larval export and local retention was not affected for larvae that only migrated up to a backscatter layer (OVM scheme *iii*, see Table 3.1 for description). When considering the impact of different OVM schemes for the same depth of release, no significant difference was found. In the same way, changing the PLD did not significantly alter the amount of exported and locally retained larvae.

The variability of the proportion of retention relative to these parameters was tested using a multifactor analysis of variance (ANOVA, Neter *et al.*, 1990) at 99% of significance. The dependent variable was the proportion of retained larvae at each island in the archipelago and the factors were PLD, species (depth of release/behavior/spawning season) and release site. Most significant parameters affecting the proportion of retention were different for MHI and PMNM sites. For the latter, the highest F-value was for species (F-value: 60.41,  $p < 2e-16$ ), followed by area of release (F-value: 16.32,  $p < 2e-16$ ) and then PLD (F-value: 13.15,  $p: 0.000415$ ). For the MHI, the highest F-values were for area of release (F-value: 28.397,  $p < 2e-16$ ) and then species (F-value: 8.950,  $p: 0.000231$ ). The PLD was not significant.

### **3.2.4 Comparison of regional and global HYCOM**

It was demonstrated in Chapter 2 that at a fine spatial resolution, the connectivity patterns obtained using velocity fields from the global and regional HYCOM were significantly different. However, the regional HYCOM grid does not cover the entire extent of the Hawaiian Archipelago, and consequently, it was desirable to use the global HYCOM velocity fields to estimate transport between the MHI and the PMNM. For this purpose, it was necessary to compare the transport and connectivity patterns obtained with velocity fields from the two models at broader spatial scales. For this experiment, eggs and larvae exhibiting OVM were released every 5 days from the polygons of the MHI region (Figure 3.2) and tracked during one year for 30 and 60 days. To assess differences at broader spatial scales, the resulting patterns of larval export and retention were grouped by islands, instead of individual sites (Figure 3.4). In this case, no significant difference was found for the proportion of larvae exported and locally retained between the regional and global HYCOM, both at yearly and monthly temporal scales (Figure 3.4). In addition, the connectivity matrices for broader spatial scales (calculated for islands instead of individual polygons) were calculated. No significant differences were found between the connectivity generated using the velocity fields from the two HYCOM implementations (results not shown). However, for finer spatial resolutions, when all release polygons were considered, several differences arose between the connectivity matrices from the two HYCOM implementations (Figure 3.5), as expected based on Chapter 2's results. The global HYCOM tended to yield higher local retention, while the regional HYCOM showed more dispersion and export, notably around Maui

County (Maui, Moloka‘i, Lana‘i, and Kaho‘olawe). The contrasting patterns reflected the different representation of circulation features by the two implementations, specifically eddies and coherent structures, which influence connectivity patterns (as discussed in Chapter 2). Considering these results, output from the global HYCOM were used to study larval connectivity along the full extent of the Hawaiian Ridge, including both the MHI and the PMNM, at broader spatial scales, i.e., with spawning/destination sites grouped by islands. The regional HYCOM was used to focus on dispersal and connectivity from the MHI’s reserves.

### **3.2.5 Adaptation to bottomfish species**

After defining key parameters, the biological model was adapted for three snapper species: *Etelis coruscans* (onaga), *Etelis carbunculus* (ehu) and *Pristipomoides filamentosus* (opakapaka). Their preferred depth range and spawning seasons were used as the depth and time of egg release (Table 3.2). In the global HYCOM experiments, the spawning and retention sites were a 10 km wide region around the land contour at the depth of spawning, subdivided into 10 km radius polygons (Figure 3.1). From each spawning site, 100 larvae were released every 5 days. For the regional HYCOM experiments, the spawning sites were the bottomfish reserves (Figure 3.2, the reserve J was subdivided into 4 release sites of equal size). The number of larvae released was scaled by the area (km<sup>2</sup>) of bottomfish essential fish habitat (EFH) available at each reserve (which is the 0-400m depth range, values shown in Table 3.3). The retention sites were a 14 km wide region around the land contour at the depth of spawning (Figure 3.2).



For both models, two experiments were conducted for each species to consider a range of PDLs. Larvae were advected for 30 and 60 days, and larvae older than 20 and 45 days, respectively, found within the limits of a retention site were considered retained (referred to hereafter as viable larvae) and removed from the simulation. The OVM matrix was derived from the vertical concentrations of lutjanid larvae for the Hawaiian region (Boherlet and Mundy, 1996) combined with ontogenic migration surveys for lutjanids in the Atlantic Ocean (Huebert, 2009) and calibrated by the previously described sensitivity analysis. The mortality coefficient used was calculated so the e-folding time scale of the larval cohort is equal to their PLD. The period of the simulations was from 2006 to 2010 for larvae advected with velocities from the global HYCOM and from 2009 to 2010 for the regional HYCOM.

Using this IBM, it was calculated population connectivity, proportion of retention, local retention and export, as defined by Paris and Cowen (2004), Pineda *et al.* (2007) and Paris *et al.* (2007). The proportions of larvae (retained and exported) were a ratio based on the amount of retained larvae, not considering larvae dispersed to open waters. Thus, the proportion of larvae retained at each destination site ( $j$ ) was given by the number of larvae retained at each site ( $j$ ), divided by the number of larvae retained at all sites. Similarly, the proportion of viable larvae exported from each release site ( $i$ ) was calculated by dividing the number of viable larvae released at each site ( $i$ ) by the number of larvae retained at all sites. The connectivity patterns were represented by a matrix of probabilities, where the rows are the spawning areas (sources, node  $i$ ) and the columns are the larvae destinations (sinks, node  $j$ ) (Paris *et al.*, 2007). The content of each matrix

cell element represents the probability of larvae leaving the spawning site and arriving at a retention zone. The content of the cell elements  $i=j$  represents the probability of local retention. The Kaho‘olawe Island Reserve (Figure 3.2) was considered along with the twelve bottomfish reserves (BRFAs) for the analyses of larval supply and reserve connectivity. This island and surrounding marine environment are reserved for of exclusive use by Native Hawaiians (Lowe, 2004). In practice, it acts as a bottomfish reserve since no commercial bottomfishing is allowed.

### **2.2.6 Evaluation of potential reserves**

The objective of this experiment is to identify candidate areas for potential reserve designation in the future, based exclusively on larval dispersal characteristics. Candidate areas were evaluated on three aspects: i) efficiency as release sites; ii) efficiency as retention sites; and iii) connectivity with all sites. This experiment followed the same setup as the regional HYCOM experiments with one modification: an equal amount of larvae (100) was released at each site. Using the particle trajectories, the proportions of i) viable larvae release per site, and ii) larval retention per site were calculated. Proportions were based on the number of larvae found (or produced) in a site divided by the total number of larvae retained (at all sites). The number of connections were based on the connectivity matrices, considering the number of connections each site had with other sites, both as an exporter and as a receiver of larval subsidy. The average and standard deviation of proportions and number of connections were calculated for all scenarios of the three species and two PLDs. The 40% of the sites which presented higher values of

viable larvae release, retention and connections were defined as the best spawning, destination and most connected sites, respectively. Results were contrasted with indicators of habitat suitability and presence of bottomfish species, based on research surveys (Parke, 2007, Christopher Kelley, *personal communication*) and pounds of bottomfish commercially landed from 2005 to 2011. Fishery data were obtained from the Hawai‘i Division of Aquatic Resources (HDAR), grouped by fishery reporting zones (Figure 3.11). Estimated amount of bottomfish habitat available per zone was adapted from Parke (2006, Figure 3.12). It is important to highlight that the catch data is likely to present errors (see Parke, 2006), and was used here as a rough indicator of bottomfish presence. It is mandatory in the State of Hawai‘i for commercial fishermen to self report catch information, including location. However, to maintain the privacy of their fishing grounds, they indicate within which HDAR’s reporting area they caught the fish. In some instances, it can be difficult for the fishermen to accurately relay their catch location to the reporting areas, what can lead to inaccuracies.

### **3.3 Results**

#### **3.3.1 Papahānaumokuākea Marine National Monument and Main Hawaiian Islands**

Despite differences in the connectivity matrices due to species specific biological traits, it was possible to identify common features in the matrices for all species (Figure 3.6). Primarily, the direct connectivity between the PMNM and the MHI was found to be limited for all species and scenarios. Larvae originating in the PMNM tended to be locally retained and not exported to the MHI. However, the islands, banks and atolls

within the PMNM were well connected by larval dispersal. The only disruption of simulated larval transport appeared between the Lisianski Island and the Pearl and Hermes Reef. Similarly, larvae released in the MHI were mostly locally retained. In contrast to the PNMN, the islands in this region showed less interconnectivity, specially the three southernmost (Hawai'i, O'ahu and the Maui-Moloka'i-Lana'i-Kaho'olawe complex). The highest degree of dispersal was observed from the opakapaka experiment using a PLD of 60 days and OVM to the surface. The variance of the connectivity matrices for all the possible cases was calculated to quantify differences between species, pelagic larval durations and behaviors (Figure 3.6b). The variance values were low when compared with the probabilities shown for specific cases (Figure 3.6a), indicating that the main patterns of connectivity described here were robust among species and behaviors.

Analysis of the connectivity matrices revealed the presence of 4 distinct dispersal zones. These zones were mostly self-contained, but still showed limited connectivity with other zones (marked by black boxes in Figure 3.6a and Figure 3.7). These zones were as follows: 1) from the Island of Hawai'i to O'ahu, 2) from Kaua'i to Necker, 3) from French Frigate shoals to Lisianski, and 4) from Pearl and Hermes Reef to Kure Atoll. The mean and standard deviation of the probability of local retention for each block of islands was calculated considering all possible scenarios (Figure 3.7). The standard deviation was much smaller than the probability of local retention. This result showed that these regions remained mostly self-contained for all species, PLDs and behaviors, suggesting that physical processes probably underlie these patterns. The averaged flow structure (Figure 3.1), showed the existence of persistent jets in this region. Large potential vorticity (PV)

gradients, often associated with jets, can act as barriers to transport in the ocean (Dritschel and McIntyre, 2008). The PV was calculated by  $(f + \zeta)/H$ , where H is depth of a target isopycnal (depth of the thermocline),  $\zeta$  is the relative vorticity averaged from surface to the depth H and f is the Coriolis parameter. Velocity and density fields were taken from the global HYCOM, and the PV for each day was averaged from 2006 to 2011. Results (not shown) indicated that there are no evident PV barriers coinciding with the boundaries between the self contained zones.

The connectivity matrices (Figure 3.6a) indicated that the islands in zone 2 (from Kaua‘i to Necker), are important stepping stones, promoting larval exchange between the PMNM and the MHI. In order to verify if those islands are ecological corridors, the number of connections each site presented with other sites, both as an exporter and as a receiver of larval subsidy, was calculated. Considering all scenarios, the islands from zone 2, along with Gardner Pinnacles and French Frigate Shoals, showed the highest number of connections. This result further indicated that the islands between Kaua‘i and Necker are indeed an ecological corridor.

### **3.3.2 Reserves within the Main Hawaiian Islands**

Two key questions that should be investigated regarding the MHI bottomfish reserves are: i) are they potentially self-supporting populations?, and ii) are they potentially replenishing the overall fishery? To answer these questions, an evaluation of the fate of larvae spawned inside reserves was undertaken. It was estimated how much of the larvae released inside reserves were: i) locally retained, ii) exported to other protected

areas, and iii) exported to unprotected fishing sites. Results were based on experiments using the regional HYCOM and a scaled release of eggs. The connectivity and proportion patterns showed small variances between different species and PLDs, as seen in the global HYCOM. Thus, the averaged connectivity and proportion for all species and PLDs were considered for the following analyses. Results clearly showed that viable larvae released inside reserves were mostly likely to be exported to fishing sites (Figure 3.8a). Smaller percentages of larvae were likely to be retained locally or exported to other reserves. Those patterns were variable along the archipelago (Figure 3.8a). The reserves showing the greater number of connections with other reserves were the Kaho‘olawe Island Reserve (O), and BRFAs E, F, G and K. It is important to highlight that Kaho‘olawe is not designed as a BRFA by the State of Hawai‘i. Nonetheless, this reserve received larval subsidy from six different BRFAs during the simulation period, helping to increase the connectivity of the reserve network. BRFAs E, F and G are located relatively close to each other: southeast O‘ahu, Penguin Bank and north Moloka‘i. Larvae from these locations were likely transported through Kaiwi, Pailolo and Kalohi Channels, which separate the islands, increasing their distribution range. Dispersal by the North Hawaiian Ridge Current (NHRC) could also influence the observed connectivity. This current flows along the north side of the Hawaiian ridge oriented primarily northwestward, but it is a weak current which changes in direction and intensity (Firing *et al.*, 1999), potentially leading to the dispersal of larvae in multiple directions. Notice that BRFA A, located in the northernmost part of the MHI, exhibited connections to more southerly reserves, but these occurred during isolated events and was not recurrent.

When considering the proportion of larvae exported (Figure 3.8b), the largest amount was exported to fishing sites. There was no significant difference between the proportion exported to other reserves and locally retained, as tested by a pairwise t-test at 99%. Some reserves were more efficient at producing viable larvae. BRFA F (Penguin Bank) and K, along with the Kaho‘olawe Island Reserve, produced most of the viable larvae (65%). Considering retention, the reserves retained 22% of all viable larvae, while 78% were retained in fishing sites. BRFA C, K, and the Kaho‘olawe Island Reserve accounted for 47% of all larvae retained inside reserves. BRFA A showed both the lowest production and retention of viable larvae. BRFAs B, E, G, H, J, and M also showed lower values of local retention. Some of those reserves received larval subsidy from other reserves (such as B and E, see Figure 3.8a), however other areas were dependent on larvae from fishing sites to sustain their populations. It is important to mention that all results indicated the importance of the Kaho‘olawe Island Reserve and of the Penguin Bank (BRFA F) in helping rebuilding stocks of bottomfish in the MHI.

### **3.3.3 Potential reserves**

The standard deviations of the scenarios (species and PLDs) were much smaller than the averaged connectivity, indicating that the resulting patterns of retention, export and number of connections were robust among species. In the following experiments, the release of eggs was not scaled by the amount of available bottomfish habitat. However, the sites showing higher larval export, retention, and a higher number of connections were the same for the constant and scaled release experiments, despite observed

differences in the magnitude of export and retention. The average retention, export, and number of connections of the best exporters, destination and most connected sites, respectively, were significantly different from the other sites as tested by an ANOVA and a multiple comparison test at 95% significance. Most of the sites presenting the higher production of viable larvae are located on the leeward side of islands within Maui County (i.e., Maui, Moloka'i, Lana'i, and Kaho'olawe), O'ahu, and Hawai'i (Figure 3.9a). Only three of the best export sites are located inside reserves, including the Kaho'olawe Island Reserve. The best destination sites were more spread out among the islands in comparison to the best exporter sites (concentrated on the leeward region) or most connected sites (concentrated on Maui County and south O'ahu) (Figure 3.9b). Most reserves were good retention sites, with the best being: C (south Kaua'i), E (east O'ahu), F (Penguin Bank), G (north Moloka'i), J (east Maui), K (north Hawai'i Island), L (east Hawai'i Island), M (south Hawai'i Island) and around the Kaho'olawe Island Reserve. Sites around Maui County (Maui, Moloka'i, Lana'i, and Kaho'olawe) were the most connected, along with south O'ahu and a few Hawai'i Island sites (Figure 3.9c). Six reserves were among the most connected, five BRFAs (E, F, H, J, K) and the Kaho'olawe Island Reserve.

### **3.4. Discussion**

#### **3.4.1. Connectivity along the archipelago**

Simulations of larval dispersal and connectivity matrices can potentially provide information about the evolutionary connectivity of organisms, indicating, for instance,



transport barriers and isolated populations (Cowen *et al.*, 2006, Baums *et al.*, 2006). Moreover, models and matrices can also help elucidate patterns of ecological connectivity (Jones *et al.*, 2009). While small larval or adult exchanges of few individuals among distinct populations might lead to panmixia (Wright, 1931), strong flows are necessary to support a population (Botsford, 2003). Therefore, ecological connectivity provides vital information for management (Botsford, 2003, Botsford *et al.*, 2009). In this study, the potential existence of four, mostly self-contained zones is an indication that those zones are self-resilient, not receiving large larval fluxes from other regions to sustain their populations. The existence of self-sustained zones implies the need for distinct management measures within each zone. However, this is not an indication of genetic structure along the archipelago. For instance, no genetic structure was found for *Pristipomoides filamentosus* (Gaither *et al.* 2011) or for *Epinephelus quernus* (Rivera *et al.* 2011), a grouper species not considered in this study. The lack of genetic structure is a consequence of both larval dispersal and adult migration. The simulations conducted in this Chapter indicated that larval exchange occurs between different zones (Figures 3.6a and 3.7). The probability of this exchange was small, however it is potentially enough to lead to panmixia of the populations. In addition, analysis of conventional tags from a State wide program showed that although 80% of the recaptures of tagged fish occurs within 0 to 22 km of their release location, a few individuals migrated more than 300 km along the archipelago (Kobayashi, 2008). Such large migrations can also contribute to the homogenization of the stock across the archipelago (Gaither *et al.*, 2011).

The connectivity matrices showed a high degree of larval transport among PMNM sites, even when considering the discontinuity in larval transport between Lisianski Island and the Pearl and Hermes Atoll. Meanwhile, limited connection by larval transport emerged within the MHI, with the southernmost islands showing especially high levels of local retention. These results contradict previous Lagrangian modeling research in the region, all of which showed higher local retention in the PMNM sites and higher larval exchange and connectivity within the MHI's release sites (Kobayashi, 2006, Kobayashi and Polovina, 2006, Rivera *et al.*, 2011). However, this Chapter's results agreed with a comprehensive population genetics study, which considered the genetic structure of 27 different species in the Hawaiian Archipelago (Toonen *et al.*, 2011). In their study, the authors found that the MHI showed genetic differentiation and population structure among its islands, while the PNMN emerged as a well homogenized region. The results here indicated for the first time that larval transport is potentially playing a role in shaping population dynamics along the archipelago. The resolution of the used hydrodynamic models, combined with sensitivity analyses and calibration for individual species are factors which contributed to reveal these patterns. Nonetheless, the boundaries of the four self-sustaining zones found in this study matched the location of genetic barriers found by Toonen *et al.* (2011). The averaged flow structure (Figure 3.1) was characterized by the presence of persistent jets. The Lagrangian nature of the flow suggests that larvae would be transported away from the islands, in disagreement with the modeling results which showed local retention and exchange between different banks and islands. Despite the steady sheared flow structure, no metrics such as FSLE or PV

barriers indicated the presence of persistent barriers to larval transport. The averaged PV gradient calculated for the boundary regions of the self contained zones did not suggest inhibition of transport. In the same way, the averaged FSLEs in the region calculated for the geostrophic flow from 2005 to 2010 did not show persistent structures (see Figure 6 from Calil and Richards, 2010). Future studies should further explore the role of the physical environment in shapping these barriers to larval transport.

Simulation results revealed limited direct connectivity by larval transport between the PMNM and the MHI. However, larval exchange between MHI and PMNM did occur in the region from Kaua‘i to Necker, suggesting that this area acted both as a stepping stone and an ecological corridor, facilitating larval transport and gene flow between the protected stocks from the north and the heavily fished stocks in the south. This transport was primarily oriented from the MHI to the PMNM, which was also observed by Rivera *et al.* (2011) and Toonen *et al.* (2011). Therefore, it is vital to protect stocks and habitat located around these islands to protect their potentially vital ecological function. This result highlights the importance of the reserves in zone 2 (reserves A, B and C) to preserve the integrity of the bottomfish stocks. This is particularly important when it is considered that reserve A (located at Ka‘ula Rock) seemed to depend primarily on larval subsidy from other sites to support a population. By episodic events, this reserve could export larvae as far south as Kaho‘olawe, further increasing the chances of genetic mixing. In addition, the role of zone 2 as an ecological corridor calls attention to Middle Bank. This important fisheries habitat is located between the MHI and the PMNM, and only a small part of the bank is protected by the PMNM. Its location is inefficient for

management and fishery regulations. Indeed, there is no control of fisheries activities at Middle Bank. To reassess the importance of the bank, larval dispersal was simulated for one year while excluding this and other submerged banks as release/destination sites. The model results indicated that for ehu (*Etelis carbunculus*), no connection existed in this particular year between the PMNM and the MHI (results not shown). This is a further indication of the importance of this bank in maintaining the connectivity and therefore the integrity of the stocks located in the MHI and the PMNM.

#### **3.4.2 Reserves within the Main Hawaiian Islands**

Most of the viable larvae released inside the MHI reserves were exported to fishing sites (Figure 3.8a), while the probability of export to other reserves was very low. Reserves should be networked for optimal effectiveness, particularly in cases where the fishery is severely depleted (Pelc *et al.*, 2010, Gaines *et al.*, 2010). Reserves that potentially generated higher production of viable larvae were ones with more bottomfish habitat (Table 3.3). These sites can potentially support higher egg production, which the results indicated was an important factor for successful export in the study region, as observed for the Kaho‘olawe Island Reserve as well as BRFA K and F (Penguin Bank). This conclusion agrees with previous modeling work of reserves efficiency (Pelc *et al.*, 2010, Grüss *et al.*, 2012). The size of the protected areas was also related to successful larval retention: bigger reserves tended to retain more larvae. However, the placement of reserves in areas favorable to transport and retention was also important, as observed for reserve C. Despite relatively small size, it represented 10% of the network larval

retention. Many reserves had low local retention and relied on larval subsidies from fishing sites to sustain their populations. In this scenario, the designation of more reserves, or the extension of the existent reserves, could increase the integration and efficiency of the reserve network. Smaller reserves, located at strategic locations (such as reserve C), can increase larval retention and connectivity, as can larger reserves that support higher production, connectivity, larval export and retention.

### **3.4.3 Evaluation of potential reserves**

It is not surprising that areas in the Maui-Moloka'i-Lana'i-Kaho'olawe complex and O'ahu were well connected. A greater concentration of sites were found there compared to the relatively isolated sites of the northern islands. Likewise, it is expected that the leeward (east) of the islands would present more connections. As discussed in Chapter 2, larvae released from leeward sites can become entrapped and recirculated by eddy features, increasing their distribution range. Some sites were among the most efficient for the three aspects analyzed. These sites are located as follows: south O'ahu (3 sites), leeward Lana'i (1 site), Kaho'olawe (4 sites), south Maui (2 sites) and leeward Hawai'i (3 sites). However, by contrasting these results with an indication of fishing stocks presence (given by pounds captured, presence of fish on research surveys and availability of bottomfish habitat) three areas appeared as suitable candidates for further research (Figure 3.10).

The first potential reserve site was the region east of reserve C, south of Kaua'i, which appeared as an effective spawning and destination site. Despite not figuring among

the 40% most connected sites, it was potentially well connected with Ni‘ihau, Ka‘ula rock and its reserves. This is crucial, as the reserves located in those islands seemed to rely on larval subsidies from non-protected sites. Further, this area appeared to be an important connector between the MHI and the PMNM, making it fundamentally important to enhance its protection. The second site was the area south of Ka‘ena point, O‘ahu, which the model suggested to be a good destination and export site, and well connected to other reserve sites. Furthermore, a significant amount of bottomfish habitat is present in this area (Figure 3.12). Indeed, the HDAR fishery reporting zone surrounding this region supports a fishery of about 3,000 pounds of bottomfish/year (averaged over the period from 2005 to 2011, Figure 3.11). Thus, this area is likely to support an elevated production of eggs, which in turn can increase the amount of viable larvae exported. Another area in South O‘ahu, around the Pearl Harbor region, also met the three criteria evaluated here. However, the area does not offer good quality bottomfish habitat (Figure 3.12, Christopher Kelley, *personal communication*). Also, no fish were reportedly caught in this area from 2005 to 2011. Therefore, the region was not considered suitable for consideration as a future bottomfish reserve, despite having the desired larval dispersal characteristics.

The last potential reserve site was located in the northeast Hawai‘i Island, which was well connected, and figured as a good spawning and retention site. This area had a significant amount of habitat, and HDAR catch reports indicated an average of 11,000 pounds of bottomfish landed each year (Figure 3.12). Thus, this region can potentially produce a considerable amount of eggs, and increase connectivity with other reserves,

particularly the ones located around Hawai‘i Island, Maui and Moloka‘i. It is important to highlight that the Kaho‘olawe Island Reserve was one of the areas appearing as a potential bottomfish reserve. This result confirmed the importance that the protection of the waters surrounding Kaho‘olawe have for the conservation of bottomfish fisheries. Finally, the site located south of Maui, which met all three criteria evaluated, was not suggested as a protected area due to its proximity to the Kaho‘olawe Island Reserve.

#### **3.4.4 Future directions**

For successful reserve designation, future studies must clarify adult behavior of the bottomfish species, focusing in particular on their movement range and reproductive strategies. Theoretical models indicated that adult fish movement can impact the efficiency of reserves (Grüss *et al.*, 2011). In the MHI, a conventional tag-recapture study has shown that while *P. filamentosus* can move between banks and islands, their typical behavior is to remain in and around the bank where they were tagged (Kobayashi, 2008). Additional studies are now in progress but have yet to show that this species or any other bottomfish species undertake long migrations (Christopher Kelley, *personal communication*). The presence of protected areas can influence these patterns, either by density-dependent (Norman and Jones, 1984) or density-independent mechanisms, such as behavioral polymorphism (Grüss *et al.*, 2010). At least one study focusing on snappers showed that reserves decreased the adults dispersal range (Parsons *et al.*, 2010). It is still unknown whether the existence of reserves is altering the behavior of fish in Hawai‘i. Further, it is necessary to understand the spawning behavior of these species, because it

can alter their distributions. Snappers are known to form spawning aggregations in other regions (Lindeman *et al.*, 2000, Claro and Lindeman, 2003, Sala *et al.*, 2003). Aggregations usually occur at specific sites, which need to be protected to ensure the spawning stock safety (Karnauskas *et al.*, 2011). Understanding the adult behavior and their changes relating to the reserves are fundamental to produce better predictions of larval dispersal and to secure the enhancement and sustainability of fishing populations.



Table 3.1. Parameters tested in the sensitivity analyses and their respective values

<b>Experiment</b>	<b>Description</b>	<b>HYCOM</b>
<b>a) Number of eggs</b>	Minimum number of eggs necessary for the model to reach stability, i.e., a constant level of larval retention, which does not change with increased egg release. The values tested were: 10, 30, 50, 100 and 500 eggs	global
<b>b) Interval of release</b>	The interval of release must represent the scales of variability of the flow and balance computational needs. Intervals of spawning (in days) considered were: 1, 2, 4, 5, 7 and 10. The decorrelation time scale was also calculated for velocity fields from the global HYCOM	global
<b>c) Depth of spawning</b>	<b>(i)</b> no buoyant, no vertically migrating larvae were released at surface, 10, 30, 50, 100 and 200 m, <b>(ii)</b> buoyant and vertically migrating larvae were released at 75 and 200 m	global and regional
<b>d) Buoyancy</b>	Four different buoyancy values: <b>(i)</b> absence of buoyancy, <b>(ii)</b> estimate buoyancy from typical egg density values and climatological values of water density for the study region, <b>(iii)</b> positive buoyant with fast ascendancy in water column, and <b>(iv)</b> positive buoyant with slow ascendancy in water column	global
<b>e) Ontogenic Migration</b>	Three different schemes: <b>(i)</b> absence of OVM, <b>(ii)</b> older larvae migrating vertically in the water column, up to the surface, following distributions from Boherlet and Mundy (1996) and Huebert (2009), and <b>(iii)</b> larvae spawned at 75 m and 200 m migrating up to 25 m and 100 m, respectively, simulating a concentration of larvae at deeper backscatter layers	global and regional
<b>f) Diffusivity</b>	Four diffusion values $\kappa$ ( $m^2/s$ ): <b>(i)</b> 0.009, <b>(ii)</b> 0.06, <b>(iii)</b> 0.2, <b>(iv)</b> 0.9	global and regional
<b>g) PLD</b>	Two different values for PLD (and competency period): <b>(i)</b> 30 (15), <b>(ii)</b> 60 (40)	global and regional

Table 3.2. Preferred depth and spawning season for the three deep-water bottomfish species considered in this study. The preferential depth range corresponds to the range where 93% of occurrences for a determined species were registered, based on literature reviews, and Hawai'i Undersea Research Laboratory (HURL) database (<http://www.soest.hawaii.edu/HURL/index.html>)

<b>Species</b>	<i>Pristipomoides filamentosus</i>	<i>Etelis coruscans</i>	<i>Etelis carbunculus</i>
<b>Local Name</b>	opakapaka	onaga	ehu
<b>Preferential depth range</b>	80-240 m	200-320 m	160-360 m
<b>Spawning season</b>	June to December Kikkawa (1984), Ralston (1981)	June to November Everson <i>et al.</i> (1989)	July to September Everson (1984)

Table 3.3. Area (km<sup>2</sup>) of essential fish habitat (EFH) available for each reserve and number of released eggs for the scaled experiment. The number of released eggs was based on the habitat area of each reserve. Reserve “O” corresponds to the Kaho‘olawe Island Reserve.

<b>Reserve</b>	<b>A</b>	<b>B</b>	<b>C</b>	<b>D</b>	<b>E</b>	<b>F</b>	<b>G</b>	<b>H</b>	<b>J</b>	<b>K</b>	<b>L</b>	<b>M</b>	<b>O</b>
<b>Essential fish habitat (0-400 m) area (km<sup>2</sup>)</b>	35	31	30	87	61	203	35	51	53	363	37	26	164
<b>Number of released eggs</b>	138	124	119	342	239	797	140	201	210	1429	144	100	647

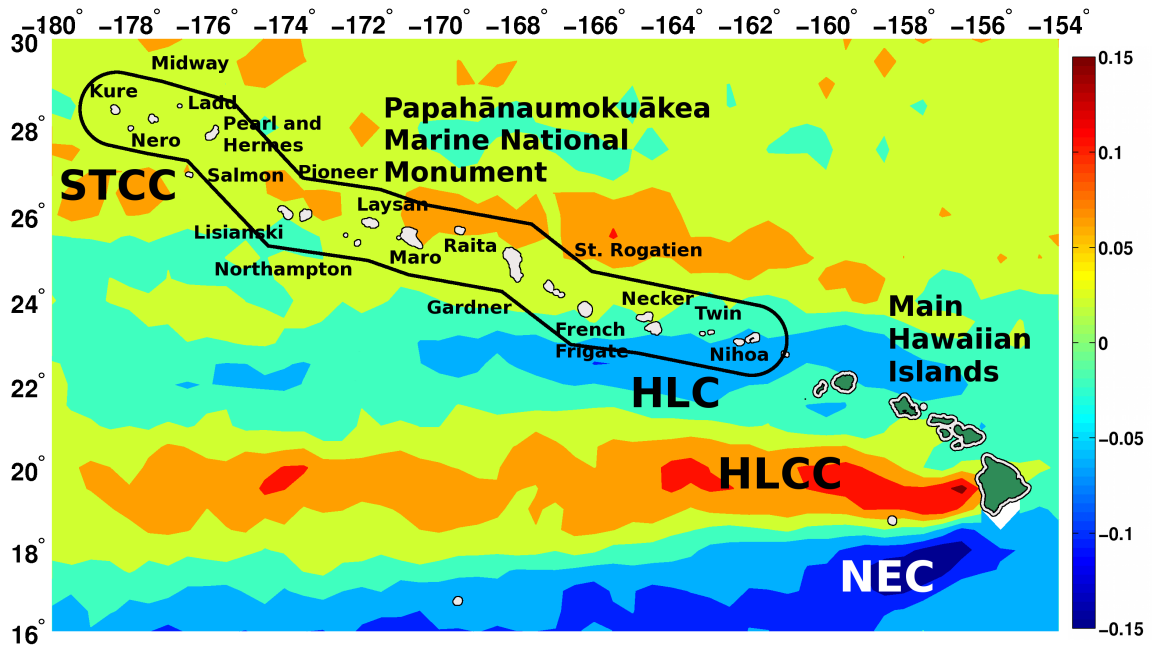


Figure 3.1. Study Area. The location of the Papahānaumokuākea Marine National Monument (PMNM), Main Hawaiian Islands (MHI) and mean currents are indicated in the map (in m/s). The background represents the geostrophic zonal velocity from AVISO, averaged from 2004 to 2011. NEC stands for the North Equatorial Current, HLCC for Hawaiian Lee Counter Current, HLC for the Hawaiian Lee Current, and STCC for Subtropical Counter Current. White areas represent release/destination sites at 75 m depth.

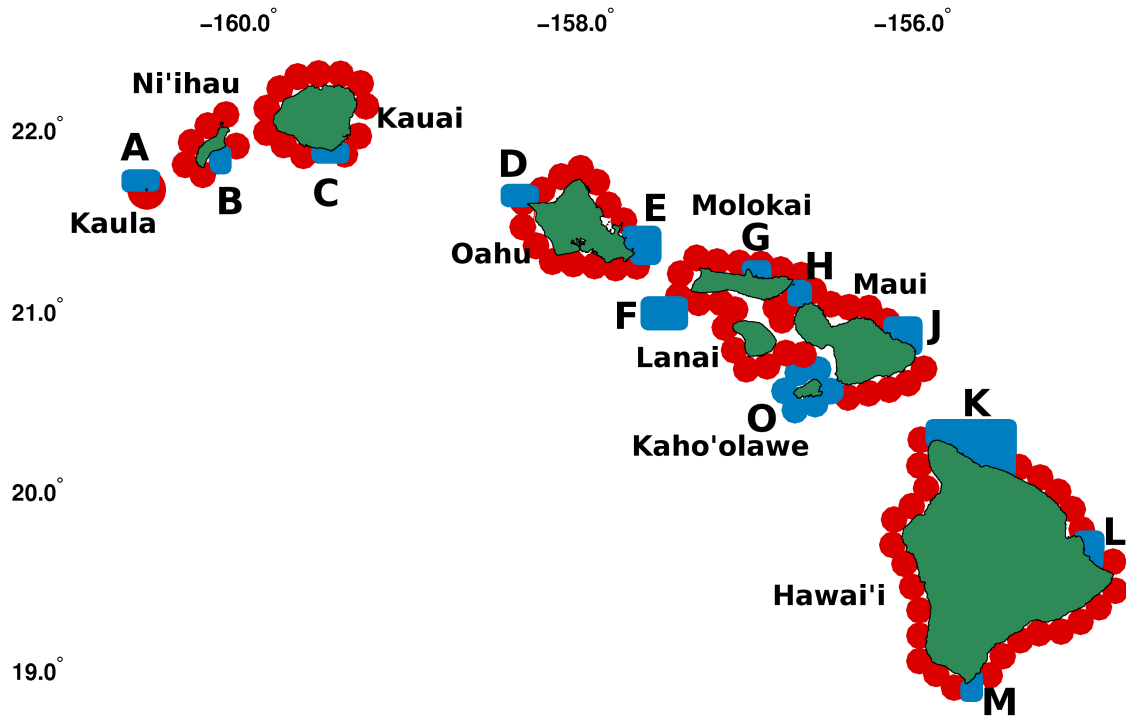


Figure 3.2. Map of the Main Hawaiian Islands. The polygons are a 14 km wide region around the land contour at 75 m. The bottomfish reserves (BRFAs) are shown in blue, and are named with the letters from A to M. The Kaho'olawe Island Reserve is also shown in blue, and is indicated with the letter O. The red polygons are the "fishing" sites: zones where bottomfish is found and are open to bottomfish fisheries.

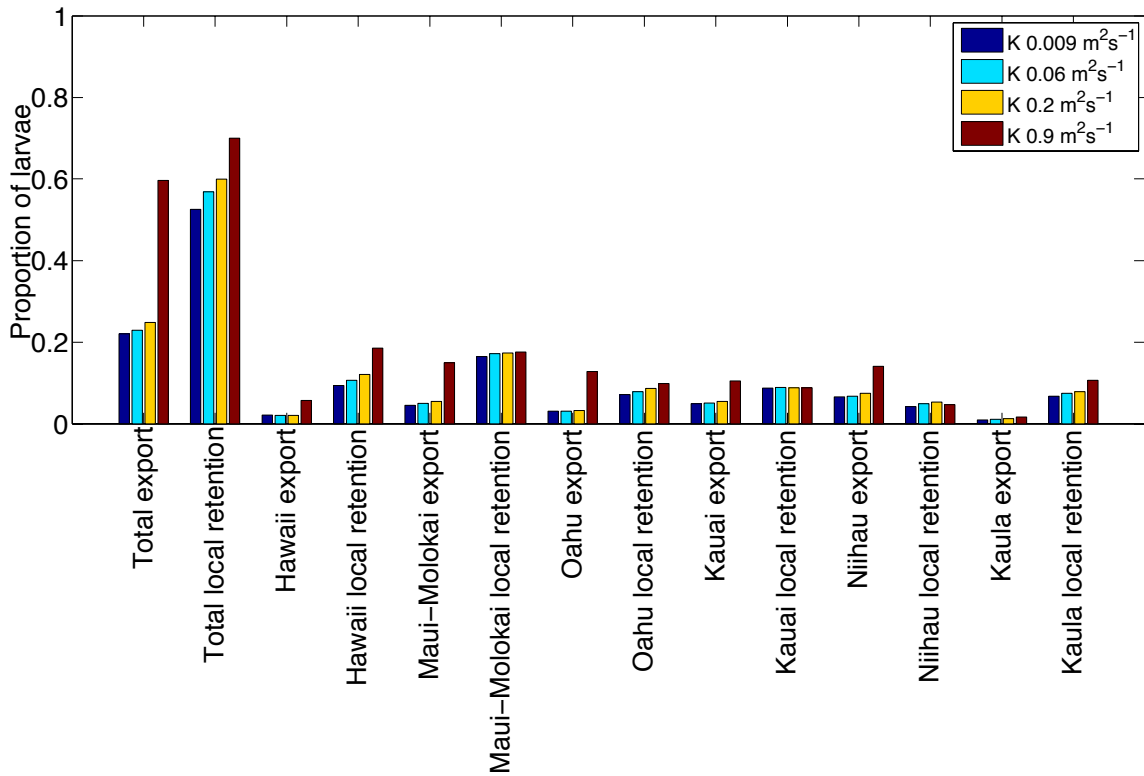


Figure 3.3. Local retention and export per island considering different diffusion coefficients. For one year, 100 larvae were released every five days at 75 m and dispersed for 30 days using global HYCOM flow fields. Larvae were actively buoyant and presented ontogenic vertical migration (OVM). The proportion of retained larvae was given as: (number of viable larvae)/(total larvae released) and was based on 72 releases for each diffusion coefficient.

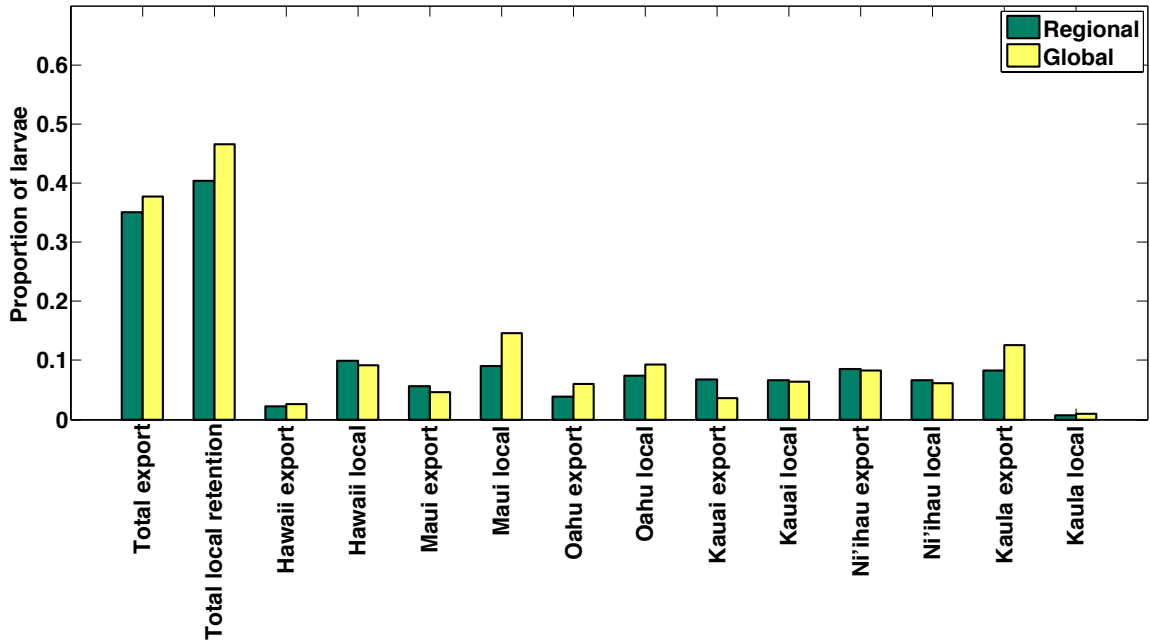


Figure 3.4. Local retention and export per island considering larvae advected using velocities from the regional and global HYCOM. For one year, 100 larvae were released every five days at 75 m and dispersed for 30 days using global and regional HYCOM velocities. Larvae were actively buoyant and presented ontogenic vertical migration (OVM). The proportion of retained larvae was given as: (number of viable larvae)/(total larvae released) and was based on 72 releases for each implementation of HYCOM.

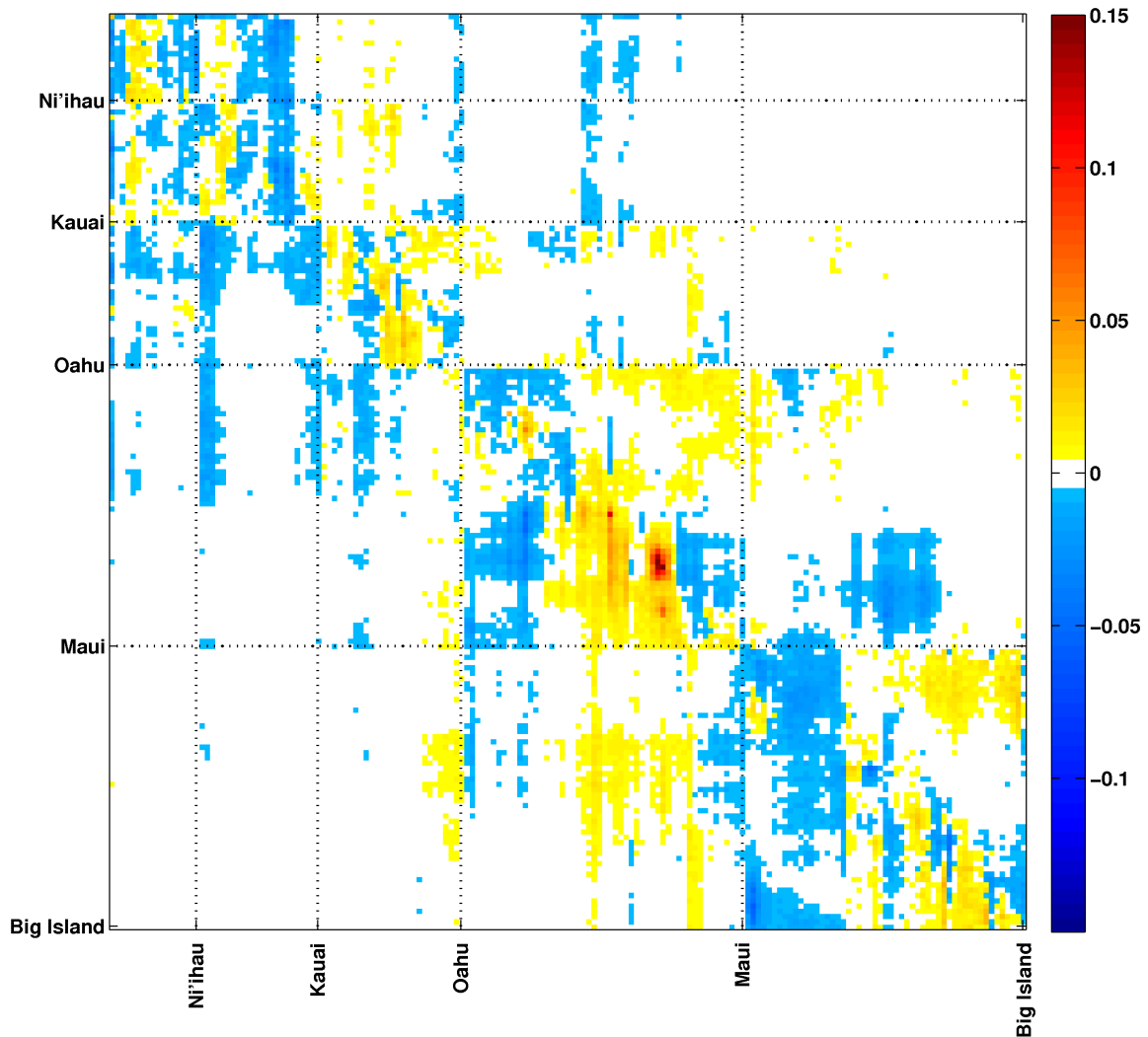
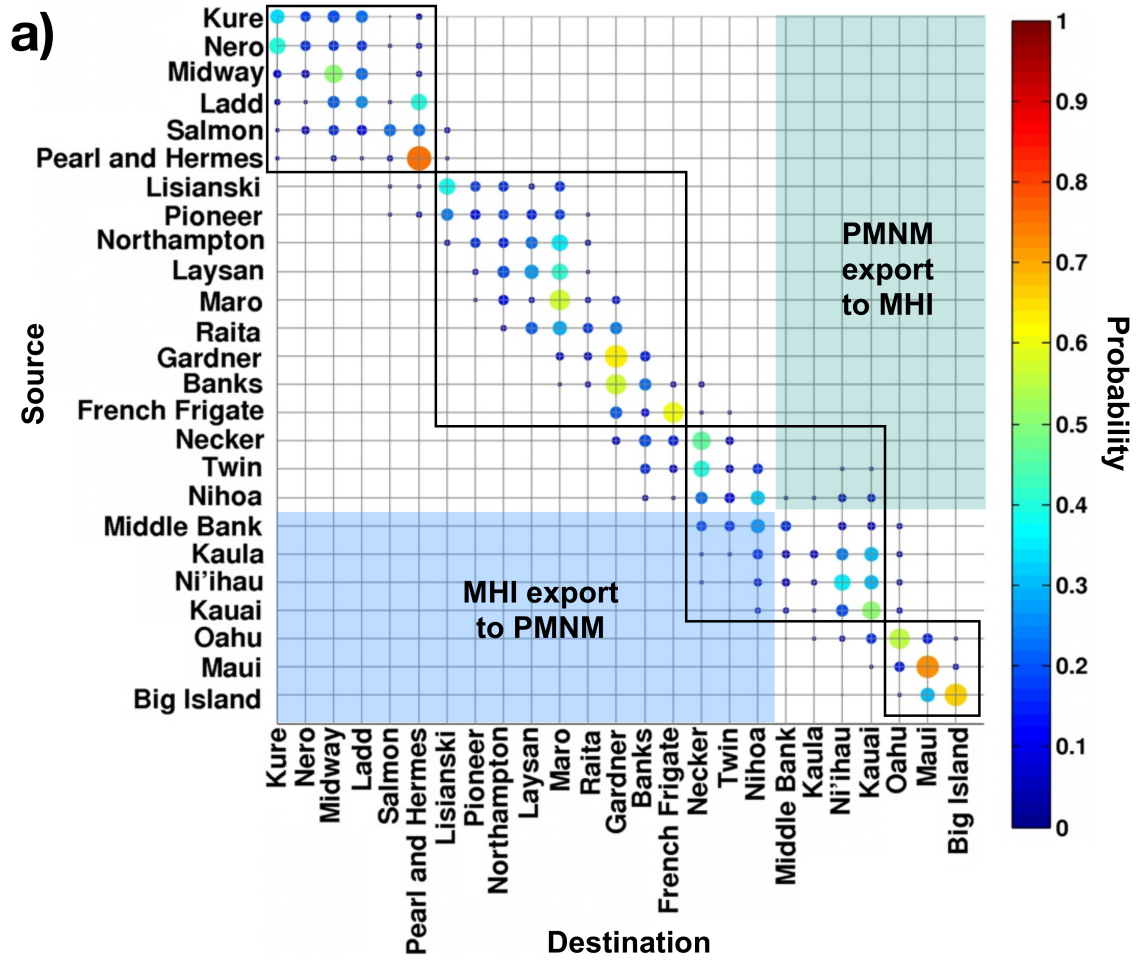


Figure 3.5. Difference between the connectivity matrices for larvae advected with velocities from the global and regional HYCOM. Positive (negative) values represent higher retention using velocities from the global (regional) HYCOM. This figure shows the probability of transport among all release and destination polygons (see polygons on Figure 2), and it is based on 84 releases for each implementation of HYCOM. For two years, from June to December 100 larvae were released every 5 days at 75 meters depth and dispersed for 30 days. Larvae were actively buoyant and presented ontogenic vertical migration.





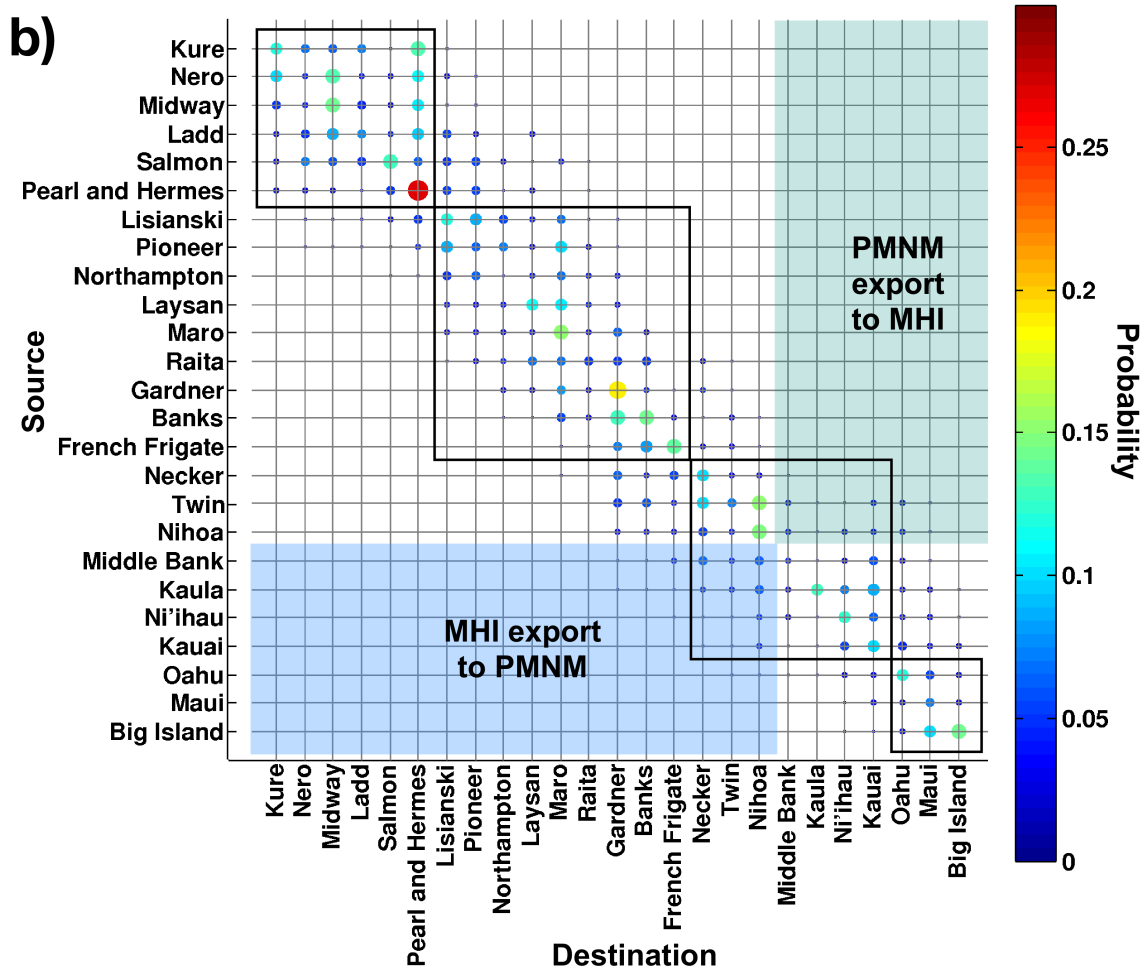


Figure 3.6. (a) Connectivity matrix for opakaopaka (*Pristipomoides filamentosus*) for a pelagic larval duration (PLD) of 30 days, based on 210 releases. (b) Variance of the connectivity matrices calculated considering twelve scenarios: three species, two PLDs and ontogenic vertical migration (OVM) schemes, based on 1920 releases. The shaded areas represent the transport among the Papahānaumokuākea Marine National Monument (PMNM) and the Main Hawaiian Islands (MHI). Black boxes represent zones where larvae released are mostly locally-retained. At (a) the probability at each cell ( $i,j$ ) is given by the number of particles leaving the spawning site  $i$  and arriving at the settlement site  $j$ , divided by the number of particles leaving the spawning site  $i$  and arriving at any settlement site. Therefore, when calculating the probability matrix, only the retained particles were considered.

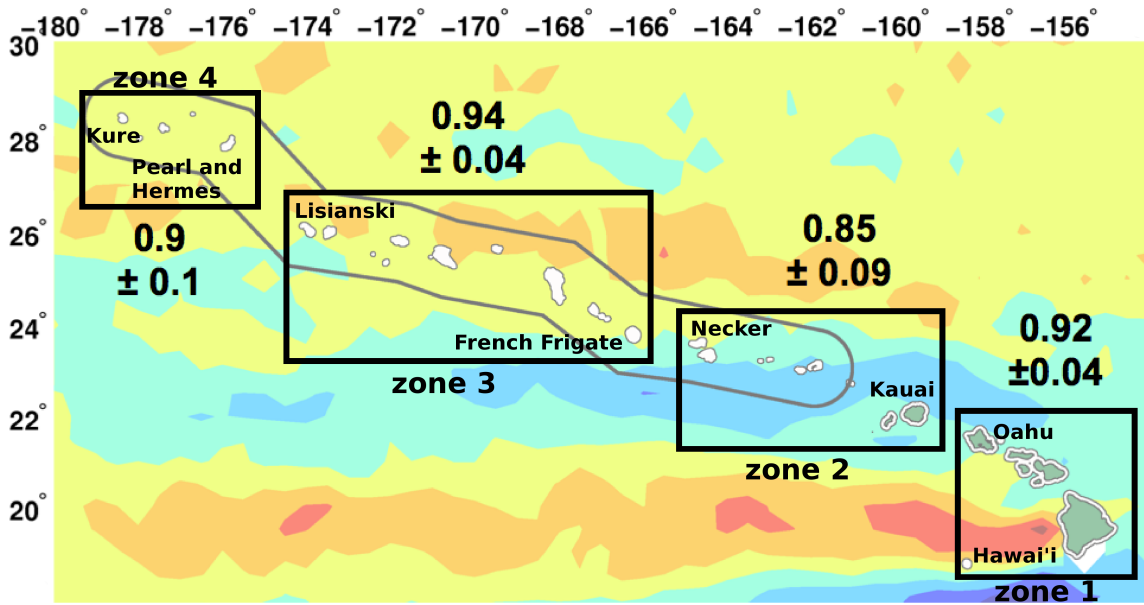


Figure 3.7. Limits of the self-contained zones (black boxes). Most of the larvae released at each one of these zones are locally retained. The mean and standard deviation of the probability of local retention is indicated for each group of islands. These values were calculated considering twelve scenarios: three species, two PLDs and ontogenic vertical migration (OVM) schemes, based on 1920 releases. White areas represent release/destination sites at 75 m depth.

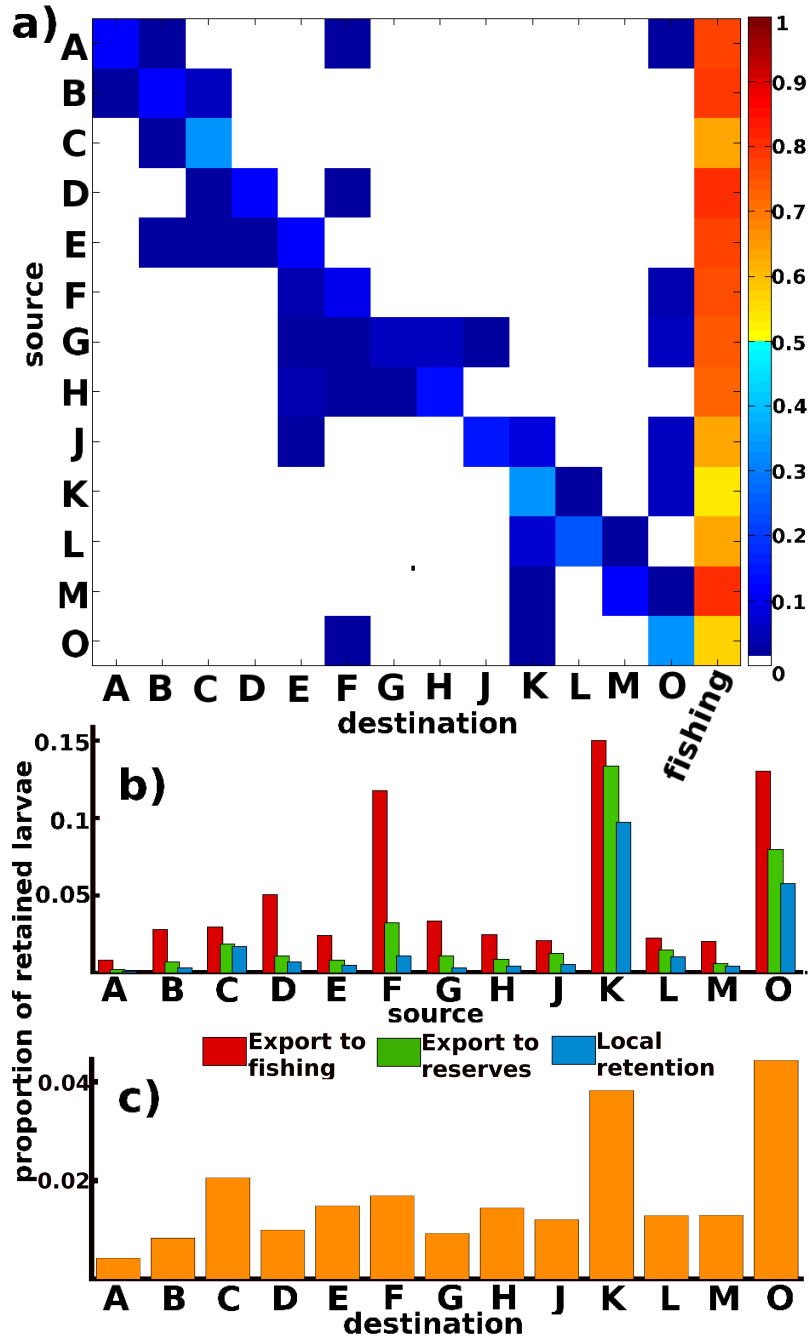


Figure 3.8. (a) Connectivity matrix for larvae released inside reserves; (b) Destination of viable larvae released inside each reserve; (c) Proportion of larvae received by each reserve. Both proportions and the connectivity matrix are averaged for the three species and for pelagic larval durations (PLD) of 30 and 60 days, based on 384 releases. (a-b) were calculated considering only larvae released inside reserves; (c) considered larvae released (and retained) at fishing sites and reserves.

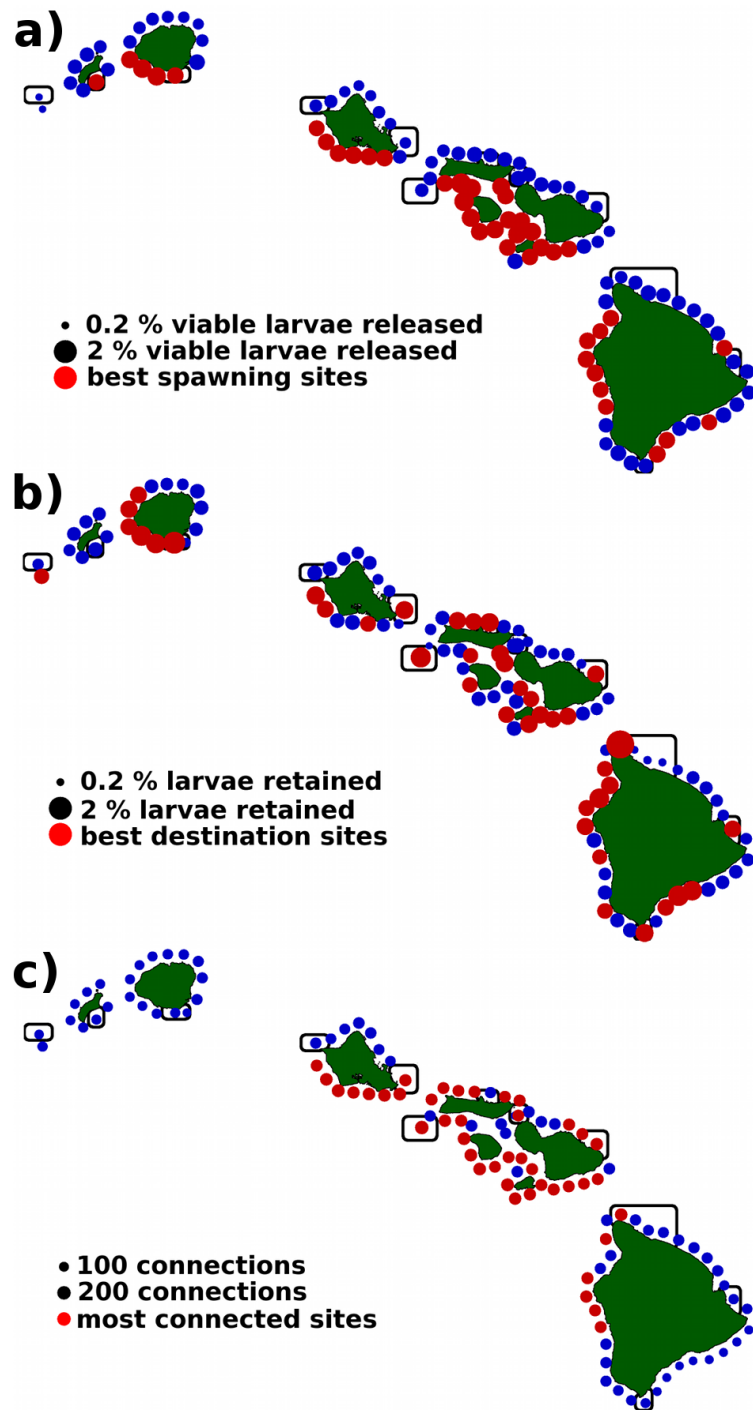


Figure 3.9. Proportion of (a) viable larvae released per spawning site, (b) viable larvae at destination sites, and (c) number of connections. Existing reserves boundaries are shown in black. The 40% of the sites presenting the higher values of viable larvae release, larval retention and number of connections, were defined as the best spawning, destination and most connected sites, respectively. Proportions are based on the total number of viable larvae, not considering larvae dispersed to the ocean. Values were averaged for three species and two pelagic larval durations, based on 384 releases.

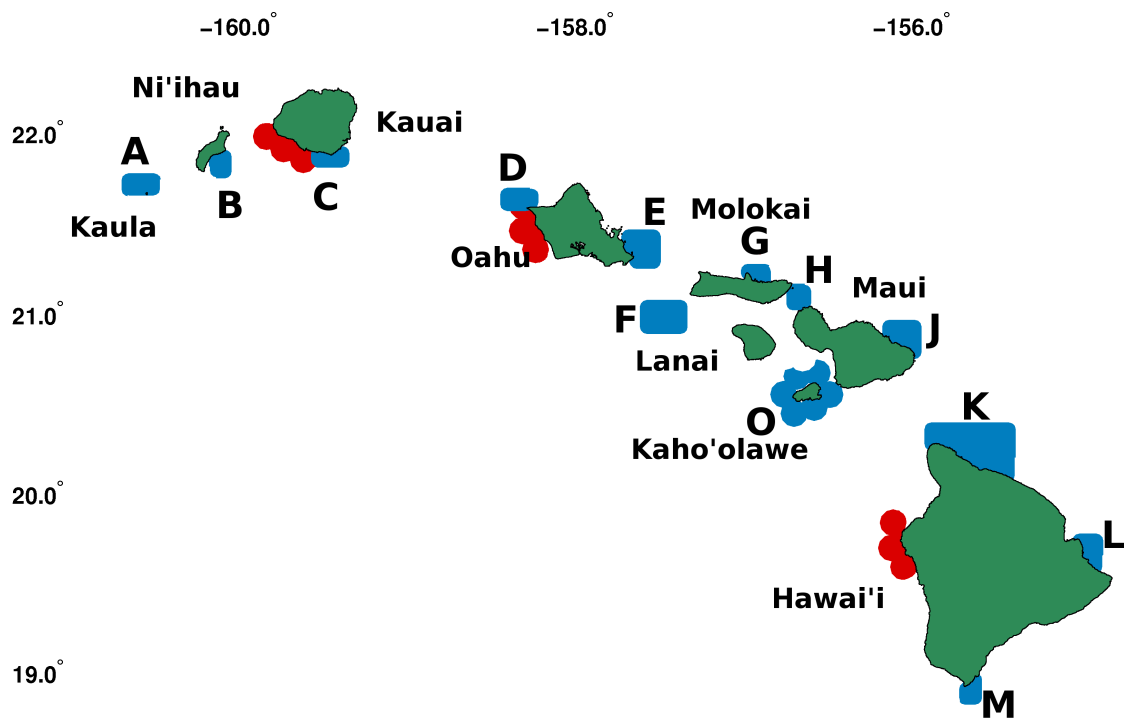


Figure 3.10. Candidate sites for future reserve designation are shown in red. Existing reserves boundaries are shown in blue. Candidate areas were evaluated on three aspects regarding larval dispersal: i) efficiency as release sites; ii) efficiency as retention sites; iii) connectivity. Indicators of habitat suitability and presence of bottomfish species were also considered (Parke, 2007, Christopher Kelley, personal communication, Hawai'i Division of Aquatic Resources).

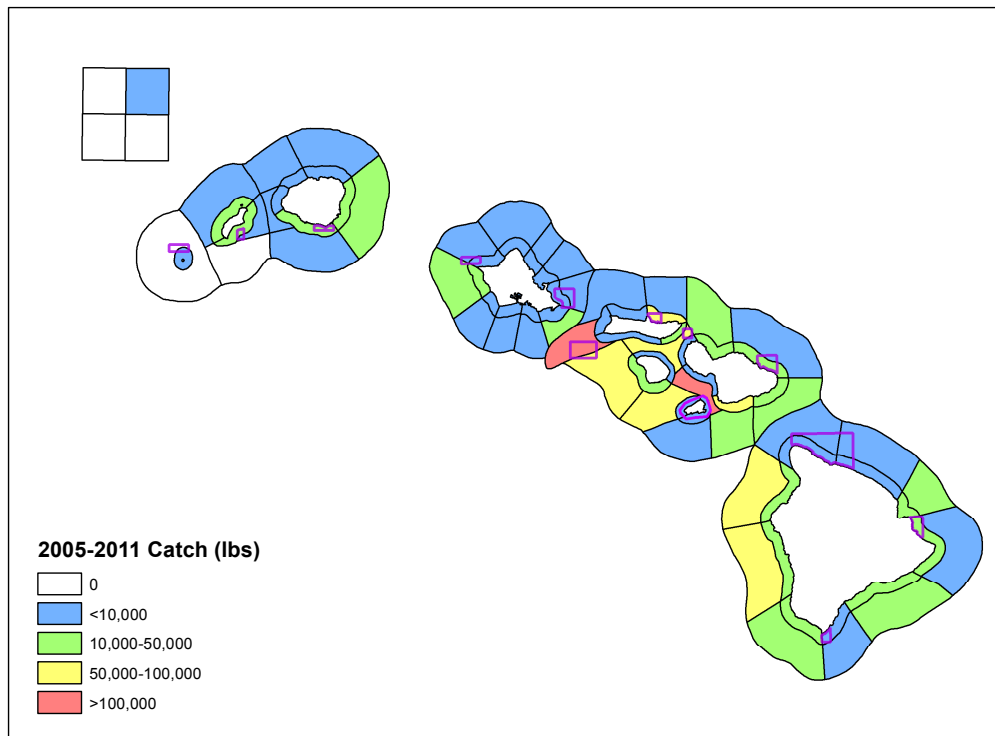


Figure 3.11. Pounds of bottomfish caught per fishery reporting zone of the Hawai'i Division of Aquatic Resources (HDAR), from 2005 to 2011. Bottomfish reported include the following species: *Pristipomoides filamentosus* (opakapaka), *Etelis carbunculus* (ehu), *Etelis coruscans* (onaga), *Epinephelus quernus* (hapu'upu'u), *Pristipomoides sieboldi* (kalekale), *Aphareus rutilans* (lehi), *Seriola dumerili* (kahala) and *Pristipomoides zonatus* (gindai). It is important to highlight that prior to 2011 the catch from Middle Bank (northern most squares) could be recorded as part of the Papahānaumokuākea Marine National Monument (PMNM) catch. In 2011, after the closure of the PMNM, 5,750 lbs of bottomfish were recorded as caught in the Middle Bank region, representing most of the catches in the region from 2005-2011.

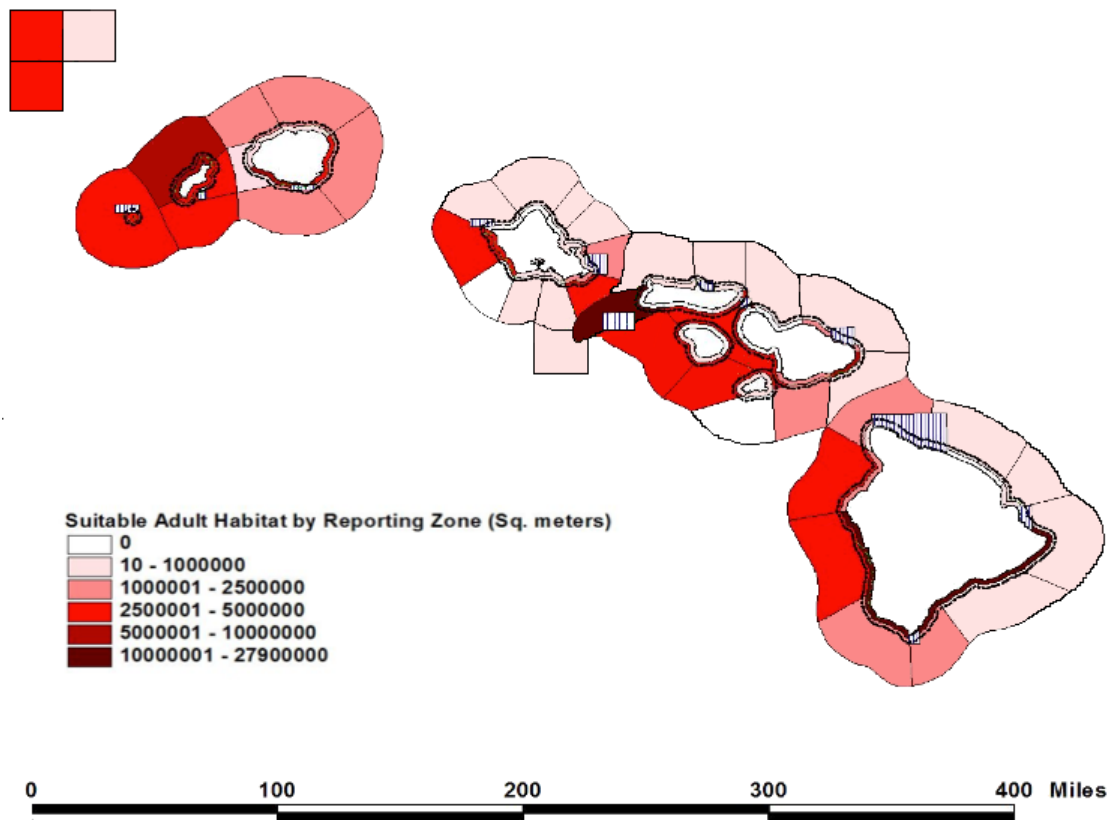


Figure 3.12. Location of the Hawai'i Division of Aquatic Resources (HDAR) fishery reporting zones, indicating the area of bottomfish habitat (m<sup>2</sup>) per zone. From Parke (2007).



## Chapter 4

### Early life stage dispersal of yellowfin tuna (*Thunnus albacares*) in the Hawaiian Region

#### 4.1 Introduction

Yellowfin tuna (*Thunnus albacares*) is one of the most important commercially harvested tuna species in the Pacific, and represents a large percentage of Hawaiian longline, handline, and troll fisheries (Western Pacific Regional Fishery Management Council, 2009). Understanding yellowfin tuna movement patterns throughout its life history is imperative to adequately manage these fisheries (Palumbi, 2004). Previous research on this species in the Hawaiian region contradicted prevailing opinion that all tuna species are highly migratory (Sibert and Hampton, 2003, Schaefer *et al.*, 2007, Wells *et al.*, 2011). Information obtained from both conventional and electronic tagging studies revealed that yellowfin tuna are characterized by short range movement around the Hawaiian Islands, seamounts, and feeding aggregating devices (FADS) (Itano and Holland, 2000, Sibert and Hampton, 2003, Dagorn *et al.*, 2007). Moreover, analyses of otolith chemical and stable isotope signatures concluded that one year old yellowfin sub-adults caught in the Hawaiian inshore fisheries were locally spawned (Wells *et al.*, 2011). However, questions regarding the origin of the tuna fished, and the degree of stock mixing due to tuna movement at different life stages, remain unanswered. This study focused on the early life stages of yellowfin tuna, aiming to elucidate their distribution

and retention patterns in the waters surrounding the Main Hawaiian Islands (MHI, Figure 4.1).

The spawning of yellowfin tuna in the study region reveals an unmistakable seasonal cycle, with spawning taking place from April to November, and peaking between June and August (Figure 4.2, Itano, 2000). Yellowfin tuna spawning activity were observed to onset when surface water temperatures exceed 24°C (Itano, 2000). Investigated here is if larval retention is a key factor in the optimization of seasonal spawning strategies of yellowfin tuna around the MHI. This was accomplished by incorporating output from a three-dimensional model that simulates ocean circulation (HYCOM) into a biological model (Connectivity Modeling System, CMS) that depicts adult spawning strategies, larval development, behavior, and dispersal (Paris *et al.*, 2007, Helgers and Paris, 2011). This methodology revealed potential characteristics of yellowfin tuna larval dispersal pathways in the Hawaiian archipelago. Specifically, this study evaluated if larvae spawned around the MHI and Cross Seamount were locally retained, and if biological traits affect yellowfin tuna larvae retention and seasonal variability. Finally, estimates of inshore-offshore larval distribution patterns, and its implications for larval survival, were explored.

## **4.2 Methodology**

### **4.2.1 Hydrodynamic model**

This study used the hydrodynamic model HYCOM, a primitive equation ocean circulation model, as the generalized vertical coordinate allow the defined vertical grid

spacing to be based on the vertical structure of the ocean: isopycnic (density-following) in stratified ocean interior, level (pressure-following) in unstratified regions such as the surface mixed layer, and sigma (terrain-following) in coastal and shelf seas (Bleck, 2002). Flow fields from a regional implementation of HYCOM (Jia *et al.*, 2011) were used to examine larval dispersal characteristics. The Hawai'i regional HYCOM ("regional HYCOM" hereafter) is configured in a nested subdomain covering the MHI (16-26°N, 150-166°W) within the global HYCOM (<http://hycom.org/global>), which supplies model fields for initialization and at the four open lateral boundaries. The regional HYCOM has 32 vertical layers and a horizontal resolution of 0.04° (~4 km). Away from the lateral boundary zones where open boundary conditions were applied, the bathymetry is replaced by the General Bathymetric Chart of the Oceans database (GEBCO, 0.016°, <http://www.gebco.net/>) which captured the regional relief features, providing an improved representation of the islands' coastlines. The regional HYCOM was forced at the surface with output from a regional atmospheric model, the Weather Research Forecasting system (WRF, <http://www.soest.hawaii.edu/MET/Faculty/wrf/arw/index.html>), with a resolution of 0.06°. No data assimilation was applied in the regional HYCOM (c.f. Jia *et al.*, 2011). Operational output from the regional implementations of HYCOM was found at [http://apdrc.soest.hawaii.edu/datadoc/hycom\\_hawaii.phd](http://apdrc.soest.hawaii.edu/datadoc/hycom_hawaii.phd).

#### **4.2.2 Individual-based Model**

This study used a Connectivity Modeling System (CMS), an Individual-based model (IBM) system developed to address larval transport questions at multiple spatial and temporal scales (Paris *et al.*, 2007, Helger and Paris, 2011, Paris *et al.*, submitted).

Deterministic movement in the model was simulated by a fourth order Runge-Kutta integration scheme of the simulated velocity field, while the turbulence was modeled by simple diffusion (Paris *et al.*, 2007). The used horizontal coefficient of diffusivity was 0.2 m<sup>2</sup>/s, estimated from Okubo (1971). Biological traits parameterized in the model included egg buoyancy, ontogenic vertical migration (OVM), coast avoidance, and mortality. Yellowfin tuna's preferential habitat was represented by the spawning sites. Larval OVM was parameterized in the model by a matrix of probability density functions (PDFs). The matrix contained the probabilities of vertical distribution of eggs/larvae for each time step. Vertical velocities were not considered to displace larvae, as it was assumed that larvae kept their vertical position, as observed from *in situ* studies (Paris and Cowen, 2004, Paris *et al.*, 2007). In nature, larvae swim to avoid becoming stranded on land. This behavior was parameterized in the model with a variable spatial interpolation scheme of the velocity field around the particle, which ensured that the particle would remain within the water grid points (c.f. Helger and Paris, 2011). The model output was used to determine the proportions of retained larvae, their spatial distributions, and onshore-offshore dispersal probabilities. The onshore-offshore dispersal probabilities reflect the probability of larval dispersal in the cross-shelf direction from all spawning sites. The probability at each distance range  $x$  and time  $t$  was given by the number of larvae found within the distance range  $x$  divided by the number of larvae found from 0 to 90 km offshore. Thus, larvae dispersed to open ocean waters were not considered in the analysis.

### **4.2.3 Adaption to Yellowfin tuna**

The spawning activity of yellowfin tuna in the Central Pacific region was characterized by Itano (2000). In the Hawaiian Islands inshore waters, spawning occurs close to the surface, from spring to fall, peaking between June and August. The spawning events in the model were therefore restricted to this period and depths of up to 50 meters. The influence of spawning locations on larval dispersal characteristics was tested, with the following locations considered: a) inshore, i.e. a distance of 20 nautical miles (nm) from the 400 m isobath, and b) oceanic, i.e., between 20 nm to 50 nm from the 400 m isobath; as shown on Figure 4.1. Larval dispersal was tracked for 30 days, a period similar to yellowfin larvae transition time, which occurs approximately three weeks after hatching (Kaji *et al.*, 1999, Margulies *et al.*, 2007a, Wexler *et al.*, 2011). Other parameters of the model were defined by a sensitivity analyses described below.

### **4.2.4 Sensitivity analyses**

Beyond addressing key parameters that influence larval dispersal, a sensitivity analysis is necessary to obtain reliable results and test the model's robustness (Edwards *et al.*, 2007, Pineda *et al.*, 2007). The parameters tested here were: a) number of eggs released, b) mortality, and c) ontogenic migration. The first tested variable was the minimum number of eggs necessary for the model to reach stability. Reaching stability was defined as a constant amount of retained larvae within inshore and offshore locations at the end of the simulation (c.f. North *et al.*, 2009). The number of eggs released were: i) 800, ii) 400, iii) 160, iv) 80, and v) 40. The mortality schemes tested were: i) absence of mortality, ii) a constant mortality index equal to the half life of the larval cohort, iii) a

spatio-temporal variable mortality coefficient.

A variable mortality coefficient was included in this study because specific ranges of turbulent dissipation rate were observed to substantially increase the encounter rates of larvae and their prey (Cury and Roy, 1989, Muelbert *et al.*, 1994, MacKenzie and Kiørboe, 1995). Laboratory studies confirmed that the survival of yellowfin tuna larvae is enhanced at specific ranges of wind-induced turbulence (Margulies *et al.* 2001, Kimura *et al.*, 2004). Margulies *et al.* (2007b) converted the optimal turbulent dissipation rate to wind velocities, using a boundary layer model (c.f. MacKenzie and Legget, 1993), and estimated that the survival of larvae concentrated at 10 m depth was three times higher for surface wind velocities from 2.6 to 3.5 m/s. Considering these results, a mortality index was created, varying in both time and space (c.f. Table 4.1). Surface wind velocities were obtained from the WRF Hawai'i Regional model (<http://www.soest.hawaii.edu/MET/Faculty/wrf/arw/index.html>) and binned into 0.2 x 0.2 degrees bins. The mortality index was calculated from the binned wind field for each day of simulation, following the values shown in Table 4.1. Similarly, the number of larvae at each bin was computed and the mortality rates were applied daily for each bin.

Available studies indicate that yellowfin tuna larvae do not perform a diel vertical migration (Suzuki, 1994, Boehlert and Mundy, 1994). However, ontogenic changes in their buoyancy might play an important role in determining their vertical distributions (Boehlert and Mundy, 1994), and were included in the model. Three different vertical migration schemes were considered: larvae concentrated at i) 10 to 20 meters, ii) near surface layers (0 to 10 meters), and iii) deeper layers (20 to 30 meters). The vertical

distributions were based on laboratory and field observations (Matsumoto, 1958, Leis, 1991, Boherlet and Mundy, 1994, Margulies *et al.*, 2007a, Llopiz, 2009). Most *in situ* studies revealed large concentrations of larvae at the upper mixing layer, restricted to the upper 50 m of the water column (Matsumoto, 1958, Leis, 1991, Boherlet and Mundy, 1994, Llopiz, 2009). Margulies *et al.* (2007a) studying eggs and larvae in captivity, reported that after fertilization eggs had a strong positive buoyancy and became negatively buoyant only 2 to 4 hours before hatching.

The sensitivity simulation results showed that varying the number of released eggs did not significantly affect the proportion of retained larvae within inshore or offshore regions (results not shown), with a minimum of 40 eggs released per spawning site. Similarly, the proportion of larval retention from different mortality schemes (absence of mortality, constant mortality, and spatially-temporally varying mortality) were not significantly different (Figure 4.3). In the same way, using different OVM schemes did not substantially affect the proportion of retained larvae (Figure 4.4). Further, different mortality or migration schemes did not significantly affect inshore-offshore larval distributions. All results were tested with a t-test, at 95%. Considering these results, no mortality coefficient was applied to the larvae. Their behavior was parameterized by the first OVM scheme, with larvae concentrated between 10 to 20 meters depth. The number of eggs released per spawning site was based on Itano (2000, Figure 4.2). A minimum of 40 eggs (per release site) were released in November, while a maximum of 800 eggs were spawned in July.

### 4.3 Results

Numerical experiments allowed the determination of retention patterns for different months as a function of spawning locations. It also allowed the identification of regions where a higher proportion of viable larvae are released. When all spawning locations were considered, the results showed that about 20% of the released eggs were retained within 20 nautical miles (37 km) of the MHI and Cross Seamount, and another 20% was retained from 20 nm to 50 nm (from 37 to 92 km). The time evolution showed that after 20 days, the proportion of larvae retained within these limits was nearly constant, i.e., values of retention were not significantly different (Figure 4.4).

When all spawning sites were considered there was no seasonality on the proportion of retained larvae either at inshore or offshore areas. Also, the small values of the standard deviations indicated a small inter-annual variability of retention (Figure 4.5). Likewise, when considering individual spawning sites, the monthly retention for each one of the sites did not present a clear pattern of seasonal variation. However, the monthly retention for some spawning sites presented higher interannual variation than shown in Figure 4.5 (results not shown).

Comparing the successful retention of larvae released at inshore and offshore areas (Figure 4.6), it was found that larvae originating inshore were more likely to be retained than those spawned offshore. The spawning sites which produced the least amount of viable larvae were Kaua‘i, Ni‘ihau and Ka‘ula. The most successfully retained larvae were released at spawning sites around Hawai‘i Island and Cross Seamount.



The time evolution of the cross-shore direction larval distribution probabilities (inshore-offshore, Figure 4.7) showed that the proportion of larvae nearshore (less than 10 km from the coast) tended to increase with time. After 16 days of dispersal, when larvae are transitioning to piscivory, the proportion of larvae in nearshore sites was significantly higher than open ocean sites (more than 10 km from the coast), as tested by an ANOVA and a multiple comparison test at 95% significance. This result held true for larvae released exclusively at offshore sites. However, for larvae released at inshore sites, the proportion of larvae at nearshore sites was significantly different from open ocean sites for transitioning juveniles, or after 26 days of dispersal. The proportion of larvae retained from 35 to 80 km offshore was approximately of 60%, for stages older than feeding larvae (6 days of dispersal) and all release scenarios.

To evaluate the existence of persistent larval dispersal pathways or accumulation zones, the larval distributions over the study area were calculated from the larval trajectories for each release, and distributions were averaged over the entire simulation time (Figure 4.8). The standard deviation of the larval distributions were much bigger than the average patterns (result not shown). No clear dispersal pathways or accumulation zones appeared on the averaged larval distributions, suggesting that dispersal patterns are highly variable. To assess the importance of time evolving eddying field on the observed larval dispersal patterns, an experiment was conducted with larvae dispersed by the averaged velocity field from the regional HYCOM, with all other IBM parameters unaltered. The velocities of the hydrodynamic model were averaged for the spawning period of yellowfin tuna from 2009 to 2011. When larvae were dispersed with the

averaged flow, the proportion of retained larvae increased to about 70% of the released larvae. Larvae were dispersed predominantly in the northeastward direction (Figure 4.9), and were also recirculated by the gyres located around the islands of Hawai‘i, Maui, Kaho‘olawe, and Moloka‘i.

## **4.4 Discussion**

### **4.4.1 Patterns of larval retention**

According to the results, the physical environment during yellowfin tuna spawning season was favorable for larval retention. Simulations results showed that after 20 days of dispersal, the number of retained larvae was nearly constant, at both inshore (less than 37 km from the islands) and offshore (less than 92 km) regions around the MHI and Cross Seamount. This was a strong indication that yellowfin tuna larvae released in Hawai‘i were locally retained. Despite the high amount of larval retention (40%), no persistent pathways or concentration zones were present for the period of simulation. The high standard deviations of the monthly larval distributions corroborates the conclusions of Chapter 2 that the environment around the MHI and Cross Seamount is highly variable, and that the timing of spawning can play an important role in larval dispersal patterns. Indeed, larvae dispersed by the averaged flow field showed even larger retention values (Figure 4.9), implying that the time evolving eddying flow contributed to disperse larvae at the spatio-temporal scales considered in this study (Figure 4.8). In Chapter 2, it was shown that at finer scales the time evolving eddying field increased connectivity around the island of Hawai‘i. In the same way, at the broader spatial scales considered here, the eddying field contributed to increase the dispersion of larvae in multiple

directions. Larvae dispersed by the averaged flow fields and released around O‘ahu, Kaua‘i, Ni‘ihau and the windward sides of Maui and Moloka‘i followed predominately northeastward trajectories, in the direction of propagation of the North Hawaiian Ridge Current (NHRC) and the Hawai‘i Lee Current (HLC). On the other hand, larvae released on the leeward side of Maui, Moloka‘i, Kaho‘olawe, Hawai‘i, and at Cross Seamount were recirculated in the leeward gyres of the averaged flow field. Those pathways of dispersal were not apparent in the averaged larval distributions (Figure 4.8).

In any case, retention rates in nature are likely a function of the dispersal caused by the physical environment, as shown here, and the biological traits of the larvae, particularly swimming ability, which was not considered in the presented simulations. *Thunnus albacares* larval developmental patterns have been shown to be variable and dependent on temperature, density of larvae, and food availability (Jeanne Wexler, *personal communication*). Larvae in the post-flexion stage usually transition to piscivory from 2 to 3 weeks after hatching (Wexler *et al.*, 2011). By this stage, larvae have developed strong swimming abilities. Indeed, yellowfin tuna larvae from 25 to 30 days post-hatching start to exhibit schooling behavior (Jeanne Wexler, *personal communication*). The favorable physical environment for retention may increase the probability of larval survival, particularly at the critical onset periods for piscivory and schooling, when larvae can exhibit cannibalism. Proximity to islands during early life stages is believed to benefit the larvae from a range of species. Nearshore environments might present a higher abundance of prey than offshore areas (Leis, 1982, Boehlert and Mundy, 1996), which can be crucial for oceanic islands surrounded by oligotrophic

environments. *Thunnus* spp. larvae in other subtropical regions generally displayed an omnivorous diet before piscivory (Llopiz *et al.*, 2010), indicating their ability to take advantage of a food rich environment. Further, a food rich environment decreases the pressure of cannibalism from larger individuals on smaller-sized organisms, as estimated with computer simulations that considered a range of pelagic larvae and laboratory studies of *Thunnus orientalis* (bluefin tuna) larvae (Nishimura and Hoshino, 1999, Ishibashi *et al.*, 2012).

Moreover, it is likely that yellowfin tuna larvae are able to detect the coast through a range of physical and biological cues, such as noise, chemical stimuli, and visual signals, as shown for other species (Kingsford *et al.*, 2002, Leis *et al.*, 2006, Gerlach *et al.*, 2007). *Thunnus* spp. larvae are able swimmers at 20 days post-hatching, and can potentially orient their movement towards the coast. Other species have shown directional swimming near a reef, in the presence of a behavioral cue, or related to foraging behavior (Leis *et al.*, 2007, Woodson and McManus, 2007, Paris *et al.*, 2009). Numerical studies revealed that behavioral swimming can potentially increase the number of larvae retained at nursery areas and decrease dispersal distances (Staaterman *et al.*, 2012).

#### **4.4.2 Larval retention and seasonality of spawning**

Although the physical environment was conducive to larval retention, no seasonal cycle was apparent in the retention patterns (Figure 4.5), indicating that other factors are optimizing the spawning cycle observed for yellowfin tuna in the Hawaiian

Islands. One of those factors is likely water temperature, which is known to play an essential role during the development of yellowfin tuna eggs and larvae (Margulies *et al.*, 2007a, Wexler *et al.*, 2011). The egg and yolk-sac stage duration of yellowfin tuna are inversely proportional to water temperatures, and growth rates of feeding larvae increase with higher temperatures within the optimal range for their survival (from 21°C to 33°C, Margulies *et al.*, 2007a, Wexler *et al.*, 2011). Higher growth and smaller hatching times can be beneficial to larvae because, simple put, bigger and highly motile larvae are better able to avoid predation and more efficiently forage for food. Food availability is another important factor affecting both larval survival and the onset of spawning. In the Hawaiian region, a recurrent annual feature are chlorophyll summer blooms, with intensity and position varying inter-annually as a result of physical and biological factors (Dore *et al.*, 2002, Dore *et al.*, 2008). As observed at Station Aloha (22°45'N, 158°W) the resultant higher nitrogen fixation from the phytoplankton summer blooms leads to an increase of mesozooplankton biomass (Landry *et al.*, 2001, Sheridan and Landry, 2004). Both favorable temperature and feeding conditions for the development of eggs and larvae have the potential to be optimizing factors for the spawning strategy of yellowfin tuna around the MHI, and deserve further investigation.

#### **4.4.3 Onshore-offshore dispersal probabilities**

The inshore-offshore dispersal probabilities obtained with the model showed that the proportion of larvae retained nearshore (less than 10 km from the coast) increased with time and independently of the release location (Figure 4.7). The simulation results

agreed with available data from ichthyoplankton surveys, which depicted higher abundances of *Thunnus* spp. larvae throughout nearshore waters, specifically at less than 5 km offshore (Miller, 1979, Leis, 1991, Boherlet and Mundy, 1994, Boehlert and Mundy, 1996, Fowler *et al.*, 2008). Two of these studies were conducted in the Hawaiian Islands (Miller, 1979, Boehlert and Mundy, 1994), the latter of which concluded that “larval *Thunnus* spp. may be island associated.”

However, the relative importance of the nearshore environment still needs to be fully understood. Available studies indicate that this importance might shift with larval development or changes in latitudes (Llopiz, 2009). For instance, in Hawai‘i, Boherlet and Mundy (1994) found a significant correlation between the size of the *Thunnus* spp. larvae sampled and their inshore-offshore distribution: smaller larvae tended to be sampled closer to shore while larger larvae were sampled farther away. This strategy might result from a tradeoff between mortality due to starvation and predation (Bakun and Broad, 2003) at different developmental stages. This behavior was not considered in the modeling process, hence the concentration of older, transitioning larvae in inshore waters, as shown in Figure 4.7d. However, simulation results revealed that the offshore environment from 35 to 80 km around the islands appeared to be conducive to the retention of older larvae (Figure 4.7d). Regardless, it is still a matter for debate if the offshore oligotrophic environment is suitable for larval survival (c.f. Llopiz, 2009). In Hawai‘i, several mechanisms can lead to sporadic enrichment of open ocean waters and are thus deserving of further investigation. Features, such as thin plankton layers (McManus and Woodson, 2012 for a review), cyclonic eddies, Rossby waves, surface

frontogenesis, and non linear Ekman pumping (Letelier *et al.*, 2000, Sakamoto *et al.*, 2004, Landry *et al.*, 2008, Rii *et al.*, 2008, Calil and Richards, 2010) can contribute to increased zooplankton concentrations, by injecting nutrients and/or enhancement of primary production at the upper layers of the ocean. However, it is unknown if the frequency, duration, and production of those features would be sufficient to sustain the survival of yellowfin tuna larvae. Simulation results corroborated the need for more studies focusing on the role that nearshore and offshore waters play in the survival of *Thunnus* spp. larvae (Fowler *et al.*, 2008, Llopiz, 2009).

Table 4.1. Table relating the wind velocity (at 10 m) categories and the mortality index applied per day at each one of the 0.2 x 0.2 degree bins. The percentage of larval survival for each mortality index illustrates a hypothetical case where a constant mortality was applied for 30 days.

<b>Wind velocities (<math>v_w</math>) m/s</b>	<b>Mortality index (<math>d^{-1}</math>)</b>	<b>Percentage of survival per day</b>	<b>Percentage of survival for 30 days</b>
$0 \geq v_w < 2$	0.003	99.7%	90%
$2 \geq v_w < 4$	0	100%	100%
$4 \geq v_w < 6$	0.003	99.7%	90%
$6 \geq v_w < 8$	0.007	99.3%	80%
$8 \geq v_w < 10$	0.011	98.9%	70%
$v_w \geq 10$	0.02	98%	60%



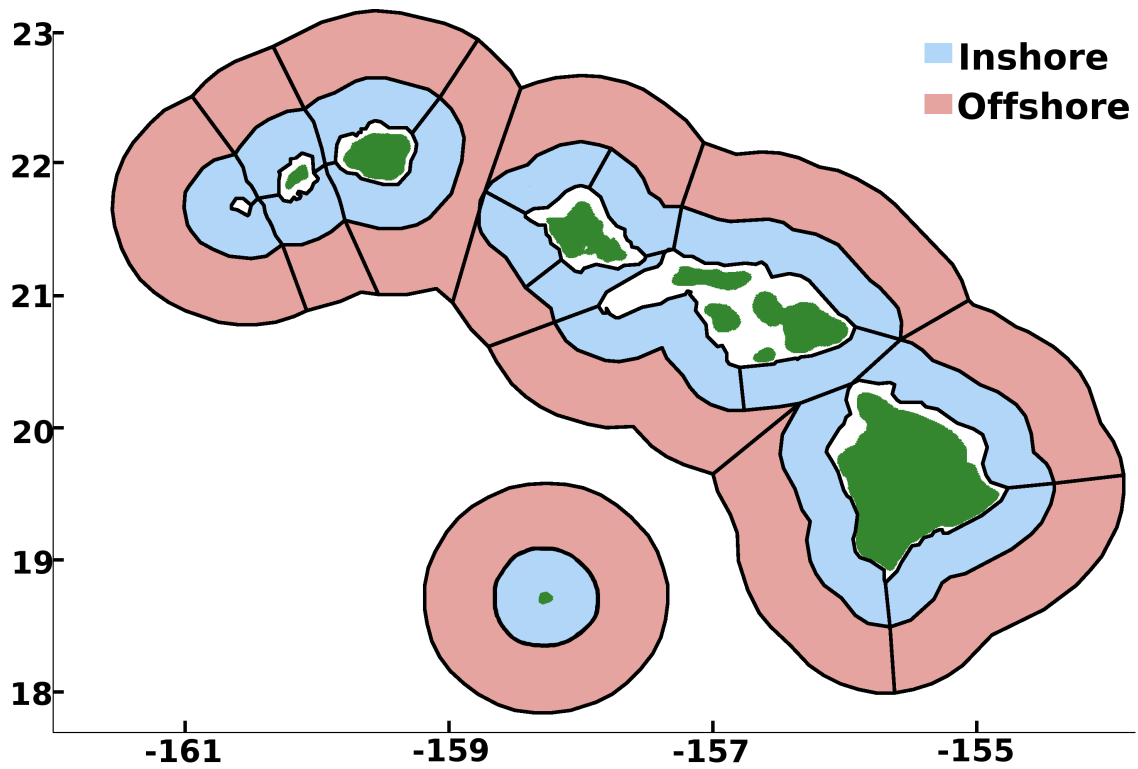


Figure 4.1. Spawning locations for yellowfin tuna. Blue areas (hereafter “inshore”) are within 20 nm (37 km) of the 400 m isobath. Pink areas (“offshore”) are from 20 nm to 50 nm (37 to 92 km) of the 400 m isobath.

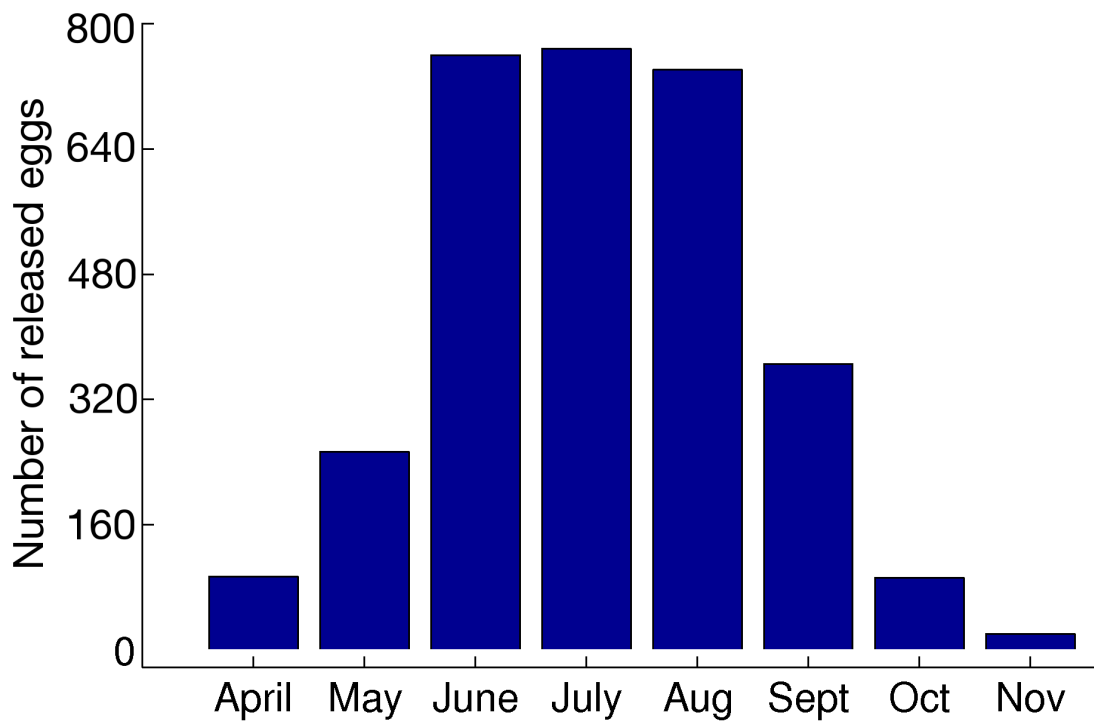


Figure 4.2. Number of eggs released per spawning area, by month of release. Percentage of spawning was based the proportion of mature yellowfin tuna in spawning condition captured per month from 1994 to 1996, as described on Itano (2000). The classification of mature females in fully yolked, atretic and spawning conditions was defined by the histological interpretation of preserved ovarian material (c.f. Itano, 2000).

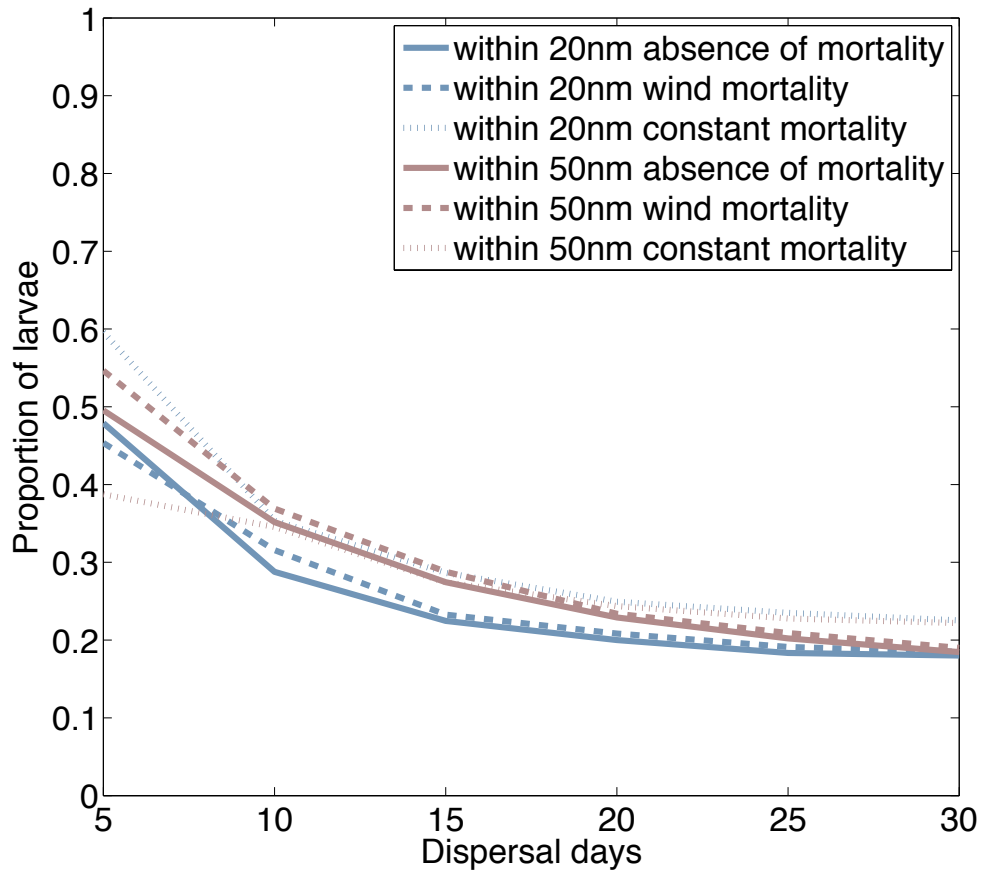


Figure 4.3. Average of proportion of larvae found within 20 nm (37 km, blue lines) and from 20 nm to 50 nm (37 to 92 km, pink line) of the Hawaiian Islands, by dispersal days. Lines show the proportion of retention from different mortality schemes, based on 100 simulations each. Larvae were released every 5 days during the yellowfin tuna spawning season for 2011.

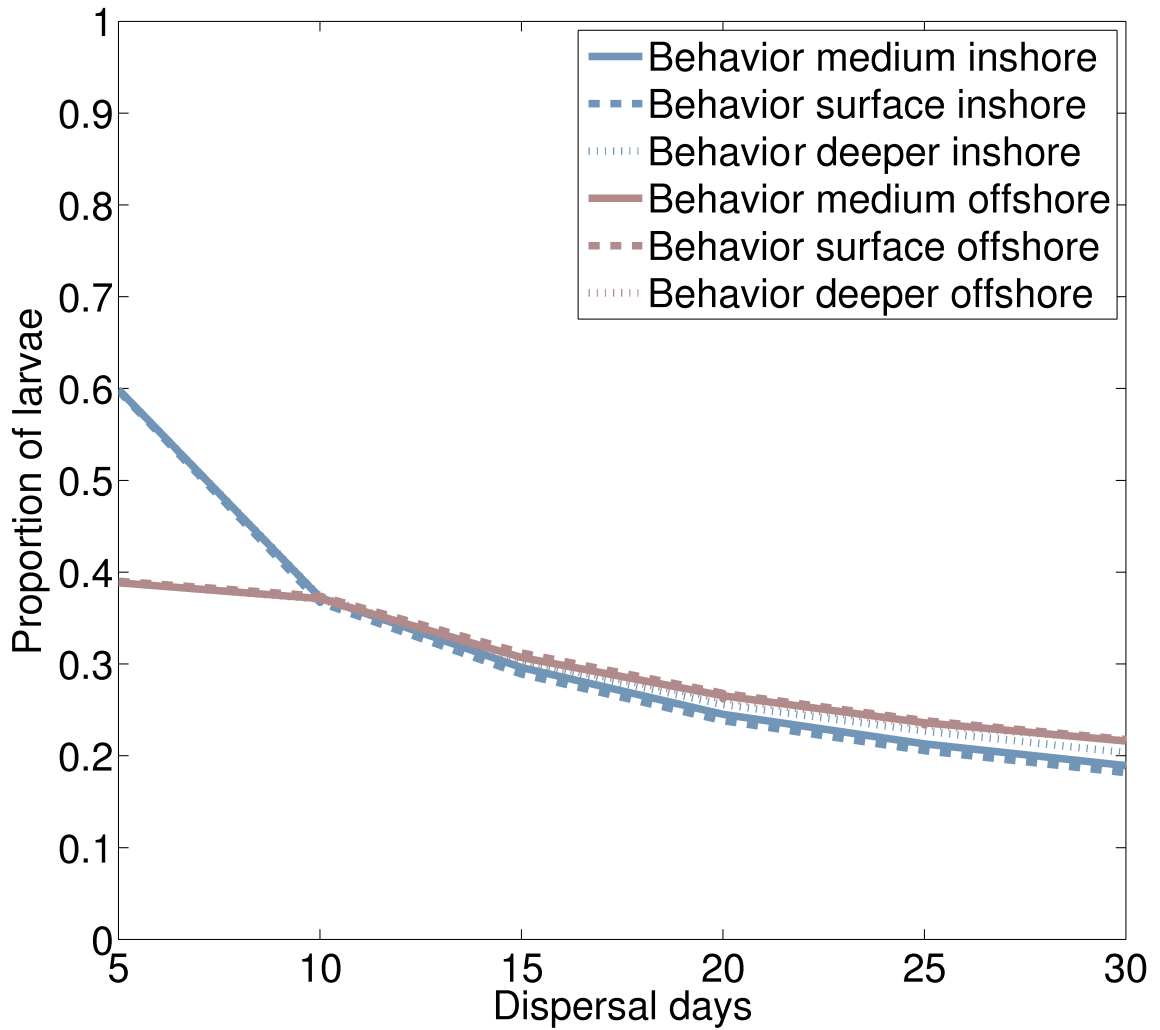


Figure 4.4. Average of proportion of larvae found within 20 nm (37 km, blue lines) and from 20 nm to 50 nm (37 to 92 km, pink line) of the Hawaiian Islands, by dispersal days. Lines show the proportion of retention from different vertical migration schemes, based on 100 simulations each. Larvae were released every 5 days during the yellowfin tuna spawning season from 2009 to 2011.

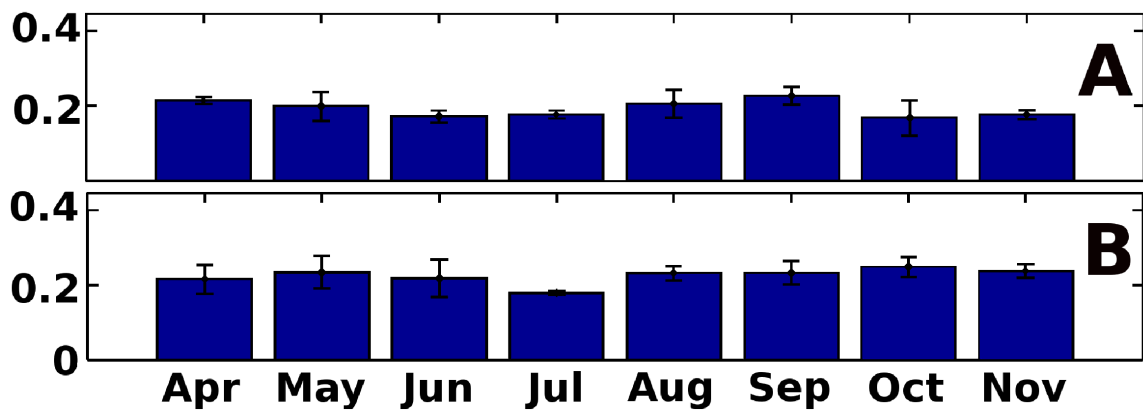


Figure 4.5. Monthly average and standard deviations of the proportion of yellowfin tuna larvae found within: (a) 20 nm (37 km) and (b) from 20nm to 50 nm (37 to 92 km) off the Hawaiian Islands; based on 100 simulations. Larvae were released every 5 days during the yellowfin tuna spawning season from 2009 to 2011.

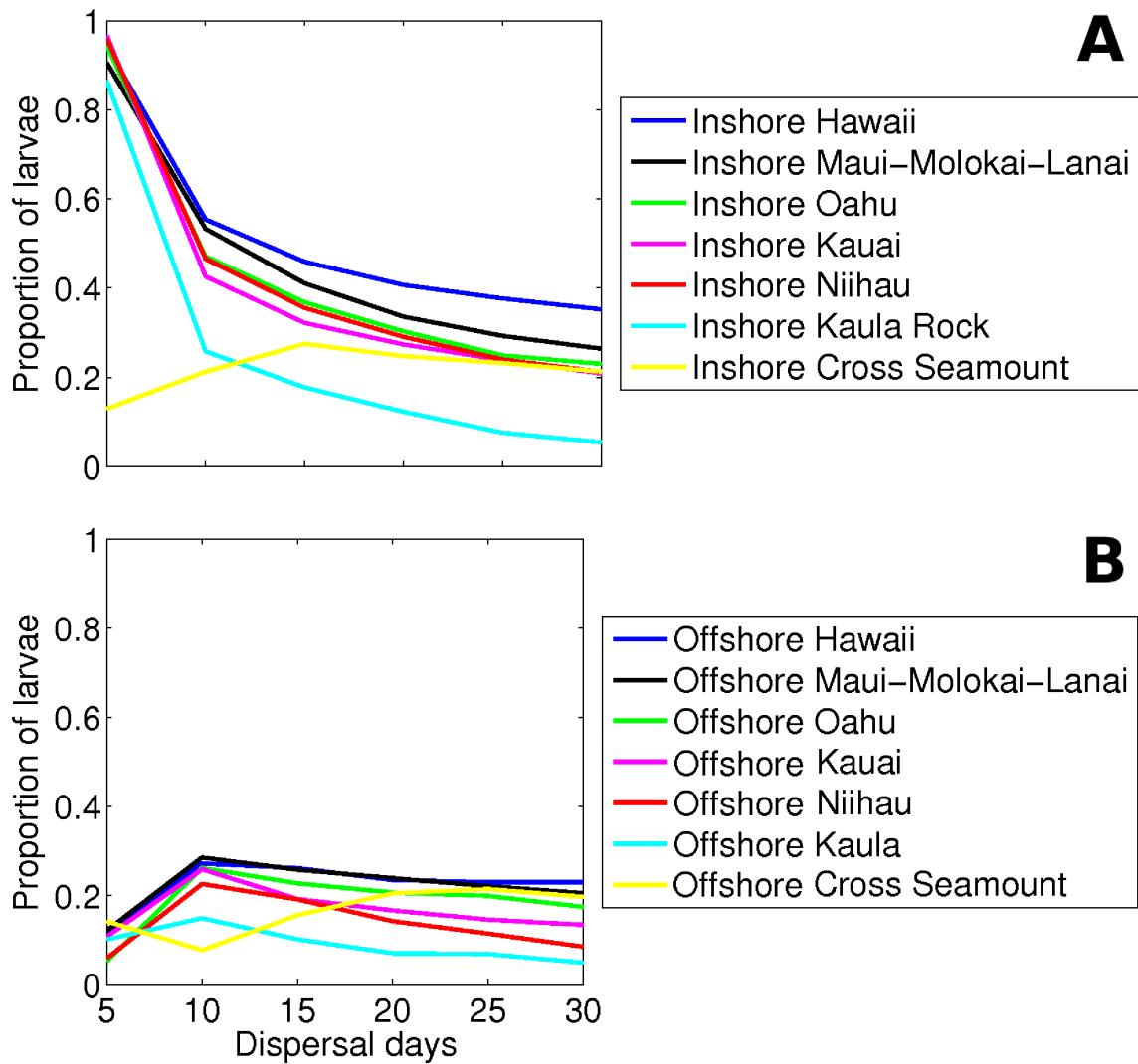


Figure 4.6. Average of the proportion of larvae found within 20 nm of the Hawaiian Islands, evolving with dispersal days, released at (a) inshore and (b) offshore spawning sites. Lines show the proportion of retention for larvae released at different sites, based on 100 simulations each. Larvae were released every 5 days during the yellowfin tuna spawning season from 2009 to 2011.

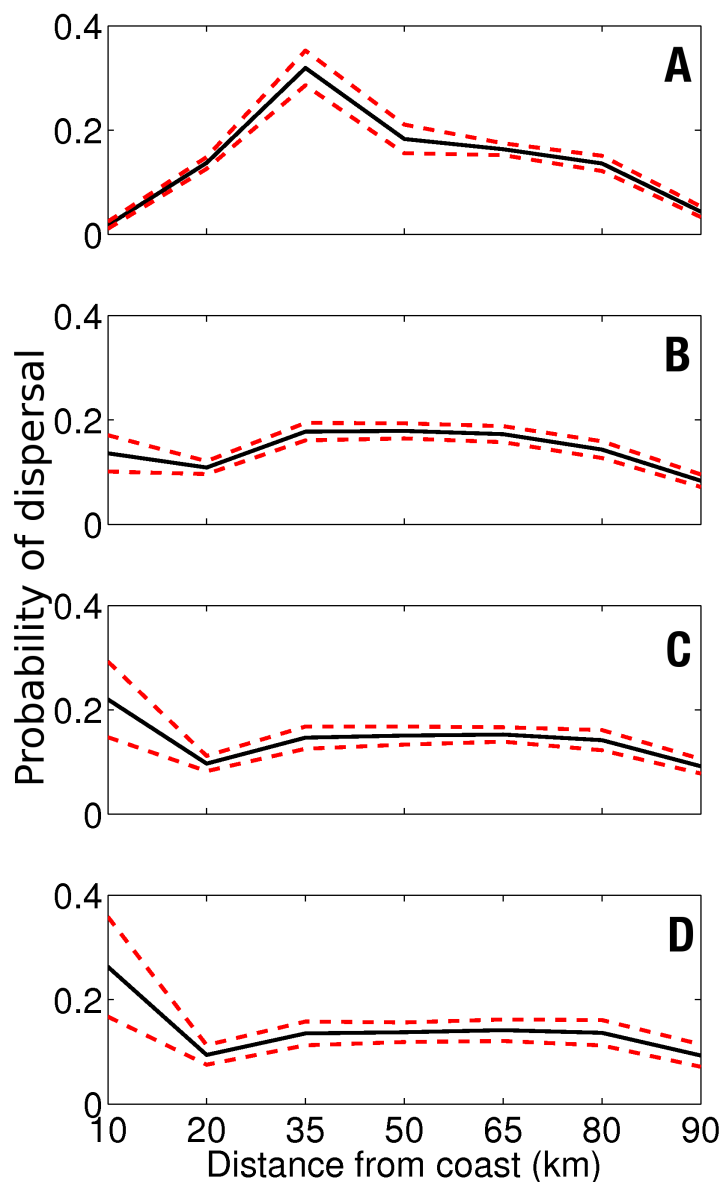


Figure 4.7. Mean (black) and standard deviations (red) of the monthly onshore-offshore dispersal probabilities of (a) hatching eggs (1 day of dispersal), (b) feeding larvae (6 days of dispersal), (c) post-flexion larvae transitioning to piscivory (16 days of dispersal), (d) transitional juvenile (26 days of dispersal). Mean and standard deviations are based on 100 simulations, during the spawning season of yellowfin tuna from 2009 to 2011. The dispersal kernels are based on the number of larvae within 90 km of the Hawaiian Islands, not considered dispersion to the open ocean. Larval stages were based on Margulies *et al.* (2007), Wexler *et al.* (2011) and Jeanne Wexler (*personal communication*).

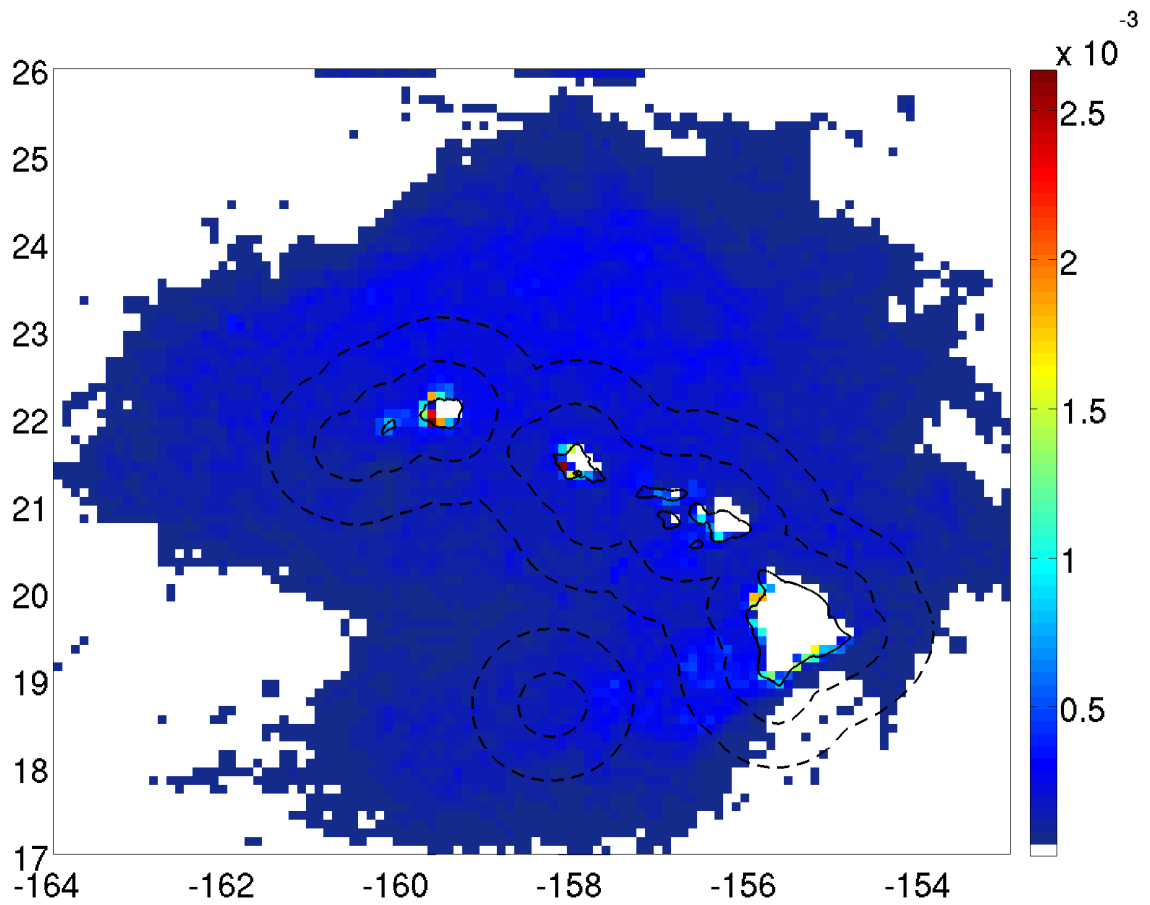


Figure 4.8. Average of the monthly larval distributions at 26 days of dispersal. The values shown are the proportion of particles found at each  $0.2 \times 0.2$  degree of the model domain, at 26 days of dispersal. Monthly larval distributions were averaged for the yellowfin tuna spawning season from 2009 to 2011.



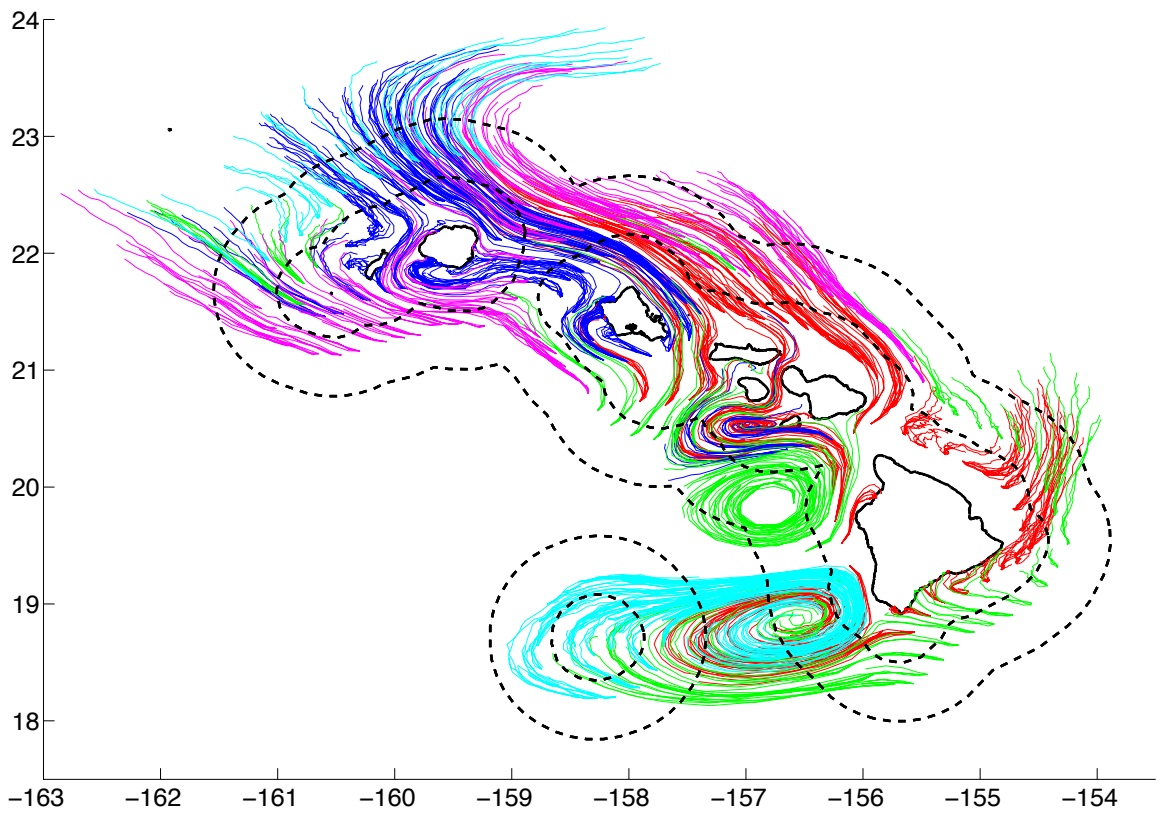


Figure 4.9. Trajectories of larvae dispersed for 30 days by the regional HYCOM flow fields averaged from 2009 to 2011. Colors are used to highlight dispersal from different areas.

## Chapter 5

### Conclusions

The specific goals of this dissertation were twofold: i) to enhance the scientific understanding of marine population connectivity in the Hawaiian region and ii) to determine the impact of ocean flow on larval dispersion characteristics around Hawai‘i. Dispersal simulations indicated that the physical environment around the Hawaiian Islands plays an important role in connectivity and retention patterns at different spatial scales.

Chapter 2 showed that the eddying flow increases connectivity and influences retention. It also revealed that both the flow field and dispersal patterns are highly variable. In this scenario, eddy events influenced transport in distinct ways, and the timing of releases played an important role in dispersal. Moreover, differences in the transport of particles and emerging connectivity patterns were apparent when comparing two different hydrodynamic model implementations (Regional and Global HYCOM). Therefore, the results highlighted the importance of hydrodynamical model flows that represent the scales of variability affecting transport and dispersion in modeling studies.

Chapter 3 indicated that the bottomfish species investigated in this study (*Pristipomoides filamentosus*, *Etelis coruscans* and *Etelis carbunculus*) share common connectivity pattern features that are driven by transport during early life stages. It also showed that there is potentially limited connectivity between the Papahānaumokuākea

Marine National Monument (PMNM) and the Main Hawaiian Islands (MHI), although, the islands, atolls, and banks located within the PMNM are well connected by larval dispersal. The potential existence of four distinct dispersal zones was also identified. These zones are mostly self-contained, i.e., larvae released in each area was mostly locally retained. The existence of these zones in the model highlight the need of further studies and indicates that distinct management measures might need to be implemented to preserve each zone's fisheries stocks.

The simulations also revealed that the islands from Kaua'i to Necker may act as stepping stones and an ecological corridor, connecting the PMNM and the MHI through larval dispersal. This further emphasizes the necessity of protecting this area. Considering the bottomfish restricted fishing areas (BRFAs), most of the viable larvae released inside of reserves during the simulations were exported to fishing sites. Thus, the reserves may be fulfilling their role to replenish depleted bottomfish fishing areas. However, the simulations also showed that the present reserve network has both limited connectivity and local retention, and that many reserves may rely on larval subsidy from fishing sites to sustain their populations. In this scenario the efficiency of the reserve network could be improved by the designation of more reserves, or by expanding the size of existing reserves by protecting additional bottomfish habitat.

Chapter 4 found that the physical environment around Hawai'i is favorable for retention during the early life stages of yellowfin tuna. However, the simulation results indicated that retention is not the main factor optimizing the yellowfin tuna's spawning season, and other factors such as favorable water temperature and food availability are

likely contributing to shaping the seasonality of spawning. The distributions of larvae by the time evolving eddying field were highly variable and no persistent dispersal pathways or accumulation zones were observed in the simulation results, apart from nearshore regions. Indeed, the modeled larval concentrations increased at inshore regions (less than 10 km from the coast) with dispersal time. Field studies have shown the accumulation of yellowfin larvae at nearshore around oceanic islands (Miller, 1979, Leis, 1991, Boherlet and Mundy, 1994, Boehlert and Mundy, 1996, Fowler *et al.*, 2008). The concentration of larvae at nearshore regions is believed to benefit the larvae from a range of species.

Despite the high variability and dispersal caused by the time evolving eddy flow, it is possible to infer that individual eddies impact the dispersal and retention of yellowfin tuna larvae, as showed in Chapter 2. Bakun (1996) proposed that the most significant physical oceanography processes influencing successful recruitment and perhaps the spawning strategy of fish are enrichment, concentration, and retention, named the “Triple triad.” Locally generated eddies in the leeward of Hawai‘i can promote these processes. In this study, it was not possible to detect enhancement processes as defined by Bakun (1996), as vertical velocities were not considered to displace larvae. However, cyclonic eddies, frontogenesis, and non linear Ekman pumping can lead to nutrient injection and enhancement of primary production (Landry *et al.*, 2008, Rii *et al.*, 2008, Calil and Richards, 2010, Karnauskas *et al.*, 2011), suggesting that such enrichment processes are taking place in the region. As showed in Figures 2.2 and S2.1, attracting Lagrangian coherent structures around eddies concentrate passive particles, and therefore, very likely larvae as well. It is important to acknowledge that this concentration refers to the

accumulation of larvae and it is not a “true concentration” (c.f. Lett *et al.*, 2008) because the model did not take larval swimming capabilities into account. Finally, the environment appeared conducive for the retention of yellowfin tuna larvae, despite the high dispersion and variability in the transport pathways. In the leeward of the MHI, individual vortices can persist for weeks, particularly in regions within 50 nm from coasts, considered here as retention sites. Larvae entrapped by gyres remain in the area, increasing the proportion of larval retention, as evident in the trajectories of particles dispersed by the average flow field.

## **5.1 Future directions**

Despite the contributions of biophysical models, the presented methodology has inherent limitations. The horizontal resolution of the hydrodynamic model implementations used (~4 km and ~8 km), does not capture the impact of smaller spatial scale processes, nor the nearshore circulation. Both processes can play a fundamental role in the retention of early life stages, and are important topics for future modeling studies in the region. Also, vertical displacements were not considered in this study. It would be beneficial for future research to consider vertical displacements, with a special focus on enhancement processes, such as those occurring at cyclonic eddies, regions of straining, frontogenesis, and non-linear Ekman pumping. Specific to yellowfin tuna, future field and laboratory studies should consider the relative importance of nearshore vs. offshore habitats for larval survival.

## Bibliography

- Almany, G.R., S.R. Connolly, D.D. Heath, J.D. Hogan, G.P. Jones, L.J. McCook, M. Mills, R.L. Pressey and D.H. Williamson (2009). Connectivity, biodiversity conservation, and the design of marine reserve networks for coral reefs. *Coral Reefs*, 28, 339-351.
- Artale, V., G. Boffetta, A. Celani, M. Cencini, A. Vulpiani (1997). Dispersion of passive tracers in closed basins: Beyond the diffusion coefficient. *Physics of Fluids*, 9, 3162–3171.
- Aurell, E., G. Boffetta, A. Crisanti, G. Paladin, and A. Vulpiani (1997). Predictability in the large: an extension of the concept of Lyapunov exponent. *Journal of Physics*, 30, 126.
- Ayata, S.D., P. Lazure, and E. Thiébaud (2010). How does the connectivity between populations mediate range limits of marine invertebrates? A case study of larval dispersal between the Bay of Biscay and the English Channel (North-East Atlantic). *Progress in Oceanography*, 87, 18-36.
- Babcock, R.C., N.T. Shears, A.C. Alcalá, N.S. Barrett, G.J. Edgar, K.D. Lafferty, T.R. McClanahan, and G.R. Russ (2010). Decadal trends in marine reserves reveal differential rates of change in direct and indirect effects. *Proceedings of the National Academy of Sciences*, 107, 18256-18261.
- Bakun, A. (1996). *Patterns in the Ocean*. Ocean Processes and marine population dynamics. La Paz, California Sea Grant College System, National Oceanic and Atmospheric Administration in cooperation with Centro de Investigaciones Biológicas del Noroeste. 323 P.
- Bakun, A., and R.H. Parrish (1991). Comparative studies of coastal pelagic fish reproductive habitats: the anchovy (*Engraulis anchoita*) of the southwestern Atlantic. *ICES Journal of Marine Science*, 48, 343-361.
- Bakun, A., and K. Broad. (2003). Environmental ‘loopholes’ and fish population dynamics: comparative pattern recognition with focus on El Niño effects in the Pacific. *Fisheries Oceanography*, 12, 458-473.
- Baums, I.B., C.B. Paris, and L.M. Cherubin (2006). A bio-oceanographic filter to larval dispersal in a reef- building coral. *Limnology and Oceanography*, 51, 1969-1981.

- Berkeley, S.A., M.A. Hixon, R.J. Larson, and M.S. Love (2004). Fisheries sustainability via Protection of age structure and spatial distribution of fish populations. *Fisheries*, 29, 23-32.
- Beron-Vera, F.J., M.J. Olascoaga, and G.J. Goni (2008). Oceanic mesoscale eddies as revealed by Lagrangian coherent structures. *Geophysical Research Letters*, 35, L12603, doi:10.1029/2008GL033957.
- Bleck, R. (2002). An oceanic general circulation model framed in hybrid isopycnic-Cartesian coordinates. *Ocean Model*, 37, 55-88.
- Bird, C.E., B.S. Holland, B.W. Bowen, and R.J. Toonen (2007). Contrasting phylogeography in three endemic Hawaiian limpets (*Cellana* spp.) with similar life histories. *Molecular Ecology*, 16, 3173-3186.
- Boehlert, G.W., and B.C. Mundy (1994). Vertical and onshore-offshore distributional patterns of tuna larvae in relation to physical habitat features. *Marine Ecology Progress Series*, 107, 1-13.
- Boehlert, G.W., and B.C. Mundy (1996). Ichthyoplankton vertical distributions near O'ahu, Hawaii, 1985-1986: data report. *NOAA Technical Memorandum NMFS-SWFS-235*. 148 P.
- Botsford, L.W., F. Micheli, and A. Hastings (2003). Principles for the design of marine reserves. *Ecological Applications*, 13, S25-S31.
- Botsford, L.W., J.W. White, M.A. Coffroth, C.B. Paris, S. Planes, T.L. Shearer, S.R. Thorrold, and G.P. Jones (2009). Connectivity and resilience of coral reef metapopulations in marine protected areas: matching empirical efforts to predictive needs. *Coral Reefs*, DOI 10.1007/s00338-009-04766-z.
- Calil, P.H.R., K.J. Richards, Y. Jia, and R.R. Bidigare (2008). Eddy activity in the lee of the Hawaiian Islands. *Deep-Sea Research II*, doi:10.1016/j.dsr2.2008.01.008.
- Calil, P.H.R., and K.J. Richards (2010). Transient upwelling hot spots in the oligotrophic North Pacific. *Journal Geophysical Research*, 115, C02003.
- Chassignet, E.P., H.E. Hurlburt, O.M. Smedstad, G.H. Halliwell, P.J. Hogan, A.J. Wallcraft, R. Baraille, and R. Bleck (2007). The HYCOM (Hybrid Coordinate Ocean Model) data assimilative system. *Journal Marine Systems*, 65, 60-83.
- Chelton, D.B., R.A. Deszoeke, and M.G. Schlax (1998). Geographical Variability of the First Baroclinic Rossby Radius of Deformation. *Journal of Physical Oceanography*, 28, 433-460.

- Christie, M.R., B.N. Tissot, M.A. Albins, J.P. Beets, and Y. Jia (2010). Larval connectivity in an effective network of Marine Protected Areas. *PloS ONE* 5, e15715.
- Claro, R., and K.C. Lindeman (2003). Spawning aggregation sites of snapper and grouper species (Lutjanidae and Serranidae) on the insular shelf of Cuba. *Gulf and Caribbean Research*, 14, 91-106.
- Cowen, R.K., C.B. Paris, and A. Srinivasan (2006). Scaling of connectivity in marine populations. *Science*, 311, 522-527.
- Cowen, R.K., G.G. Gawarkiewicz, J. Pineda, S.R. Thorrold, and F.E. Werner (2007). Population connectivity in marine systems: an overview. *Oceanography*, 20, 14-21.
- Cowen, R.K., and S. Sponaugle (2009). Larval dispersal and marine population connectivity. *Annual Review of Marine Science*, 1, 443-466.
- Crowder, L.B., J.A. Rice, T.J. Miller, and E.A. Marschall (1992). Empirical and theoretical approaches to size-based interactions and recruitment variability in fishes. In DeAngelis, D.L., and L.J. Gross (Eds.), *Individual-based models and approaches in ecology: populations, communities and ecosystems* (pp. 237-255). Chapman and Hall. New York. NY.
- Cummings, J.A. (2005). Operational multivariate ocean data assimilation. *Quarterly Journal of the Royal Meteorological Society*, 13, 3583-3604.
- Cury, P. and C. Roy (1989). Optimal environmental window and pelagic fish recruitment success in upwelling areas. *Canadian Journal of Fisheries and Aquatic Sciences*, 46, 670-680.
- Cushing, D.H. (1988). *Marine Ecology and Fisheries*. Cambridge, Cambridge University Press. 278 P.
- Dagorn, L., K.N. Holland, and D.G. Itano (2007). Behavior of yellowfin (*Thunnus albacares*) and bigeye (*T. obesus*) tuna in a network of fish aggregating devices (FADs). *Marine Biology*, DOI 10.1007/s00227-006-0511-1.
- Department of Land and Natural Resources of the State of Hawaii (2007). Title 13 of Hawaii Administrative Rules, Subtitle 4, Part V, Chapter 94: Bottomfish Management. 31 P. (online). Available from: [www.state.hi.us/oip/rules.html](http://www.state.hi.us/oip/rules.html) (Accessed 26 March 2008).
- Di Franco, A., B.M. Gillanders, G. Benedetto, A. Pennetta, G. De Leo, and P. Guidetti (2012). Dispersal patterns of coastal fish: implications for designing networks of marine protected areas. *PLoS ONE*, 7, e31681. doi:10.1371/journal.pone.0031681.



- Dickey, T., F. Nencioli, V. Kuwahara, C. Leonard, W. Black, Y. Rii, R. Bidigare, and Q. Zhang (2008). Physical and bio-optical observations of oceanic cyclones west of the island of Hawaii. *Deep-Sea Research Part II*, 55, 1195-1217.
- Dore, J.E., J.R. Brum, L.M. Tupas, and D.M. Karl (2002). Seasonal and interannual variability in sources of nitrogen supporting export in the oligotrophic subtropical North Pacific Ocean. *Limnology and Oceanography*, 46, 1595-1607.
- Dore, J.E., R.M. Letelier, M.J. Church, R. Lukas, and D.M. Karl (2008). Summer phytoplankton blooms in the oligotrophic North Pacific Subtropical Gyre: Historical perspective and recent observations. *Progress in Oceanography*, 76, 2-38.
- Dritschel, D.G. and M.E. McIntyre (2008). Multiple jets as PV staircases: The Phillips effect and the resilience of eddy-transport barriers. *Journal Atmospheric Sciences*, 65, 855-874.
- Eble, J.E., R.J. Toonen, and B.W. Bowen (2009). Endemism and dispersal: comparative phylogeography of three surgeonfishes across the Hawaiian Archipelago. *Marine Biology*, 156, 689-698.
- Edwards, K.P., J.A. Hare, F.E. Werner, and H. Seim (2007). Using 2-dimensional dispersal kernels to identify the dominant influences on larval dispersal on continental shelves. *Marine Ecology Progress Series*, 352, 77-87.
- Everson, A.R. (1984). Spawning and gonadal maturation of the ehu, *Etelis carbunculus*, in the Northwestern Hawaiian Islands. In Grigg, R.W., and K.Y. Tanoue (Eds.), *Proceedings of the Second Symposium on Resource Investigations in the Northwestern Hawaiian Islands* (pp. 128-148) Vol. 2, UNIHI-SEAGRANTMR-84-1.
- Everson, A.R., H.A. Williams, and B.M. Ito (1989). Maturation and reproduction in two Hawaiian Eteline snappers, uku, *Aprion virescens*, and onaga, *Etelis coruscans*. *Fishery Bulletin*, 87, 877-888.
- Exec. Order No. 13178, 3 C.F.R. 13178 (2000 comp.), reprinted in 65 F.R. 34909
- Exec. Order 13196, reprinted in 66 F.R. 73903.
- Firing, E., B. Qiu, and W. Miao (1999). Time-dependent island rule and its application to the time-varying north Hawaiian ridge current. *Journal of Physical Oceanography*, 29, 2671-2688.
- Flament, P., R. Lumpkin, J. Tournadre, and L. Armi (2001). Vortex pairing in an unstable anticyclonic shear flow: discrete subharmonics of the pendulum day. *Journal of Fluid Mechanics*, 440, 401-409.

- Fogarty, M.J., and L.W. Botsford (2007). Population connectivity and spatial management of marine fisheries. *Oceanography*, 20, 112-123.
- Fowler, A., J.M. Leis, and I.M. Suthers (2008). Onshore-offshore distributions and abundances of tuna larvae (Pisces: Scombridae: Thunnini) in near-reef waters of the Coral Sea. *Fisheries Bulletin*, 106, 405-416.
- Gaines, S.D., B. Gaylord, and J.L. Largier (2003). Avoiding current oversights in marine reserve design. *Ecology Applications*, 13, S32-S46.
- Gaines, S.D., B. Gaylord, L.R. Gerber, A. Hastings, and B.P. Kinlan (2007). Connecting places: the ecological consequences of dispersal in the sea. *Oceanography*, 20, 90-99.
- Gaines, S.D., C. White, M.H. Carr, and S.R. Palumbi (2010). Designing marine reserve networks for both conservation and fisheries management. *Proceedings National Academy of Sciences*, 107, 18286-18293.
- Gaither, M.R., S.A. Jones, C. Kelley, S.J. Newman, L. Sorenson, and B. Bowen, (2011). High connectivity in the deepwater snapper *Pristipomoides filamentosus* (Lutjanidae) across the Indo-Pacific with isolation of the Hawaiian Archipelago. *PLoS ONE*, 6, e28913. doi:10.1371/journal.pone.0028913.
- Gerber, R.L., L.W. Botsford, A. Hastings, H.P. Possingham, S.D. Gaines, S.R. Palumbi, and S. Andelman (2003). Population models for marine reserve design: A retrospective and prospective synthesis. *Ecological Applications*, 13, S47-S64.
- Gerlach, G., M.J. Kingsfords, K.P. Black, and V. Miller-Sims (2007). Smelling home can prevent dispersal of reef fish larvae. *Proceedings of the National Academy of Science*, 104, 858-863.
- Grimm, V. (1999). Ten years of individual-based modeling in ecology: what have we learned and what could we learn in the future? *Ecological Modelling*, 115, 129-148.
- Grorud-Covert, and S. Sponaugle (2009). Larval supply and juvenile recruitment of coral reef fishes to marine reserves and non-reserves of the upper Florida Keys, USA. *Marine Biology*, 156, 277-288.
- Grüss, A., D.M. Kaplan, S. Guénette, M.R. Callum, and L.W. Botsford (2010). Consequences of adult and juvenile movement for marine protected areas. *Biological Conservation*, 144, 692-702.
- Grüss, A., D.M. Kaplan, and D.R. Hart (2011). Relative impacts of adult movement, larval dispersal and harvester movement on the effectiveness of reserve networks. *PLoS ONE*, 6, e19960. doi:10.1371/journal.pone.0019960.

- Haller, G., and G. Yuan (2000). Lagrangian coherent structures and mixing in two-dimensional turbulence. *Physica D*, 147, 352-370.
- Harrison, H.B., D.H. Williamson, R.D. Evans, G.R. Almany, S.R. Thorrold, G.R. Russ, K.A. Feldheim, L. Van Herwerden, S. Planes, M. Srinivasan, M.L. Berumen, and G. P. Jones (2012). Larval export from marine reserves and the recruitment benefit for fish and fisheries. *Current Biology*, 22, 1023-1028.
- Hastings, A., and L.W. Botsford (2003). Comparing designs of marine reserves for fisheries and for biodiversity. *Ecological Applications*, 13, S65-S70.
- Helgers, J., and C.B. Paris (2011). *Connectivity Modeling System User's Guide*. 39 P.
- Hjort, J. (1914). Fluctuations in the great fisheries of northern Europe. Rapports et Proces-verbaux des Reunions, *Conseil international pour l'Exploration de la Mer*, 20, 1-1228.
- Huebert, K.B. (2009). Behavior and transport of pelagic coral reef fish larvae in the Straits of Florida. Ph.D. Dissertation, University of Miami, Miami, USA.
- Huggett, J., P. Freon, C. Mullon, and P. Penven (2003). Modelling the transport success of anchovy *Engraulis encrasicolus* eggs and larvae in the southern Benguela: the effect of spatio-temporal spawning patterns. *Marine Ecology Progress Series*, 250, 247-262.
- Ishibashi, Y., T. Miki, Y. Sawada, and M. Kurata (2012). Effects of feeding conditions and size differences on aggressive behaviour and cannibalism in the Pacific bluefin tuna *Thunnus orientalis* (Temminck and Schlegel) larvae. *Aquaculture Research*, 1-9, doi:10.1111/j.1365-2109.2012.03203.x.
- Itano, D.G., and K.N. Holland (2000). Movement and vulnerability of bigeye (*Thunnus obesus*) and yellowfin tuna (*Thunnus albacares*) in relation to FADs and natural aggregation points. *Aquatic Living Resources*, 13, 213-223.
- Itano, D. (2000). *The reproductive biology of Yellowfin Tuna (*Thunnus albacares*) in Hawaiian waters and the western Tropical Pacific Ocean: Project Summary*. SOEST Publication 00-01, JIMAR Contribution, 00-328.
- Jia, Y., P.H.R. Calil, E.P. Chassignet, E.J. Metzger, J.T. Potemra, K.J. Richards, and A.J. Wallcraft (2011). Generation of mesoscale eddies in the lee of the Hawaiian Islands. *Journal of Geophysical Research*, 116, C11009, doi:10.1029/2011JC007305.
- Johannes, R.E. (1978). Reproductive strategies of coastal marine fishes in the tropics. *Environmental Biology of Fishes*, 5, 251-252.

- Jones, G.P., G.R. Almany, G.R. Russ, P.F. Sale, R.S. Steneck, M.J.H van Oppen, and B.L. Willis (2009). Larval retention and connectivity among populations of corals and reef fishes: history, advances and challenges. *Coral Reefs*, 28, 207-325.
- Joseph, B., and B. Legras (2002), Relation between kinematic boundaries, stirring and barriers for the Antarctic Polar Vortex. *Journal Atmospheric Sciences*, 59, 1198–1212.
- Kaji, T., M. Tanaka, M. Oka, H. Takeuchi, S. Ohsumi, K. Teruya, and J. Hirokawa (1999). Growth and morphological development of laboratory-reared yellowfin tuna *Thunnus albacares* larvae and early juveniles, with special emphasis on the digestive system. *Fisheries Science*, 65, 700-707.
- Karnauskas, M., L.M. Chérubin, and C.B. Paris (2011). Adaptive significance of the formation of multi species fish spawning aggregations near submerged capes. *PLoS ONE* 6, e22067. doi:10.1371/ journal.pone.002206728.
- Kikkawa, B.S. (1984). Maturation, spawning, and fecundity of opakapaka, *Pristipomoides filamentosus*, in the Northwestern Hawaiian Islands. In Grigg, R.W., and K.Y. Tanoue (Eds.), *Proceedings of the Second Symposium on Resource Investigations in the Northwestern Hawaiian Islands* (pp. 149-160). Vol. 2, UNIH-SEAGRANT-MR-84-01.
- Kimura, S., H. Nakata, D. Margulies, J.M. Suter, and S.L. Hunt (2004). Effect of oceanic turbulence on the survival of yellowfin tuna larvae. *Nippon Suisan Gakkaishi*, 70, 175-178.
- Kingsford, M.J., J.M. Leis, A. Shanks, K.C. Lindeman, S.G. Morgan, and J. Pineda (2002). Sensory environments, larval abilities and local self-recruitment. *Bulletin of Marine Science*, 70, 309-340.
- Kitajima, C., Y. Yamane, S. Matsui, Y. Kihara, and M. Furuichi (1993). Ontogenetic Change in buoyancy in the early stage of Red Sea Bream. *Nippon Suisan Gakkaishi*, 59, 209-216.
- Kobayashi, D. (2006). Colonization of the Hawaiian Archipelago via Johnston Atoll: a characterization of oceanographic transport corridors for pelagic larvae using computer simulation. *Coral Reefs*, 25, 407-417.
- Kobayashi, D.R. (2008). Spatial connectivity of Pacific insular species: Insights from modeling and tagging. Ph.D. Dissertation. University of Sydney, Sydney, Australia.
- Kobayashi, D.R., and J.J. Polovina (2006). Simulated seasonal and interannual variability in larval transport and oceanography in the Northwestern Hawaiian Islands using satellite remotely sensed data and computer modeling. *Atoll Research Bulletin*, 543, 365-390.

- Kool, J, C.B. Paris-Limouzy, S. Andrefouet, and R.K. Cowen (2009). Complex migration and the development of genetic structure in subdivided populations: an example from Caribbean coral reef ecosystems. *Ecography*, 32, 1-10.
- Landry, M.R., H. Al-Mutairi, K.E. Selph, S. Christensen, and S. Nunnery (2001). Seasonal patterns of mesozooplankton abundance and biomass at Station ALOHA. *Deep-Sea Research II*, 48, 2037-2061.
- Landry, M.R., M. Decima, M.P. Simmons, C.C.S. Hannides, and E. Daniels (2008). Mesozooplankton biomass and grazing responses to Cyclone Opal, a subtropical mesoscale eddy. *Deep-Sea Research II*, 1378-1388.
- Leis, J.M. (1982). Nearshore distributional gradients of larval fish (15 taxa) and planktonic crustaceans (6 taxa) in Hawai'i. *Marine Biology*, 72, 89-97.
- Leis, J.M., T. Trnski, M. Harmelin-Vivien, J.P. Renon, V. Dufour, M.K. El Moudni, and R. Galzin. (1991). High concentrations of tuna larvae (Pisces: Scombridae) in near-reef waters of French Polynesia (Society and Tuamotu Islands). *Bulletin of Marine Sciences*, 48, 150-158.
- Leis, J.M. (2006). Are larvae of demersal fishes plankton or nekton? *Advances in Marine Biology*, 51, 59-141.
- Leis, J.M., K.J. Wright, and J.N. Johnson (2007). Behavior that influences dispersal and connectivity in the small, young larvae of a reef fish. *Marine Biology*, 153, 103-117.
- Lehahn, Y., F. d'Ovidio, M. Levy, and E. Heifetz (2007). Stirring of the northeast Atlantic spring bloom: A Lagrangian analysis based on multi satellite data. *Journal of Geophysical Research*, 112, C08005.
- Letelier, R.M., D.M. Karl, M.R. Abbott, P. Flament, M. Freilich, R. Lukas, and T. Strub (2000). Role of late winter mesoscale events in the biogeochemical variability of the upper water column of the North Pacific Subtropical Gyre. *Journal of Geophysical Research*, 105, 723-728.
- Lindeman, K.C., R. Pugliese, G.T. Waugh, and J.S. Ault (2000). Developmental patterns within a multispecies reef fishery: management applications for essential fish habitats and protected areas. *Bulletin of Marine Science*, 66, 929-956.
- Llopiz, J.K. (2009). The Trophic Ecologies of Larval Billfishes, Tunas, and Coral Reef Fishes in the Straits of Florida: Piscivory, Selectivity, and Niche Separation. Ph.D. Dissertation. University of Miami, Miami, USA.
- Llopiz, J.K., D. E. Richardson, A. Shiroza, S.L. Smith, and R.K. Cowen (2010). Distinctions in the diets and distributions of larval tunas and the important role of appendicularians. *Limnology and Oceanography*, 55, 983-996.

- Lobel, P.S. (1989). Ocean current variability and the spawning season of Hawaiian reef fishes. *Environmental Biology of Fishes*, 24, 161-171.
- Lobel, P.S. (2011). Transport of reef lizardfish larvae by an ocean eddy in Hawaiian waters. *Dynamics of Atmospheres and Oceans*, DOI: 10.1016/j.dynatmoce.2011.01.001.
- Lobel, P.S., and A.R. Robinson (1986). Transport and entrapment of fish larvae by ocean mesoscale eddies and currents in Hawaiian waters. *Deep-Sea Research*, 33, 483-500.
- Lobel, P.S., and A.R. Robinson (1988). Larval fishes and zooplankton in a cyclonic eddy in Hawaiian waters. *Journal Plankton Research*, 10, 1209-1223.
- Lubchenco, J., S.R. Palumbi, S.D. Gaines, and S. Andelman (2003). Plugging a Hole in the Ocean: The Emerging Science of Marine Reserves. *Ecological Applications*, 13, S3-S7.
- Lowe, M.K. (2004). The status of inshore fisheries ecosystems in the Main Hawaiian Islands at the dawn of the millenium: Cultural impacts, fisheries trends and management challenges. In Friedlander, A.M. (Ed.), *Status of Hawai'i's coastal fisheries in the new millennium*. Proceedings of the 2001 Fisheries Symposium sponsored by the American Fisheries Society, Hawai'i Chapter. Honolulu, Hawai'i.
- Lumpkin, C.F. (1998). Eddies and Currents of the Hawaiian Islands. Ph.D. Dissertation. University of Hawai'i at Mānoa, Honolulu. USA.
- Lumpkin, R., and P. Flament (2001). Lagrangian statistics in the central North Pacific. *Journal Marine Systems*, 29, 141-155.
- MacKenzie, B.R., and W.C. Leggett (1993). Wind-based models for estimating the dissipation rates of turbulent energy in aquatic environments: empirical comparisons. *Marine Ecology Progress Series*, 94, 207-216
- MacKenzie, B.R. and T. Kiørboe (1995). Encounter rates and swimming behavior of pause-travel and cruise larval fish predators in calm and turbulent laboratory environments. *Limnology and Oceanography*, 40, 1278-1289.
- McManus, M.A., and C.B. Woodson (2012). Plankton distribution and ocean dispersal. *The Journal of Experimental Biology*, 215, 1008-1016
- Mann, K.H., and J.R.N. Lazier (2006). *Dynamics of Marine Ecosystems: Biological-Physical Interactions in the Oceans* (3<sup>rd</sup> ed.). Blackwell. 495 P.
- Man, A., R. Law, and N.V.C. Polunin (1995). Role of marine reserves in recruitment to reef fisheries: a metapopulation model. *Biological Conservation*, 71, 197-204.

- Margulies, D., J.B. Wexler, K.T. Bentler, J.M. Suter, S. Masuma, N. Tezuka, K. Teruya, M. Oka, M. Kanematsu, and H. Nikaido (2001). Food selection of yellowfin tuna, *Thunnus albacares*, larvae reared in the laboratory. *Interamerican Tropical Tuna Communication Bulletin*, 22, 9–51 H.
- Margulies, D., J.M. Suter, S.L. Hunt, R.J. Olson, V.P. Scholey, J.B. Wexler, and A. Nakazawa (2007a). Spawning and early development of captive yellowfin tuna (*Thunnus albacares*). *Fisheries Bulletin*, 105, 249-265.
- Margulies, D., V.P. Scholey, J.B. Wexler, R.J. Olson, J.M. Suter and S.L. Hunt (2007b). *A review of IATTC research on the early life history and reproductive biology of scombrids conducted at the Ashotines Laboratory from 1985 to 2005*. Inter-American Tropical Tuna Commission, Special Report 16. Inter-American Tropical Tuna Commission, La Jolla, USA, 63 P.
- Matsumoto, W.M. (1958). Description and distribution of larvae of four species of tuna in central Pacific waters. *Fisheries Bulletin*, 58, 31-72.
- Miller, J.M. (1979). Nearshore abundance of tuna (Pisces: Scombridae) larvae in the Hawaiian Islands. *Bulletin of Marine Science*, 29, 19-26.
- Mitchum, G.T. (1995). The source of 90-day oscillations at Wake Island. *Journal of Geophysical Research*, 100, 2459-2475.
- Muelbert, J.H., M.R. Lewis, and D.E. Kelley (1994). The importance of small-scale turbulence in the feeding of herring larvae. *Journal of Planktonic Research*, 16, 927-944.
- Munday, P., J.M. Leis, J.M. Lough, C.B. Paris, M.J. Kingsford, M.L. Berumen, and J. Lambrechts (2009). Climate change and coral reef connectivity. *Coral Reefs*, 28, 379-395.
- Neter, J., W. Wasserman, and M. Kutner (1990). *Applied linear statistical models*. (3<sup>rd</sup> ed.). Irwin. 1181 P.
- Nishimura, K., and N. Hoshino (1999). Evolution of cannibalism in the larval stage of pelagic fish. *Evolutionary Ecology*, 13, 191-209.
- Norman, M.D., and G.P. Jones (1984). Determinants of territory size in the Pomacentrid reef fish, *Parma victoriae*. *Oecologia*, 61, 60-69.
- North, E.W., A. Gallego, and P. Petitgas (Eds.) (2009). *Manual of recommended practices for modelling physical – biological interactions during fish early life*. International Council for the Exploration of the Sea (ICES), Cooperative Research Report N° 295. 111 P.

- Okubo, A. (1971) Oceanic diffusion diagrams. *Deep Sea Research*, 18, 789-802.
- Okubo, A. (1994). The role of diffusion and related physical processes in dispersal and recruitment of marine populations. In Sammarco, P.W., and M.L. Heron (Eds.), *The Bio-Physics of Marine Larval Dispersal* (pp. 5-32). Washington: American Geophysical Union.
- Olascoaga, M.J., F.J. Beron-Vera, L.E. Brand, and H. Koçak (2008). Tracing the early development of harmful algal blooms on the West Florida Shelf with the aid of Lagrangian coherent structures. *Journal Geophysical Research*, 113, C12014.
- Otinno, J.M. (1989). *The Kinematics of Mixing: Stretching, Chaos, and Transport* Cambridge University Press, New York.
- d'Ovidio, F., V. Fernandez, E. Hernandez-Garcia, and C. Lopez (2004). Mixing structures in the Mediterranean Sea from finite-size Lyapunov exponents. *Geophysics Research Letters*, 31, L17203.
- d'Ovidio, F., J. Isern-Fontanet, C. Lopez, E. Hernandez-Garcia, and E. Garcia-Lardona (2008). Comparison between the Okubo-Weiss parameter and finite-size Lyapunov exponents computed from altimetry in the Algerian basin. *Deep-Sea Research I*, 56, 15-3. doi:10.1016/j.dsr.2008.07.014.
- Palumbi, S. (2004). Marine reserves and ocean neighborhoods: The spatial scale of marine populations and their management. *Annual Review Environment and Resources*, 29, 31-68.
- Paris, C.B. (2010). Reef Interconnectivity and larval dispersal. In Hopley, D. (Ed.), *Encyclopedia of Modern Coral Reefs: Structure, Form and Process* (pp. 881-889). Springer-Verlag.
- Paris, C.B., R.K. Cowen, K.M.M. Lwiza, D. Wang, and D.B. Olson (2002). Multivariate objective analysis of the coastal circulation of Barbados, West Indies: implication for larval transport. *Deep-Sea Research I*, 49, 1363-1386.
- Paris, C.B., and R.K. Cowen (2004). Direct evidence of a biophysical retention mechanism for coral reef fish larvae. *Limnology and Oceanography*, 49, 1944-1979.
- Paris, C.B., L.M. Cherubin, and R.K. Cowen (2007). Surfing, spinning, or diving from reef to reef: effects on population connectivity. *Marine Ecology Progress Series*, 347, 285-300.
- Paris, C.B., A. Clement, and R. Cowen (2008). Influence of projected temperature changes in the Caribbean on the pelagic phase and population networks of a common reef fish. Abstract, session 071, Ocean Sciences Meeting, Orlando, USA.



- Paris, C.B., J-O. Irrisson, G. Lacroix, O. Fiksen, J.M. Leis, and C. Mullon (2009) Connectivity. In North, E., A. Gallego, and P. Petitgas (Eds.), *Manual of Recommended Practices or Modelling Physical-Biological Interactions in Fish Early-Life History* (pp. 63-76). International Council for the Exploration of the Sea (ICES), Cooperative Research Report N° 295.
- Paris, C.B., J. Helgers, and E. van Sebille. The connectivity modelling system: tracking biotic and abiotic particles in the ocean. Submitted to *Environmental Modelling and Software*.
- Parke, M. (2007). *Linking Hawaii Fisherman Reported Commercial Bottomfish Catch Data to Potential Bottomfish Habitat and Proposed Restricted Fishing Areas using GIS and Spatial Analysis*. U.S. Dep. Commerce, NOAA Tech. Memo, NOAA-TM-NMFS-PIFSC-11, 37 P.
- Parsons, D.M., M.A. Morrison, and M.J. Slater (2010). Responses to marine reserves: Decreased dispersion of the sparid *Pagrus auratus* (snapper). *Biological Conservation*, 143, 2039–2048.
- Patzert, W.C. (1969). Eddies in Hawaiian waters. *Hawai'i Institute of Geophysics* 69-8, 51 p.
- Pelc, R.A., W.W. Warner, S.D. Gaines, and C.B. Paris (2010). Detecting larval export from marine reserves. *Proceedings of the National Academy of Sciences*, doi: 10.1073/pnas.0907368107.
- Pineda, J., J.A. Hare, and S. Sponaugle (2007). Larval transport and dispersal in the coastal ocean and consequences for population connectivity. *Oceanography*, 20, 22-39.
- Planes, S., G.P. Jones, and S.R. Thorrold (2009). Larval dispersal connects fish population in a network of marine protected areas. *Proceedings of the National Academy of Sciences*, 106, 5693-5697.
- Polovina, J.J., P. Kleiber, and D.R. Kobayashi (1999). Application of TOPEX-POSEIDON satellite altimetry to simulate transport dynamics of larvae of spiny lobster, *Panulirus marginatus*, in the Northwestern Hawaiian Islands, 1993-1996. *Fishery Bulletin*, 97, 132-143.
- Pooley, S. (1987). Demand considerations in fisheries management - Hawaii's market for bottom fish. In Polovina J.J., and S. Ralston (Eds.), *Tropical snappers and groupers: biology and fisheries management* (pp. 605-638). Boulder, CO: Westview Press.
- Presidential Proclamation 8031. Establishment of the Northwestern Hawaiian Islands Marine National Monument, Washington, DC, 71, Fed. Reg. 36443, June 26, 2006.

- Qiu, B., D.A. Koh, C. Lumpkin, and P. Flament (1997). Existence and formation mechanism of the North Hawaiian Ridge Current. *Journal of Physical Oceanography*, 27, 431:444.
- Qiu, B., and T.S. Durland (2002). Interaction between an island and the ventilated thermocline: Implications for the Hawaiian Lee Countercurrent. *Journal of Physical Oceanography*, 32, 3408-3426.
- Ralston, S. (1981). A study of the Hawaiian deepsea handline fishery with special reference to the population dynamics of opakapaka, *Pristipomoides filamentosus* (Pisces: Lutjanidae). Ph.D. Dissertation, University of Washington, Seattle, USA.
- Rii, Y.M., S.L. Brown, F. Nencioli, V. Kuwahara, T. Dickey, D.M. Karl, and R.R. Bidigare (2008). The transient oasis: Nutrient-phytoplankton dynamics and particle export in Hawaiian lee cyclones. *Deep-Sea Research II*, 55, 1275-1290.
- Rivera, M.A.J., K.R. Andrews, D.R. Kobayashi, J.L.K. Wren, C.D. Kelley, G.K. Roderick, and R.J. Toonen (2011). Genetic analyses and simulations of larval dispersal reveal distinct populations and directional connectivity across the range of the Hawaiian Grouper (*Epinephelus quernus*). *Journal of Marine Biology*, doi: 10.1155/2011/765353.
- Roberts, C.M., and J.P. Hawkins (1997). How small can a marine reserve be and still be effective? *Coral Reefs*, 16, 150.
- Rypina, I.I., L.J. Pratt, J. Pullen, J. Levin, and A.L. Gordon (2010). Chaotic advection in an archipelago. *Journal Physical Oceanography*, 40, 1988-2006.
- Sakamoto, C.M., D.M. Karl, H.W. Jannasch, R.R. Bidigare, R.M. Letelier, P.M. Walz, J.P. Ryan, P.S. Polito, and K.S. Johnson (2004). Influence of Rossby waves on nutrient dynamics and the plankton community structure in the North Pacific subtropical gyre. *Journal of Geophysical Research*, 109, doi:10.1029/2003JC001976
- Sala, E., O. Aburto-Oropeza, G. Paredes, and G. Thompson (2003). Spawning aggregations and reproductive behavior of reef fishes in the Gulf of California. *Bulletin of Marine Science*, 72, 103-121
- Sale, P.F. (1970). Distribution of larval acanthuridae off Hawai'i. *Copeia*, 1970, 765-766.
- Sammarco, P.W., and M.L. Heron (1994). *The Bio-Physics of Marine Larval Dispersal*. American Geophysical Union. Washington, USA.
- Schaefer, K.M., D.W. Fuller, and B.A. Block (2007). Movements, behavior, and habitat utilization of yellowfin tuna (*Thunnus albacares*) in the northeastern Pacific Ocean, ascertained through archival tag data. *Marine Biology*, 152, 503-525.

- Sheridan, C.C., and M.R. Landry (2004). A 9-year increasing trend in mesozooplankton biomass at the Hawai'i Ocean Time-series Station ALOHA. *ICES Journal of Marine Science*, 61, 457-463.
- Siebert, J., and J. Hampton (2003). Mobility of tropical tunas and the implications for fisheries management. *Marine Policy*, 27, 87-95.
- Sinclair, M. (1988) *Marine populations: An essay on population regulation and speciation*. Washington, Washington Sea Grant Program. 252 P.
- Spalding, S. (2006). History of the Hawai'i bottomfish fishery. *Hawai'i Fishing News*, 32, 16-18.
- Sponaugle, S., T. Lee, V. Kourafalou, and D. Pinkard (2005). Florida Current frontal eddies and the settlement of coral reef fishes. *Limnology Oceanography*, 50, 1033-1048.
- Staaterman, E., C.B. Paris, and J. Helgers (2012). Orientation behavior in fish larvae: A missing piece to Hjort's critical period hypothesis. *Journal of Theoretical Biology*, 304, 188-196.
- Steneck, R.S., C.B. Paris, S.N. Arnold, M.C. Ablan-Lagman, A.C. Alcala, M.J. Butler, L.J. McCook, G.R. Russ, and P.F. Sale (2009). Thinking and managing outside the box: coalescing connectivity networks to build region-wide resilience in coral reef ecosystems. *Coral Reefs*, DOI 10.1007/s00338-009-0470-3.
- Suzuki, Z. (1994). A review of the biology and fisheries for yellowfin tuna (*Thunnus albacares*) in the Western and Central Pacific Ocean. In Shomura, R.S., J. Majkowski, and S. Langi (Eds), *Interactions of pacific tuna fisheries. Volume 2: Papers on biology and fisheries* (pp. 108-137). *FAO Fisheries Technical Paper*, 336/2.
- Toonen, R.J., K.R. Andrews, I.B. Baums, C.E. Bird, G.T. Concepcion, T.S. Daly-Engel, J.A. Eble, A. Faucci, M.R. Gaither, M. Iacchei, J.B. Puritz, J.K. Schultz, D.J. Skillings, M.A. Timmers, and B.W. Bowen (2011). Defining boundaries for ecosystem-based management: a multispecies case study of marine connectivity across the Hawaiian Archipelago. *Journal Marine Biology*, doi:10.1155/2011/460173.
- Walsh, W.J. (1987). Patterns of recruitment and spawning in Hawaiian reef fishes. *Environmental Biology of Fishes*, 18, 257-276.
- Wells, R.J., J.R. Rooker, and D.G. Itano (2011). Nursery origin of yellowfin tuna in the Hawaiian Islands. *Pelagic Fisheries Research Program Newsletter*, 15, 1-6 (online). Available from: [http://www.soest.hawaii.edu/PFRP/newsletters/2011\\_annual\\_issue.pdf](http://www.soest.hawaii.edu/PFRP/newsletters/2011_annual_issue.pdf) (Accessed 20 December 2011).

- Werner, F.E., R.K. Cowen, and C.B. Paris (2007). Coupled biophysical models: Present capabilities and necessary developments for future studies of population connectivity. *Oceanography*, 20, 54-69.
- Western Pacific Regional Fishery Management Council (2006). *Information and Management Alternatives Regarding Overfishing in the Hawai'i Bottomfish Fishery* (online). Available from: <http://www.wpcouncil.org/bottomfish/Documents/MaterialforPubliMeetings-2006-Jan4FinalDraft.pdf> (Accessed 26 March 2008).
- Western Pacific Regional Fishery Management Council (2009) *Pelagic Fisheries of the Western Pacific Region: 2008 Annual Report*. Prepared by the Pelagics Plan Team and WPRFMC staff, Western Pacific Regional Fishery Management Council, Honolulu, Hawaii.
- Wexler, J.B., D. Margulies, and V.P. Scholey (2011). Temperature and dissolved oxygen requirements for survival of yellowfin tuna, *Thunnus albacares*, larvae. *Journal of Experimental Marine Biology and Ecology*, 404, 63-72.
- Woodson, C.B., and M.A. McManus (2007). Foraging behavior can influence dispersal of marine organisms. *Limnology and Oceanography*, 52, 2701-2709.
- Wright, S. (1931). Evolution in Mendelian populations. *Genetics*, 16, 97-159.
- Wyrtki, K. (1982). Eddies in the Pacific North Equatorial Current. *Journal of Geophysical Research*, 12, 743-749.
- Xie, S.P., W.T. Liu, and M. Monaka (2001). Far-reaching effects of the Hawaiian Islands on the Pacific ocean atmosphere system. *Science*, 292, 2057-2069.
- Zeller, D., M. Darcy, S. Booth, M.K. Lowe, and Martell (2008). What about recreational catch? Potential impact on stock assessment for Hawaii's bottomfish fisheries. *Fisheries Research*, 91, 88-90.